NTIS #

SSC-447

IN-SERVICE PERFORMANCE OF ALUMINUM STRUCTURAL DETAILS

SHIP STRUCTURE COMMITTEE

2007

Ship Structure Committee

RADM Craig E. Bone
U. S. Coast Guard Assistant Commandant,
Marine Safety and Environmental Protection
Chairman, Ship Structure Committee

Mr. W. Thomas Packard
Director,
Survivability and Structural Integrity Group
Naval Sea Systems Command

Dr. Roger Basu
Senior Vice President
American Bureau of Shipping

Mr. Joseph Byrne
Director, Office of Ship Construction
Maritime Administration

Mr. Nash
Director General, Marine Safety,
Safety & Security
Transport Canada

Mr. Kevin Batesen
Director of Engineering
Military Sealift Command

Dr. Neil Pegg
Group Leader - Structural Mechanics
Defence Research & Development Canada - Atlantic

CONTRACTING OFFICER TECHNICAL REP.
Mr. Chao Lin / MARAD
Glenn Ashe / ABS
Mr. Robert Sedat / USCG

EXECUTIVE DIRECTOR
Lieutenant Benjamin A. Gates
U. S. Coast Guard

SHIP STRUCTURE SUB-COMMITTEE

AMERICAN BUREAU OF SHIPPING
Mr. Glenn Ashe
Mr. Phil Rynn
Mr. Balji Menon
Mr. Derek Novak

DEFENCE RESEARCH & DEVELOPMENT ATLANTIC
Dr. David Stredulinsky
Mr. John Porter

MARITIME ADMINISTRATION
Mr. Chao Lin
Mr. Carl Setterstom
Mr. Richard Sonnenschein
Mr. David Heller

MILITARY SEALIFT COMMAND
Mr. Michael W. Touma
Mr. Paul Handler
Mr. James Kent

ONR / NAVSEA
Dr. Paul Hess
Dr. Jeffery E. Beach
Mr. Yapa Rajapakse
Mr. Allen H. Engle

TRANSPORT CANADA
Mr. Richard Stillwell

UNITED STATES COAST GUARD
Capt. Patrick E. Little
Mr. H. Paul Cojeen
Mr. Rubin Sheinberg
Mr. Robert Sedat

SNAME
Mr. Jaideep Sirkar
Mr. Alan Rowen
Mr. Norman Hammer
Mr. John Conlon

Member Agencies:

American Bureau of Shipping
Defence Research Development Canada
Maritime Administration
Military Sealift Command
Naval Sea Systems Command
Society of Naval Architects & Marine Engineers
Transport Canada
United States Coast Guard

Ship
Structure
Committee

Address Correspondence to:

Executive Director
Ship Structure Committee
U.S. Coast Guard (CG-3PSE/SSC)
2100 Second Street, SW
Washington, D.C. 20593-0001
Web site: http://www.shipstructure.org

SSC – 447
SR – 1434

MARCH 21, 2007

FATIGUE AND FRACTURE BEHAVIOR OF FUSION AND FRICTION STIR WELDED ALUMINUM COMPONENTS

As aluminum has become more commonplace in structural applications, extensive research of large structures has been conducted to determine in-service performance. This project provides insight into the widespread research done in Europe on fatigue testing of aluminum components. The findings from the European Recommendations for Aluminum Alloys Structures (ERAAS) have been compared with parallel research from other organizations and research universities.

In addition, the report provides an overview of Friction Stir Welding (FSW) and compares preliminary test results between both tradition fusion welding and FSW methods.

CRAIG E. BONE
Rear Admiral, U.S. Coast Guard
Chairman, Ship Structure Committee

Technical Report Documentation Page

<table>
<tr><td>1. Report No.
SSC - 447</td><td>2. Government Accession No.</td><td colspan="2">3. Recipient's Catalog No.</td></tr>
<tr><td colspan="2" rowspan="2">4. Title and Subtitle
In-Service Performance of Aluminum Structural Details</td><td colspan="2">5. Report Date
Nov. 1, 2006</td></tr>
<tr><td colspan="2">6. Performing Organization Code
5813C.FR</td></tr>
<tr><td colspan="2">7. Author(s)
R. Kramer</td><td colspan="2">8. Performing Organization Report No.
SR-1444</td></tr>
<tr><td colspan="2" rowspan="2">9. Performing Organization Name and Address
Alionscience – JJMA
311 Legget Drive
Kanata, ON (Canada) K2K 1Z8</td><td colspan="2">10. Work Unit No. (TRAIS)</td></tr>
<tr><td colspan="2">11. Contract or Grant No.</td></tr>
<tr><td colspan="2" rowspan="2">12. Sponsoring Agency Name and Address
Ship Structure Committee
C/O Commandant (G-MSE/SSC)
United States Coast Guard
2100 Second Street, SW
Washington, DC 20593-0001</td><td colspan="2">13. Type of Report
Final Report</td></tr>
<tr><td colspan="2">14. Sponsoring Agency Code
G-P</td></tr>
<tr><td colspan="4">15. Supplementary Notes
Sponsored by the Ship Structure Committee and its member agencies</td></tr>
<tr><td colspan="4">**16. Abstract**
The primary objective of the project was to compare and evaluate the design criteria and standards currently used in naval and commercial ships for the hull and structural members. This report reviewed the basic concepts in several current ship and structures regulations. The design of bottom structure, as both local structure and as part of the hull girder was the specific focus. We expected to identify factors of safety in either the load or strength formulations or both. As well as identify the best practices that incorporate latest models of structural behavior that are adequately validated by theory and experimentation. This will then be applied to new unified structural design ships.</td></tr>
<tr><td colspan="2">17. Key Words</td><td colspan="2">18. Distribution Statement
Distribution Available From:
National Technical Information Service
U.S. Department of Commerce
Springfield, VA 22151
Ph. (703) 605-6000</td></tr>
<tr><td>19. Security Classif. (of this report)
Unclassified</td><td>20. Security Classif. (of this page)
Unclassified</td><td>21. No. of Pages
104</td><td>22. Price</td></tr>
</table>

Table of Contents

List of Figures

List of Tables

1. INTRODUCTION

In accordance with the Statement of Work included in the Solicitation for this proposal, the Objectives of this project are:

1. Develop a survey of in-service performance of aluminum structural details for use by designers and fabricators of aluminum vessels. Start to fill some of the gaps identified in SSC-410, "Fatigue of Aluminum Weldments." Consideration shall be given to several types of vessels (catamarans, SES's, ACV's, SWATH's, monohulls, etc.) using aluminum details.

2. Construct a database of the in-service information and develop a rating system to assist designers and fabricators with the selection of fatigue resistant details and fabrication procedures. Coordinate the survey data with fabrication and QA procedures employed during the initial construction recommending minimum criteria that should be used to enhance the behavior of aluminum details subjected to the fatigue environment.

3. Introduce fatigue to the design stage of a vessel and address the fatigue issue up-front instead of the current practice which relegates this to a maintenance problem causing undue expense throughout the life of the vessel.

The execution of this project was unable to perform the surveys initially planned although some of the ground work was developed and is presented herein. The preliminary work included interviews with various small boat yards who indicated good success with the welding and performance of aluminum details. As anticipated, these interviews were also conducted with yards and owners that were more reluctant to provide information on relevant experience, which is understandably attributed to the competitive nature of this industry. Regardless, there is significant information regarding the performance of aluminum structural details in small and high speed aluminum craft. Gathering this information would develop a good database of information and provide designers good insight to the selection of details with improved performance in the fatigue environment.

To help compensate for the lack of survey work there is more emphasis on the existing fatigue data and design standards for aluminum structural details. This focuses on the work that has been developed in Europe, where significant effort has been devoted to the testing of small and large specimens in support of addressing the fatigue of aluminum during the design process.

1.1 Determination of Details & Classes of Details for Survey

Section 2 of this report presents the preliminary plans that had been intended for the surveys. The efforts for Section 2 included a review of all previous SSC reports to determine survey procedures successfully employed for similar efforts in steel. This effort was beneficial and helped to establish the categories of structural details that would have originally been sought during the surveys. It is worth noting that all previous SSC efforts addressed steel, large displacement vessels while the current project is focused on aluminum and aluminum high speed craft. Therefore, the classes of details defined in Section 2 would have been modified to address the differences between these types of vessels and would have evolved during the execution of the surveys.

1.2 Fatigue Behavior of Aluminum Structural Details

The information gathered from the European community regarding the fatigue of aluminum is presented in Section 3 though Section 7 of this report. This information includes some specific comparisons between different design standards, including the Aluminum Association, regarding the use of fatigue in the design of aluminum structural systems. The fatigue data presented throughout these sections are for specific structural details with their geometry provided for easy reference. Many of these details and their structural functions can be related to those used in the marine industry for estimation of design performance in the current application of aluminum craft. Additional information on environmental effects can also be obtained from design standards such as Eurocode 9, which includes knockdown factors for the Marine and Immersed environments.

Section 8 of this report presents information for Friction Stir Welding, FSW, procedures and is taken from the body of work gathered for the fatigue behavior of aluminum from European sources. It includes information on the fatigue performance of aluminum details fabricated with FSW as well as comparison to similar details fabricated with traditional fusion welding procedures.

1.3 Conclusions and Recommendations

Section 9 presents conclusions and recommendations for additional work in this field and recognizes the work that has also been done for fracture mechanics and crack propagation in aluminum details, again with reference to European sources.

2. DETERMINATION OF DETAILS & CLASSES OF DETAILS FOR SURVEY

This section of the report presents the preliminary list of details to be investigated during the vessel surveys. This list of details may evolve as the task progresses and additional "trouble spot" areas become identified. The list of details presented for this project is assumed to be readily accessible, i.e., it is assumed that there will not be any survey of details contained within tanks or other inaccessible areas such as voids. All surveys will take place while the vessel is either pier side or underway during routine operations. The Survey Team will not cause any form of damage to anything on the vessels being surveyed. There will not be any Non-destructive evaluation of structure using any techniques such as dye penetrant, magnetic particle or ultrasonic sound. All survey data shall be limited to visual recording with light tamping of a small hammer, if beneficial, to detect flaws in the metal. Photographic records of surveyed details will be developed.

2.1 List of Ship Details & Background Information

The following list of details will be specifically sought for investigation during the vessel surveys for this project:

- Bow, bottom and cross structure in way of areas subjected to repeated slam loads. (Ability to survey cross structure will depend on access.)
- Stiffener end connections, i.e., vertical bulkhead to longitudinal deck stiffening and vertical bulkhead to bottom shell stiffening.
- Typical longitudinal stiffener/transverse web frame intersection on strength deck, bottom and side shell.
- Transverse bulkhead structure in way of haunch.
- Deck beam to side frame connection in transversely framed ships.
- Details in way of hard chines.
- Machinery Foundations and structural details in way of machinery spaces.
- Waterjet and bow thruster foundations.
- Structural detailing in way of free-standing tanks.
- Structural details in way of windows, hatches and other openings/penetrations through light superstructure scantlings.

Other information sought prior to and during the surveys will include:

- Operating environment of vessel.
- Classification notation for craft certified in accordance with regulatory body requirements – is the vessel designed in accordance with regulatory requirements but unclassed?
- Aluminum alloy/temper and weld metals used in fabrication.
- In-service histories of details throughout the fleet including repair histories.
- Approximate costs, or ranking of costs, associated with maintenance of details with poor histories.

The vessel surveys will also include photographic documentation to the greatest extent practical. This will, of course, require the permission of the vessel owner/operator who will be assured of complete anonymity for all photographs used in the survey and final report, if desired.

One of the primary objectives of this project is to perform vessel surveys that will allow for the investigation of structural details and evaluate their in-service performance. This can include details and classes of details that have good in-service records as well as those that perform poorly, although the emphasis will be on the latter, i.e., structural details with poor in-service performance histories.

The preliminary list of details was based on experience with these vessels, input from the Project Technical Committee, PTC, and review of the SSC reports shown below. While it was not expected to gather specific, relevant information regarding details from the SSC reports it was expected that there might be some good insight into the survey procedures and the manner in which details are classified. The review of the SSC reports confirmed most of the expected procedures and helped to validate the efforts that are expected. The SSC reports reviewed include:

- SSC-266 “Review of Ship Structural Details”
- SSC-272 “In-Service Performance of Structural Details”
- SSC-294 “Further Survey of In-Service Performance of Structural Details”
- SSC-318 “Fatigue Characterization of Fabricated Ship Details for Design”
- SSC-367 “Fatigue Technology Assessment and Avoidance Strategies in Marine Structures”
- SSC-379 “Improved Ship Hull Structural Details Relative to Fatigue”
- SSC-400 “Weld Detail Fatigue Life Improvement Techniques”

As noted by their titles, not all of the reports address the stage of investigation associated with vessel survey. The lessons learned from the latter reports will be incorporated into the current project as applicable. Hopefully this will help to reduce the learning curve for aluminum by taking advantage of the lessons learned in treating the fatigue problem in steel.

While it is not the intention of this project to limit the details sought for investigation during survey, there are some practical limitations. Since the objective of this project is the survey of details with poor in-service performance histories, it is expected that those details included in the list above with better histories will receive less attention than those more prone to problems. It is fully expected that the relevance of such histories will become apparent prior to and during the actual surveys. The list of details provided above represents an optimistic checklist that could potentially include details with poor in-service histories. It will be difficult to completely survey all these classes of details within the scope of this project.

2.2 Review of Previous Ship Structure Committee Reports

To date, the Ship Structure Committee has published over 400 reports. Dozens of these reports, starting in 1946, deal with one or more aspects of fatigue. All but one of these reports deals with steel and virtually all information reflect displacement type vessels that operate at relatively low speed in an open ocean, unrestricted environment. The current project specifically addresses the in-service performance of structural details in aluminum vessels, with a tendency towards high-speed, although the latter is not a necessary condition. Regardless, it was well recognized that the great bulk of data and research currently contained within the SSC reports addresses steel displacement vessels and that the direct relevance to the current project may be limited.

It is interesting to note the progression of SSC reports relative to steel fatigue. There was a natural progression in the topics they covered that reflects the evolution of a continuing research project. The initial reports are similar in nature to the current project for aluminum, data gathering, survey type reports that attempt to start quantifying the in-service performance of the steel details subjected to fatigue. These are followed by reports that reflect the environments and loading histories that cause fatigue and proposals to start quantifying and predicting fatigue damage during the design stage. Subsequent reports propose improved structural details for resistance to cracking in the fatigue environment along with improved welding and fabrication procedures to minimize the crack initiation mechanism associated with all welding procedures.

The progression of SSC reports addressing steel fatigue reflects what is expected to be a similar, although abbreviated series of SSC reports for aluminum. It is expected to be abbreviated because of the potential learning curves that can be applied from steel to aluminum even though the operational and loading profiles of the respective vessel types can be significantly different.

Regardless, the review of the SSC reports conducted for the current project did provide some insight into format and procedure for the surveys, if not so much for the specific types of details. It should be noted that SSC 266, SSC 272 and SSC 294 present comprehensive classes of details to be included in vessel surveys with significant survey data included in SSC 272 and SSC 294. These are all generic details, relevant to displacement type vessels, and certainly applicable to the surveys conducted at the time for the steel ships involved.

2.2.1 SSC 266 “Review of Ship Structural Details” 1977

As mentioned above, this report contains a fairly comprehensive presentation of the typical structural details required to complete the design of any steel displacement vessel. They are global categories and suggested the manner of classification for the current project. There are 15 classes of details presented in SSC 266 as follows:

1. Clearance Cuts
2. Snipes
3. Tight Collars
4. Reeving Slots
5. Structural Intersections
6. Miscellaneous Cutouts
7. Patches
8. Stanchion end Connections
9. Tripping Brackets
10. Face Plates
11. Stiffener Ends

12. Clip Connection
13. Chock
14. Panel Stiffener
15. Beam Bracket

The details are generic and include nominal information regarding clearances, radii, weld types, gusset and chock locations, etc. A simple sketch is provided for each detail within SSC 266. It is anticipated that the current project will include sketches/photographs for all relevant details.

There are no specific results for SSC 266 that will benefit this project. In addition to defining the 15 classes of details noted above, SSC 266 summarizes much of the classification society requirements relative to structural detail development. It provides some background on damage histories found from previous work and also includes introductory ideas regarding strength and fatigue criteria for detail design.

One of the conclusions from SSC 266 is that there is very little feedback of the performance of structural details back to the designer. Since many of the aluminum vessels fabricated do not require certification of the details in the design it is expected that many of the larger fabricators may track performance for their own, internal use, but not necessarily make the data generally available to classification societies or other designers. This closely tracked performance could be considered an advantage in the competitive world of high-speed ferry design. With no incentive or requirement to provide such performance history to the class societies, it would not be unexpected if no feedback is provided.

2.2.2 SSC 272 "In-Service Performance of Structural Details" 1978

This report summarizes actual survey work performed for the project. It includes a tremendous amount of data collected on fifty (50) displacement type, steel vessels. Newport News Shipbuilding performed the task. Thirty three (33) of the fifty (50) vessels surveyed were inspected at the NNS facility while they were in for scheduled maintenance, inspections, overhauls or unscheduled emergency repairs. The average vessel had a displacement of 34,980 long tons and an LBP of 622 feet. This availability and access to such large vessels for extended periods represents a significant difference to the availability and access for the current project.

Similar to SSC 266, this project also created various classes of details for grouping the in-service performance data. SSC 272 used 12 classes of details, which along with the observed number of details, is presented in **Table 1**. SSC 272 also included the results of the survey indicating the number of failed details.

The volume of details surveyed is tremendous compared to the expectations for the current project.

Table 1 Detail Classification and Number of Observed Details in SSC 272

Detail Classification	Number of Observed Details
1. Beam Bracket	50,750
2. Tripping Bracket	20,640
3. Non-Tight Collars	16,250
4. Tight Collars	18,000
5. Gunwale Connection	100
6. Knife Edge Crossing	None found
7. Miscellaneous Cutouts	252,870
8. Clearance Cutouts	48,510
9. Structural Deck Cuts	6030
10. Stanchion Ends	6270
11. Stiffener Ends	30,760
12. Panel Stiffeners	40,030

The vessels surveyed for this project will be significantly smaller than those surveyed for SSC 272, probably in the range of 1% to 5% of the average displacement quoted above. Also, they will be fully operational and in-service, i.e., performing their daily, commercial operations, not laid-up for repair, maintenance, inspection, etc. The surveyors will be traveling to the ships, not have the convenience of ships that are laid-up for repairs or other services over relatively protracted periods of time. The level of effort for the current project will not allow for more than a few days of actual survey.

Regardless, the procedures for conducting the surveys in SSC 272 are similar to those anticipated for the current project. All surveys will be performed on readily accessible structure without causing any damage to any of the surrounding ship systems. i.e., insulation, paint, drop ceilings, etc. The surveyors on the current project may also employ small hammers or other devices to lightly tap structure suspected of containing a crack. The surveyors for the current project will not use any of the more advanced non-destructive evaluation procedures associated with typical classification society/shipyard QA procedures. None of the advanced NDE procedures were used during SSC 272.

One of the differences between the details classifications of SSC 266 and SSC 272 suggests the similar direction anticipated for the current project, i.e., the inclusion of localized, special areas. These are noted by such classes as “Gunwale Connection” and “Knife Edge Crossing” in SSC 272 whereas SSC 266 did not contain any details that approached this level of specific definition. As noted above, the current project anticipates developing classes that relate to specific areas of repeated failures on aluminum high-speed vessels.

Although its exact form is yet to be determined, the results of the surveys for the current project will also develop a database presentation for ease of access to the data. Both SSC 272 and SSC 294 also present numerous photographs helping to describe the details. Both of these reports also maintain the anonymity of all vessels included in their surveys. The reports do include the number of each type of vessel included in the survey but do not track in-service performance history as a function of the type of ship. All of these practices have been anticipated for the current project since its proposal development stage.

2.2.3 SSC 294 "Further Survey of In-Service Performance of Structural Details" 1980

This report is a continuation of the efforts in SSC 272. It was also performed by Newport News Shipbuilding and used the same approach as presented in SSC 272. The surveys completed for SSC 294 involved thirty-six (36) ships, most of which were surveyed at NNS. As a matter of completeness, **Table 2** presents the same data for SSC 294 that **Table 1** presented for SSC 272.

Table 2 Detail Classifications and Number of Observed Details in SSC 294

Detail Classification	Number of Observed Details
1. Beam Bracket	17,836
2. Tripping Bracket	13,372
3. Non-Tight Collars	4724
4. Tight Collars	2654
5. Gunwale Connection	72
6. Knife Edge Crossing	None found
7. Miscellaneous Cutouts	43,819
8. Clearance Cutouts	8797
9. Structural Deck Cuts	1504
10. Stanchion Ends	820
11. Stiffener Ends	9969
12. Panel Stiffeners	13,807

Again, it can be seen that there was a tremendous amount of data collected for SSC 294. This project had the same advantage as SSC 272, i.e., the vessels had extended availabilities as a result of being at NNS for scheduled maintenance, overhauls, etc. This advantage will not present itself for the current project.

2.2.4 Other SSC Reports Reviewed

As the SSC reports continue beyond SSC 294 the data and information relates to further stages of the fatigue evaluation/prevention cycle. Most of that information is not relevant to the objective of this section of the report, i.e., definition of the list of details to be surveyed. Limited amounts of that information will be relevant to future development of this project and a larger amount may become relevant to future projects associated with fatigue of aluminum weldments. As discussed above, this information will help to shorten the learning curve for fatigue of aluminum weldments by borrowing from the lessons learned with fatigue of steel weldments.

The preliminary list of details to be included in the vessel surveys for this project provides a good starting point that reflects the known areas of concern of poor in-service candidates. More vessel specific areas may reveal themselves as a result of the surveys. Trends between such vessel specific areas will be investigated?

It is expected that the list of details will evolve as the project continues. This will present no problem as the information will be gathered during the surveys and the survey team will have good knowledge of the areas with poor histories as a result of the preliminary discussions held with all operators.

3. FATIGUE AND FRACTURE BEHAVIOR OF ALUMINUM STRUCTURAL DETAILS

The main reason to include discussion on the European standards and Friction Stir Welding, FSW, in this report regarding in-service performance is to introduce the large volume of work that has been developed in Europe to support the use of aluminum in structural applications. The information presented in this report will help the reader understand the history and development of much of the design standards, U.S. and European, concerning aluminum. There has been extensive testing of small and large specimens developed in support of the European standards regarding fatigue of aluminum. Also, the work presented herein provides a blueprint for the progression of the development of fatigue in aluminum structural weldments that was anticipated for this and follow-up SSC reports. The same procedures used to refine the understanding of fatigue in general applications could be applied to structural details specific to aluminum and aluminum high speed craft.

3.1 Damage Tolerant Design and Fracture Analysis

This report does not include any of the specific work or reference information that is available through some of the European standards on this subject, i.e., Eurocode 9. The topic is introduced through these headings only to alert the reader that there is extensive information available. This includes design curves for da/dN, crack extension per cycle of load as a function of crack tip stress intensity. These curves can be used to estimate the remaining life in a cracked detail once crack initiation has been identified and critical crack length defined. The life is defined in number of load cycles which can then be translated into calendar time to help evaluate the criticality of joint repair. Regardless, there is significant information for crack propagation, fracture analysis and crack growth rate data through the reference provided above.

3.2 History and Development of the European Standards

The development of European specifications for the design of aluminum structures has been supported by activities that have taken place from the 1980's up to the present day when they are reaching their final stage with the drafting of the Eurocode 9 or EN 1999-1:2004.

Following the initial contacts through the establishment of the INALCO International Conference on Aluminum Weldments, the Committee for Aluminum Fatigue Data Exchange and Evaluation was formed. Its task was to unite the two databases on aluminum fatigue data started a few years earlier at Iowa State University (Prof. Dr. W. W. Sanders, Jr.) and Technical University of Munich (Prof. Dr. D. Kosteas) and expand these to include any available data. This joint project continued for several years, the data bank was later based and maintained at the Technical University of Munich (TUM), but had to be discontinued in the 1990's for lack of funds. Nevertheless, the initial statistical-regression analyses on small specimen data and data from larger specimen testing started in the 1980's at the TUM formed the basis for the first European common document.

The second phase of development is characterized by the analysis of comprehensive new data on small specimens but also encompasses a considerable amount of component tests (aluminum beams) supplied by Alusuisse, Switzerland. The project was carried out by the Section of Light Metal Structures and Fatigue at the Technical University of Munich (Kosteas) with the support of a statistician from the Pechiney Research Center in Voreppe/France, and Dr. R. Jaccard, Alusuisse, Zürich/Switzerland. This project was also discussed with researchers and company representatives from different European countries in two workshops in Zürich and Munich. A representative compilation of results was published: *Jaccard, R., Kosteas, D., Ondra, R.: Background Document to Fatigue Design Curves for Welded Aluminum Components. IIW Doc. No. XIII-1588-95.* The enhanced data led to the European Recommendations for Aluminum Alloys Structures (ERAAS) Fatigue Design Recommendations in 1992.

These evaluations were the baseline for the first drafts of the Eurocode 9 sections on aluminum fatigue design in a third development phase, enhanced by further material (including welded aluminum beam tests from other laboratories like TNO Delft/The Netherlands, The Swiss Federal University in Lausanne, and ATLSS/Lehigh University, U.S.A.) and a number of comparative analyses with other simultaneously emerging codes (International Institute of Welding, IIW, on Fatigue Design, Aluminum Association Design Manual), as well as the introduction of a number of new issues often following re-evaluation of data. During the final three years when the completed codes were being compiled, a completely new approach and change of format had to be followed. The European document EN 1990 states general provisions for the quality management, defining consequence and reliability classes for structures, definitions which ultimately lead to the adoption of respective execution classes for structural components. This also led to the split of the former single document for fatigue into a document for “design” [now EN 1999-1-3] and a document for “execution” (or manufacturing quality and control) [now EN 1090-3]. This development was undertaken for steel as well.

The classification of weld quality through allowable imperfections was undertaken after the document EN ISO 10042. Certain inconsistencies may arise in this procedure, as comparative studies at TUM with respective national specifications have shown. The issue of relevance to fatigue behavior is not yet completed for specific imperfections in this code. The quantification of the quality classes and the harmonization of imperfection limit sizes will be one of the main challenges in the coming years.

This report offers a compilation of important fatigue data and its evaluation as presented in the European specifications. Much of the fatigue data used to develop the European standards is proprietary data sponsored by private industry and is not available for general review. Instead, comparative analyses and data in the form of S-N diagrams was developed and used in the codes.

The information for the European Standards is presented in four parts in this report:

1. Section 4 presents the data described above as it was evaluated for the European Recommendations for Aluminum Alloy Structures, ERAAS, and later Eurocode 9.
2. Section 5 is a short comparison between the fatigue strengths calculated for the European Recommendations (based on the comprehensive experimental data of over 25,000 data points from small specimens and 2,500 data points from component tests) and various other aluminum design codes including The Aluminum Association, Inc., Washington, DC.

3. Section 6 summarizes, in tabular form, the background information for the definition of design fatigue strength values from the available data.
4. Section 7 presents the same experimental results as above but in a comparison to the International Institute of Welding, IIW, fatigue design rules for aluminum structures – it should be noted that it represents the status of development at the end of 1999.

3.3 Friction Stir Welding

In addition to the discussion on the European Standards, Section 8 of this report also presents general information and test results on Friction Stir Welding with some comparative test results to similar welds developed using traditional fusion processes.

The report presents a general introduction to the processes, procedures and hardware associated with FSW. It provides a comprehensive description of the mechanics underlying the FSW process and an understanding of why the basic FSW process is better for fatigue sensitive materials like aluminum compared to the traditional fusion welding procedures.

The report also presents fatigue data of 6XXX aluminum alloys using FSW with comparative data to typical fusion welding procedures, as available.

4. EUROPEAN RECOMMENDATIONS FOR ALUMINUM ALLOY STRUCTURES – FATIGUE DESIGN (ERAAS)

Early in the development of the European codes three groups of structural detail S-N curves were established with respective slope values of 7.0, 4.3 and 3.4. As a remnant of the analysis procedure for varying load spectra (especially from older fatigue design standards for steel bridges with standardized loading and factors to accommodate other specific loading sequences through the linear damage accumulation Miner-rule) the concept of parallel and equi-distant S-N curve band can still be recognized in the Eurocode document. The following discussion and figures help explain these assumptions.

4.1.1 Design S-N Curves in the ERAAS

All design S-N curves in ERAAS Fatigue are based primarily on experimental, full-scale component data. Most of this data was generated in the mid life range up to $2{\times}10^6$ cycles. Therefore, the assessment lines did not have to be conservatively extrapolated.

Design codes in the past were based almost exclusively on small specimen data in the lower fatigue life ranges. In order to obtain a safe design line, especially in the fatigue-relevant region around $2{\times}10^6$ cycles, this data had to be extrapolated and was conservative at longer lives. The procedure to formulate such design lines was to fix it at the center of gravity of existing experimental data - most often in an area around 10^4 and up to 10^5 cycles - and rotate it downward at longer lives, maintaining a conservative philosophy. Due to the new, full-scale component data at $2{\times}10^6$ cycles and above it was possible to formulate a "best-fit" design curve, fixing it at the appropriate strength value as a lower data boundary, practically corresponding to the mean minus two standard deviations strength value. A certain degree of uniformity for practical reasons or concurrence with other existing design codes was attained through an assumed slope, common for a group of structural details. The slopes are m=7.00 for parent material and m=3.37 or m=4.32 for the welded details. These values have been calculated at two characteristic stress-life pairs from the respective S-N data plots of individual datasets. This concept was checked against some other options, common in other specifications. In general, it can be demonstrated that neither an equi-distant parallel design line concept, **Figure 1**, nor other slopes than those mentioned above would better represent the experimental data. **Figure 2** demonstrates that because of the best-fit concept at $2{\times}10^6$ cycles a classification due to an equi-distant line concept would lead to lower characteristic fatigue strength. A variation of other slope values, for instance m=3.4, 3.8, 4.3 would "punish" the material for most of the structural details under consideration in relation to the introduced best-fit design line concept.

By introducing these simplifications it was still possible to obtain characteristic fatigue classes, as engineers are used to with other codes, with the advantage of a best-fit concept at the most relevant life range. No problems in practice should be expected for the different slopes during the design procedure even when calculating the equivalent damage of different spectrum loadings. In today's practice, computers are used for such calculations, all necessary equations are given within the Recommendations and software for PCs is available to perform such fatigue assessments.

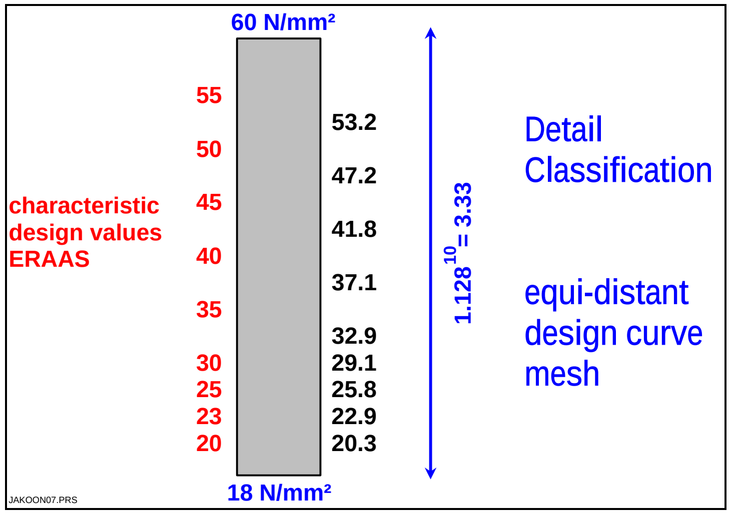

Figure 1 Equi-distant Design Curve Mesh

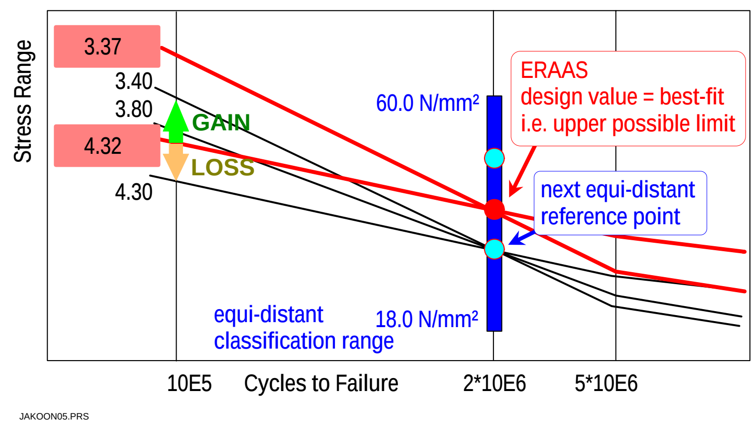

Figure 2 Effect of Classification Considering Equi-Distant and Parallel Design Line Concepts on Attainable Fatigue Strengths

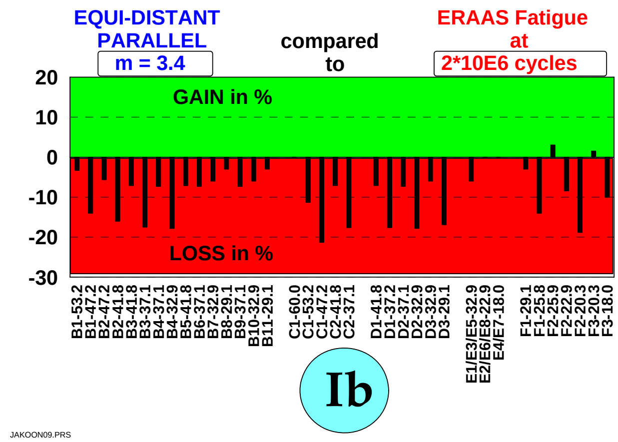

Figure 3 Example of the effect of parallel and equi-distant design lines on fatigue strength according to the different structural details after ERAAS Fatigue 1992

Using an equi-distant parallel S/N curve band result in the following:

At $2*10^6$ cycles

- a “Loss”, observed in all cases, due to the new classification at the next respective reference strength value of the equi-distant mesh, as this is, in general a lower value than the ERAAS design value resulting from the “best-fit” concept.

At 10^5cycles and a parallel band slope of 3.40

- if the original ERAAS curve had a slope of 3.37 (which is practically identical to the assumed value parallel band slope of 3.40) then the “Loss” at 10^5 cycles has the same value as above at $2*10^6$ cycles due to the new reference class value,
- if the original ERAAS curve had a slope of 4.32 (shallower than the assumed parallel band slope of 3.40) then, depending on the classification value of the detail, the “Loss” will be reduced compared to the value at $2*10^6$ cycles or may even be turned into a “Gain”

At 10^5cycles and a parallel band slope of 4.30

- if the original ERAAS curve had a slope of 3.37 (steeper than the assumed parallel band slope of 4.30) then the “LOSS” will be enhanced, compared to its value at $2*10^6$ cycles
- if the original ERAAS curve had a slope of 4.32 (which is practically identical to the assumed parallel band slope of 4.30) then the “LOSS” will maintain its value

It is evident from these comparisons that there is no “GAIN” from a classification following an equi-distant parallel band of S/N curves and the ERAAS design curve classification on the basis of a best-fit curve value at $2x10^6$ cycles serves the material far better in this area critical for applications susceptible to fatigue. The only compromise was made in adopting two sets of structural welded details with different slopes each, but parallel curves within the set. Whatever “LOSS” appears compared to effective strength values - that is the design is too conservative for short lives, where design is not generally affected by fatigue criteria.

4.1.2 Data Base of the Recommendations

The development of the ERAAS Fatigue document was based mainly on experimental fatigue data of full-scale components. Results on small specimens were only used to investigate tendencies of notch or R-ratio or plate-thickness influences. At the time, data was only provided by Alusuisse-Lonza Services [3], Austria Metal (AMAG) [4] and TUM [5, 6] on various aluminum alloys and welded structural details on extruded or built-up beams. A summary of this database is given in **Figure 4**.

All data were stored in individual datasets describing only one structural detail with typical manufacturing and loading characteristics, as part of the Aluminum Data Bank. These data sets were processed either individually or grouped together in "families" and then analyzed statistically. Approximately 160 individual data sets and 120 families have been analyzed for the fatigue data of full-scale specimen. Detailed results are covered in [3].

Further decisions and the final ERAAS document design curves were based on the systematic documentation, regression analysis and evaluation of all data, including small specimen data from different institutions as well as the small specimen data generated at TUM studying manufacturing variations in butt and fillet welded details. Results were summarized during the two workshops in Munich and Zurich and were included, along with an international comparative study on structural detail classification and fatigue strength values, in [7]. It is mainly these results that form the background for the information in this report.

Further experimental data generated at other institutions will be similarly documented and evaluated for the purpose of the new design standard Eurocode 9: Aluminum Design. Respective analyses already allow the general statement of the validity of the ERAAS Fatigue Design curves. In a few specific cases a modified or simplified structural detail classification may have to be adopted. New data on welded beams, as well as small specimens, has been produced in the last two years at:

- EPF-Lausanne by Hirt et al [18],
- ATLSS Laboratories at Lehigh University by Fisher and Menzemer [8], and
- TNO-Delft by Soetens et al. [19, 20, 21].

Only the experimental data produced at Lehigh is included in the following diagrams, and compared to existing results by TUM.

Structural Detail	ERAAS Ref. N°	Alusuisse-Lonza Number of Data-points	AMAG Number of Data-points	TUM Number of Data-points
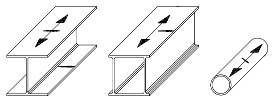	A2 A4	33 72		
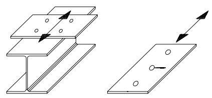	A5	20		
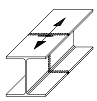	B5 B6 B7 B8	44 30 85		
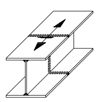	B9 B10 B11		28	17 3 40
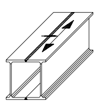	C1 C2	 17		
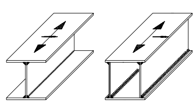	D1 D2	15	 25	5 88
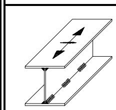	D3			57
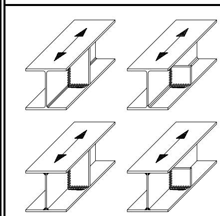	E1	116	7	159
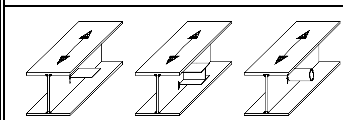	E2	124		
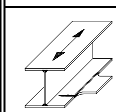	E3			
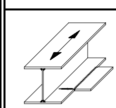	E4	118		
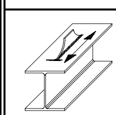	E5	58		

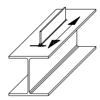	E6 E7			53
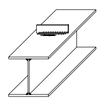	E8			22
	F1 F2			22
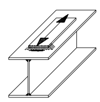	F3	27	30	69

Figure 4 Full-Scale Background Data for ERAAS-Fatigue Document

4.1.3 Base Metal 5000/6000 Series

ERAAS Detail Class A3 (simple extrusions) and A4 (Components)

Results for the 5000 alloys give values of 128 to 140 N/mm² for 2×10^6 cycles and 180 to 185 N/mm² for 1×10^5 cycles at R=0, with results approximated by 106 N/mm² at 2×10^6 cycles and 150 N/mm² at 1×10^5 cycles for R=+0.5. The general decision for simple extrusions/machined parts for both 6000/5000 alloys is to use a design curve at 95 N/mm² at 2×10^6 cycles at R=+0.5 for no environmental effects, **Figure 5**. With a slope of m=7.00 the line shows a value of 146 N/mm² at 1×10^5 cycles. In the case of environmental effects (corrosion) a value of 67 N/mm² for the 5000 series and 55 N/mm² for the 6000 series at 2×10^6 cycles and R=+0.5 and small specimens are indicated.

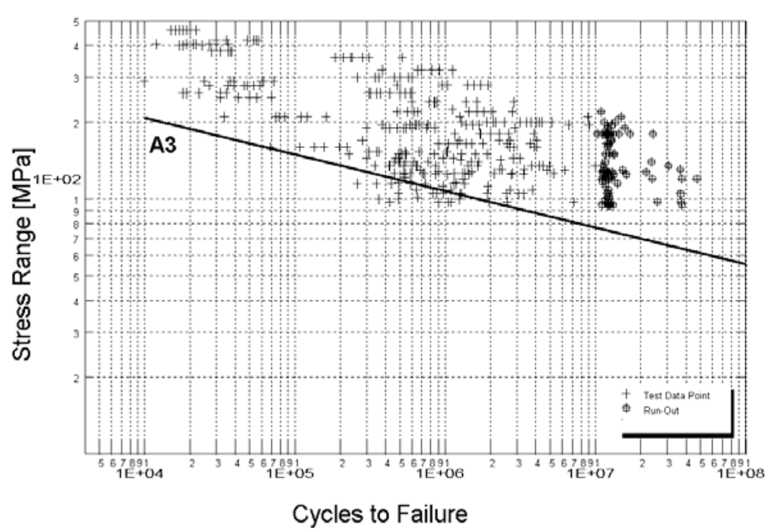

Figure 5 Base Metal 6005A (AlMgSi0) Small Specimen Data

For base metal components an uppermost strength value of 87 N/mm² at 2×10^6 cycles and R=0 was indicated for both the 5000 and 6000 alloy beams. At lower lives the 5000 series exhibited higher values. Some Alusuisse data show values of 95 N/mm² for extrusion profiles in the 6000 series. Taking into account the available information and considering respective factors in transforming strength values from R=0 and R=-1 to R=+0.5, and dropping the former proposal of different design curves for the two alloy groups the final decision was made for a design curve at R=+0.5 with 70 N/mm² at 2×10^6 cycles and a slope of m=7.00, **Figure 6**.

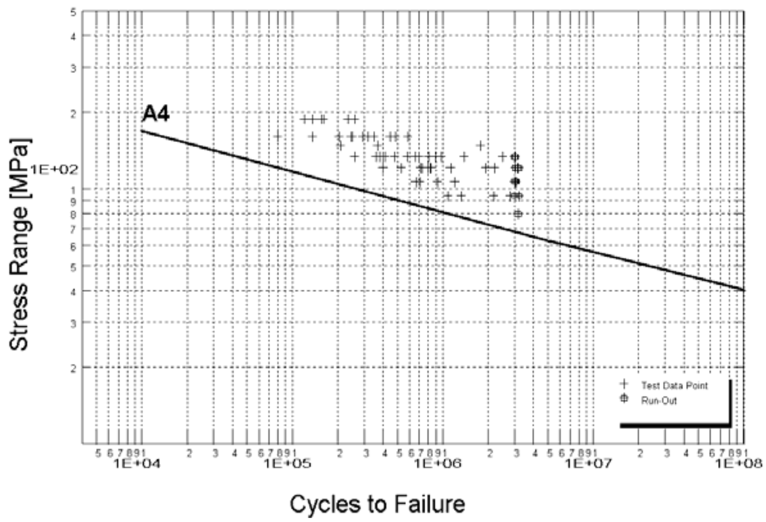

Figure 6 Base Metal 5083 (AlMg4,5Mn) Full Scale Component Data

4.1.3.1 Butt Weld, Transverse

Simple Elements – ERAAS detail classes B1 (55 N/mm²), B2 (50 N/mm²), B3 (45 N/mm²) and B4 (40 N/mm²) at 2×10^6 cycles cover various manufacturing qualities for transverse butt welds, welded from one or both sides, with overfill dressed flush or intact and are based on small specimen data [7]. The proposed design curves are maintained.

Extruded components – ERAAS detail classes B5 (45 N/mm²), B6 (40 N/mm²), B7 (35 N/mm²) and B8 (30 N/mm²) at 2×10^6 cycles cover various manufacturing qualities for transverse butt welds, welded from one or both sides, with overfill dressed flush or intact and are based on extruded shapes data [7]. The design curves of B6, B7 and B8 are maintained. Considering a re-classification of detail B5 see the following information about detail B9 for built-up components.

Built-up Components – ERAAS detail classes B9 (40 N/mm²), B10 (35 N/mm²) and B11 (30 N/mm²) at 2×10^6 cycles cover various manufacturing qualities for transverse butt welds, welded from one or both sides, with overfill dressed flush or intact and are based on built-up components data [7] (beams with longitudinal welds connecting web to flange).

Comparing the data for cases B5 and B9, extruded and built-up components with butt weld overfill ground flush, it is observed, that there respective scatter bands cannot be distinguished for all practical purposes. It is also obvious from **Figure 7** that even design curve B9 does not cover the lower life range in a satisfactory way. Here a common design line with a shallower slope is proposed as shown in **Figure 8**.

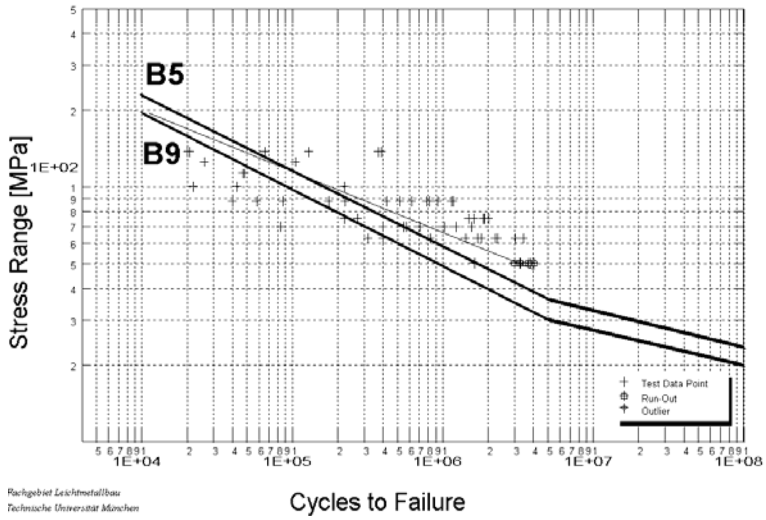

Figure 7 Transverse Butt Weld, Overfill Ground Flush, Extruded & Built-Up Components

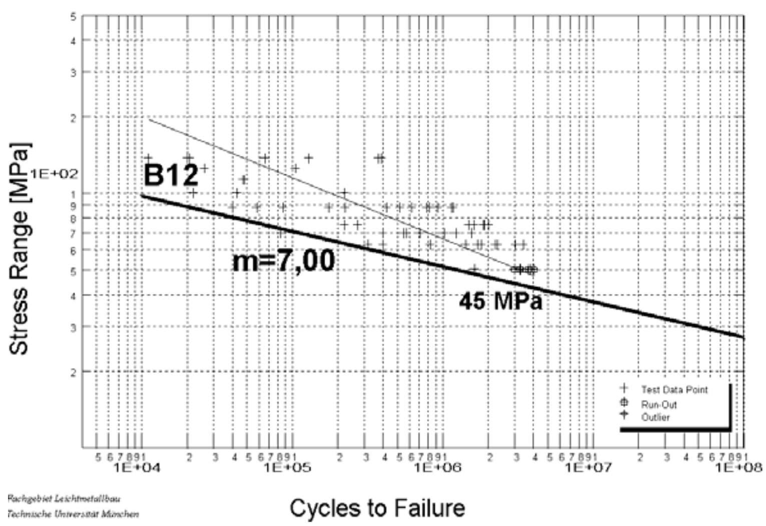

Figure 8 Proposed Design Line for Transverse Butt Weld, Overfill Ground Flush, Extruded & Built-Up Components

The respective diagrams for detail class B10 (35 N/mm²) and B11 (30 N/mm²), for welds from both sides and one side only, are given in **Figure 9** and **Figure 10**. The respective ERAAS design curves are maintained.

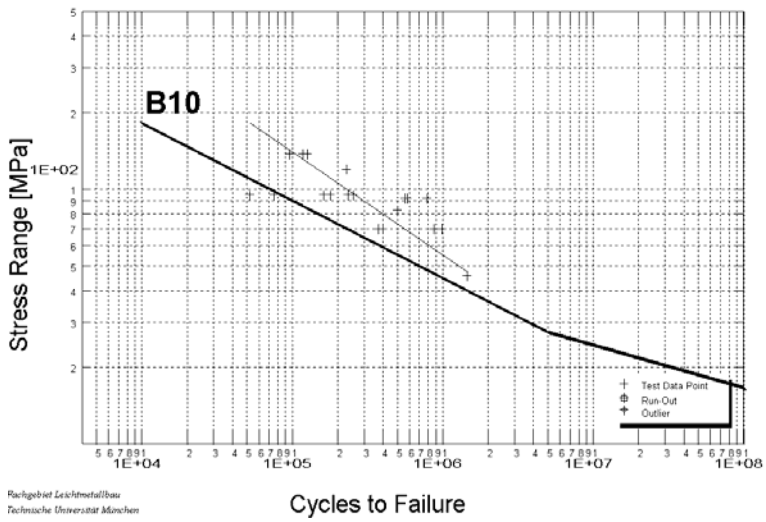

Figure 9 One-sided Transverse Butt Weld on Built-up Components

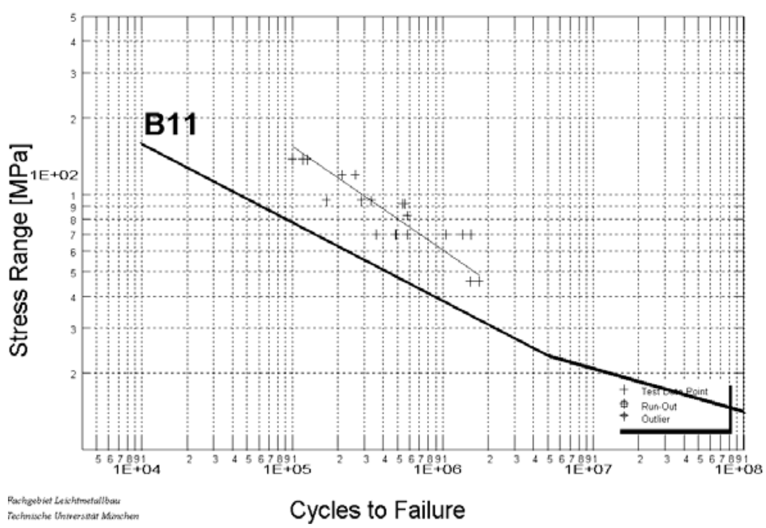

Figure 10 Two-sided Transverse Butt Weld on Built-up Components

4.1.3.2 Butt Weld, Longitudinal

ERAAS detail class C1 (60 N/mm²) (ground flush) and C2 (45 N/mm²) (as welded)

Taking into account that a minimum design value of 60 N/mm² has been adopted for base material, a design curve for detail class C1 at R=+0.5 with 60 N/mm² at 2×10^6 and a slope of m=4.32 was adopted, leading to 120 N/mm² at 1×10^5 cycles, **Figure 11**. Care must be taken to ensure a satisfactory weld root, so that fatigue cracks will not emanate from it. Appropriate backing bars may be required.

The design curve for detail C2, **Figure 12**, is defined for R=+0.5 with a strength of 45 N/mm² at 2×10^6 cycles and a slope of m=3.37

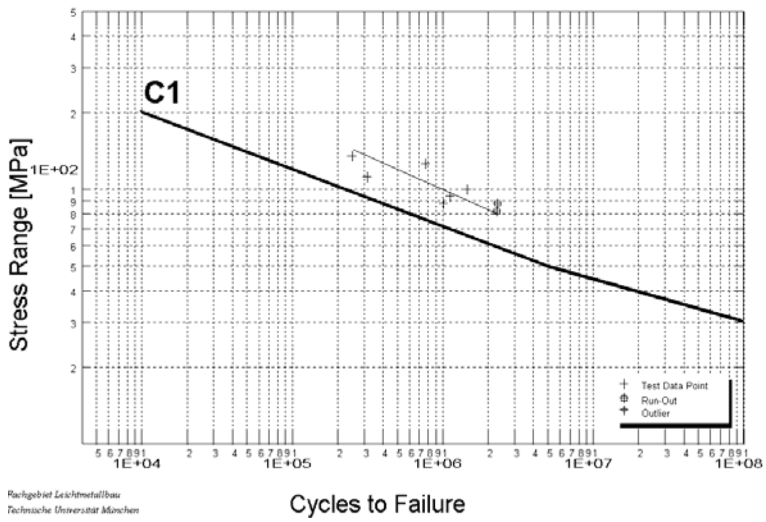

Figure 11 Longitudinal Butt Weld, Overfill Ground Flush

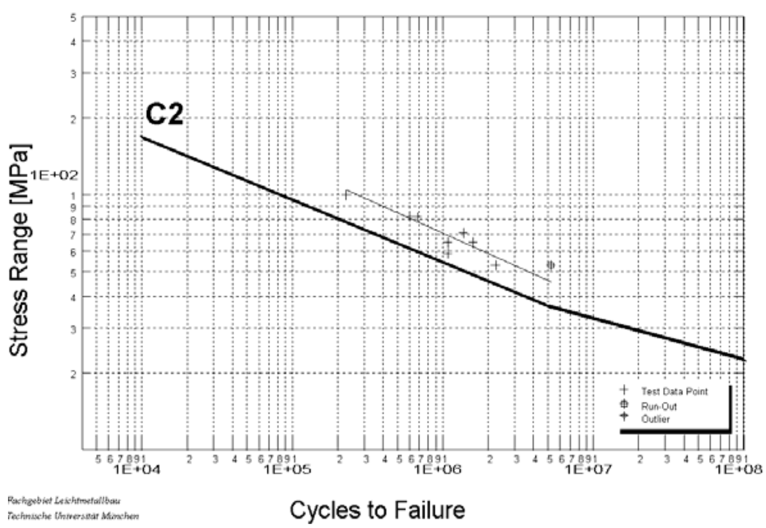

Figure 12 Longitudinal Butt Weld, As Welded

4.1.3.3 Longitudinal Fillet Welds

Detail class D1 (45 N/mm²) for longitudinal fillet weld with no stop-starts, had very few data points available. They lie in the scatter band of data points for detail class D2 (40 N/mm² - longitudinal fillet weld with stop-starts) with a tendency to higher fatigue strength values. **Figure 13** includes these data points for D1 together with data for D2. Some obvious outliers should be checked through analysis of fractured surfaces for an explanation of possible imperfections leading to their behavior. **Figure 14** shows the test results for detail class D3 (35 N/mm²) for the longitudinal intermittent fillet weld.

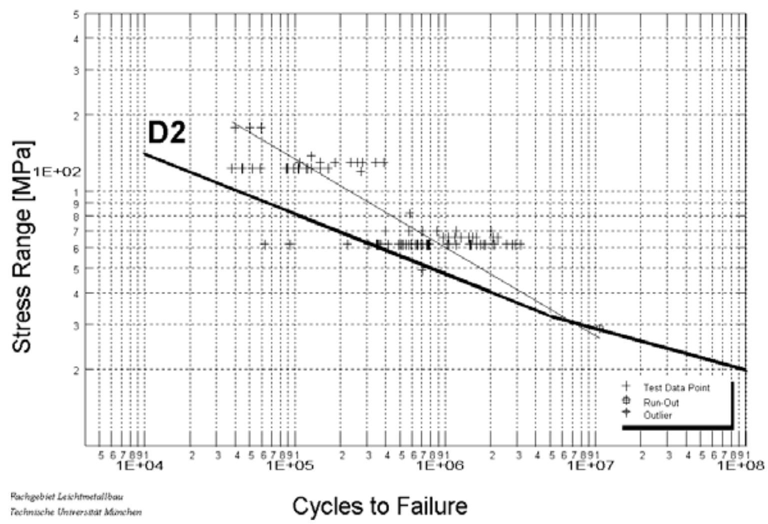

Figure 13 Longitudinal Fillet Weld with/without Stop-Starts

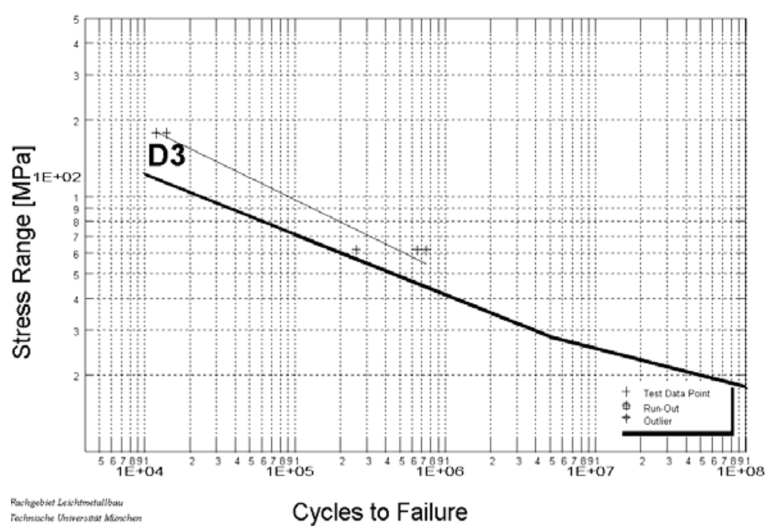

Figure 14 Intermittent Longitudinal Fillet Weld

4.1.3.4 Fillet Weld, Transverse, Non-Load-Carrying

ERAAS detail class E1 (35 N/mm²) (full and half stiffener), **Figure 15**.

Test results from Alusuisse [3] support values up to 45 N/mm². TUM beam test results of the first program [4] lie at somewhat lower fatigue strengths, but the fact that they represent failures at web stiffeners under loading points should be considered by calculating the principal stresses. TUM beam test results of the second program [6] lie in the scatter band of the previous program, especially at life ranges of 10^5 and 6×10^5 cycles. Sufficient data at high stress ranges had not been tested at that time.

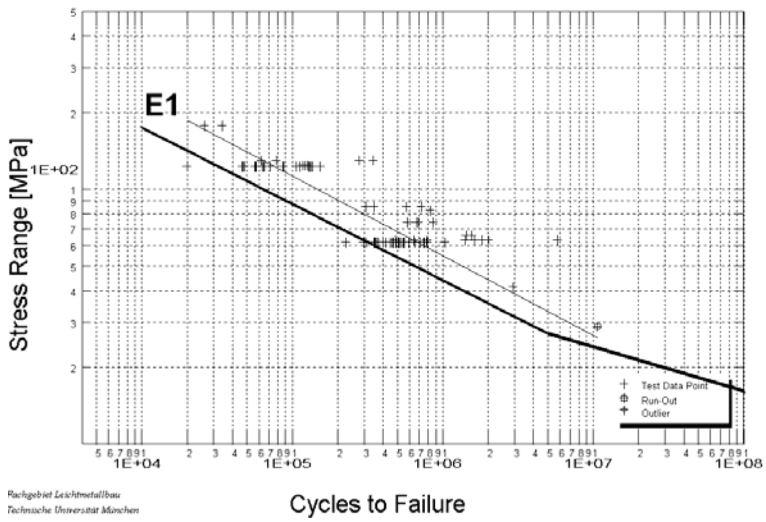

Figure 15 Fillet Weld, Transverse, Non-Load-Carrying (Web Stiffener)

Similarly, a comparison to TUM beams with a transverse vertical flange attachment from the second program [6] was undertaken. Taking into account the principal stresses and that these attachments are mounted at the outer-most part of the beam, the results fit into similar values for web stiffeners.

For TUM results an R-ratio effect appears on high stress levels ($\Delta\sigma \approx 123$ N/mm²). Longer lives could be seen for R=-1 compared to R=+0.1. A different behavior compared between full stiffeners welded on both flanges and half web stiffeners welded only on the compression flange cannot be seen. Due to the lack of information for lives above 10^6 cycles a design curve with 35 N/mm² at 2×10^6 cycles and a slope of m=3.37 was proposed, **Figure 15**.

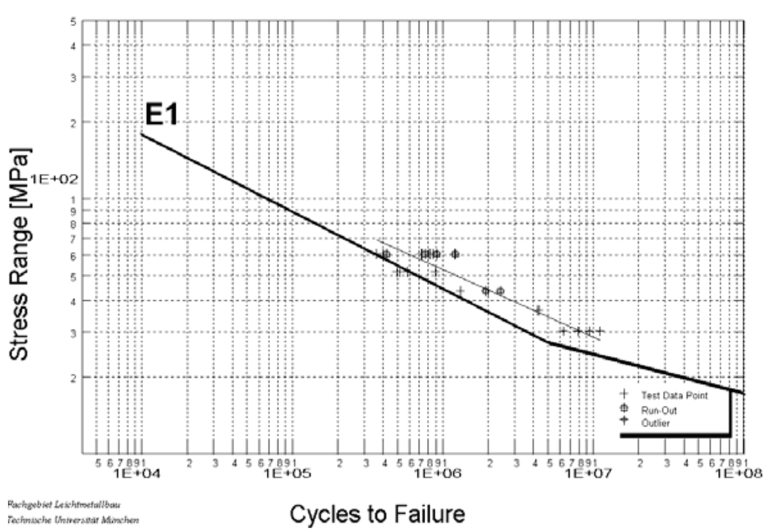

Figure 16 Transverse Fillet Weld, Non-Load-Carrying (Web Stiffener), ATLLS-Lehigh Test Results

Figure 16 shows the results from [8] which complete and verify existing TUM test data and establish the long life range fatigue behavior of the detail.

4.1.3.5 Web Attachments

ERAAS detail class E2-23 N/mm² (rectangular, circular, hollow shapes)

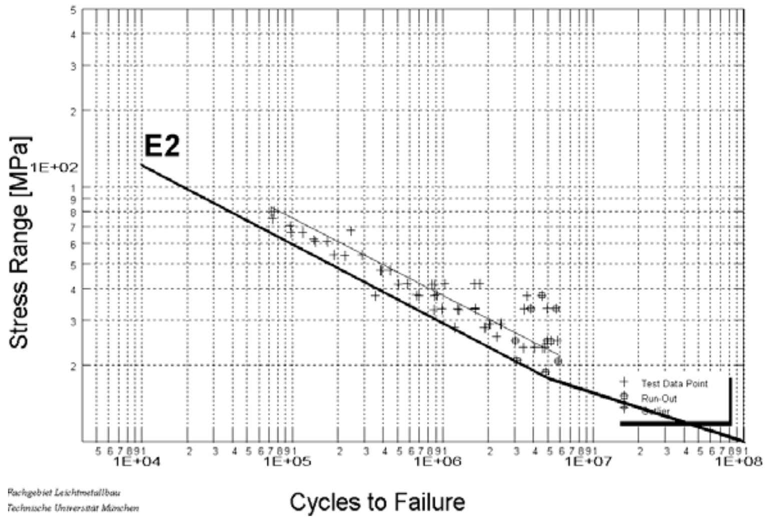

Figure 17 Web Attachments

Proposed fatigue strength values are based on ALS beam test results. These support the values at 2×10^6 cycles for both rectangular shapes and round tubes welded to the beam web. A design line with 23 N/mm² at 2×10^6 cycles and a slope of m=3.37 was adopted, **Figure 17**.

4.1.3.6 Attachment at Edge of Flange

ERAAS detail class E3 (35 N/mm²) (with transition radius, r). The design line is based on Alusuisse beam data with higher actual values especially for the higher life range, **Figure 18**. Two data points have not been taken into account in fixing the design line as they seem to be outliers.

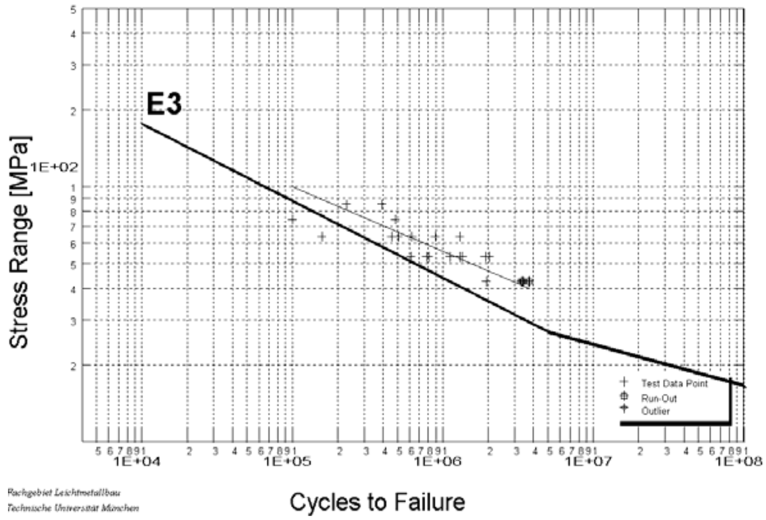

Figure 18 Attachment at Flange Edge, with transition radius, r>50 mm

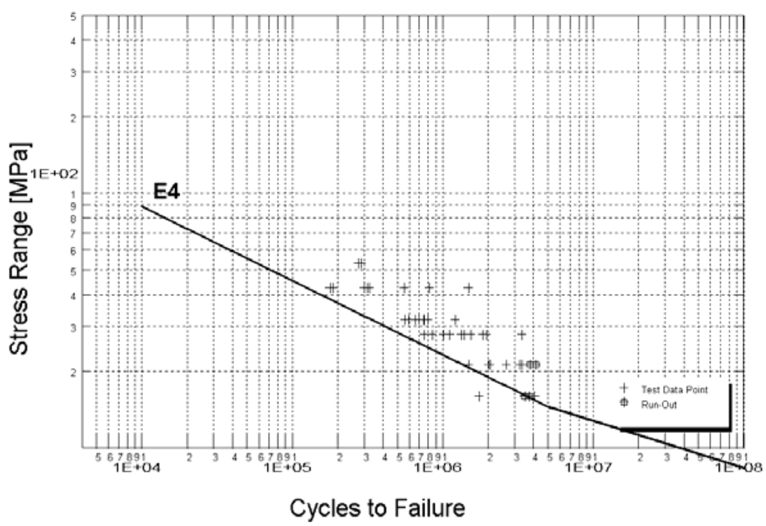

Figure 19 Attachment at Flange Edge, no transition radius

The values of the design proposal of the European Aluminum Association, EAA, have been considered and a value of 18 N/mm² at 2×10^6 cycles with a slope of m=3.37 have been adopted for E4, without any transition radius to the flange attachment, **Figure 19**.

4.1.3.7 Vertical Attachment on Flange

ERAAS detail class E5 (35 N/mm²), longitudinal on extruded beam with transition radius. No actual data available, design line assumed in accordance to attachment at flange edge, detail E4. Design curve maintained but experimental verification is desirable for extruded or built-up beams.

ERAAS detail class E6 (23 N/mm²), longitudinal on extruded beam without transition radius and ERAAS detail class E7 (18 N/mm²), longitudinal on built-up beam without transition radius. S-N diagrams indicate somewhat higher fatigue strength values for Alusuisse test results on extruded beams in comparison to TUM test results on built-up beams, **Figure 20**. Observing all data points, especially those in the region around 2×10^6 cycles resulting from Alusuisse tests with extruded beams, the proposal to treat both extruded and built-up beams with a single design curve appears to be a logical solution, **Figure 21**.

ERAAS detail class E8 (23 N/mm²), transverse on built-up beam. The design curve is based on the evaluation of a total of 22 data points distributed on three stress levels. It has been considered to propose a design line at 25 N/mm² with a slope of 4.32, **Figure 22**.

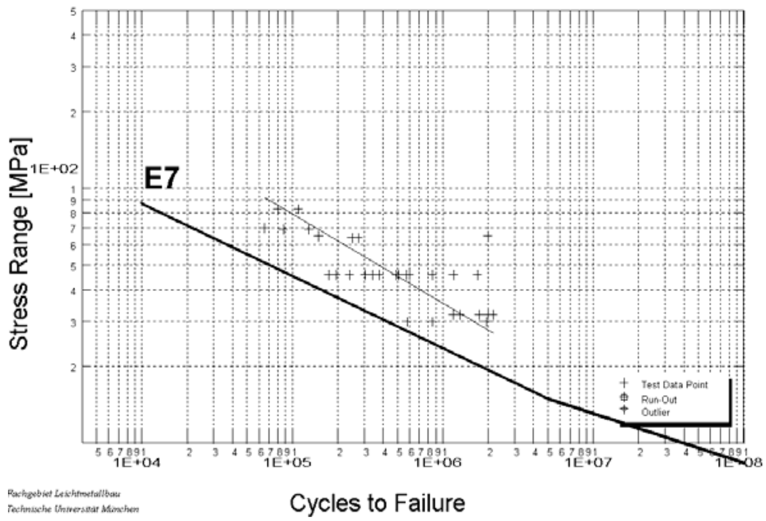

Figure 20 Vertical Attachment (Long'l) - Flange of Built-up Beam, no transition radius

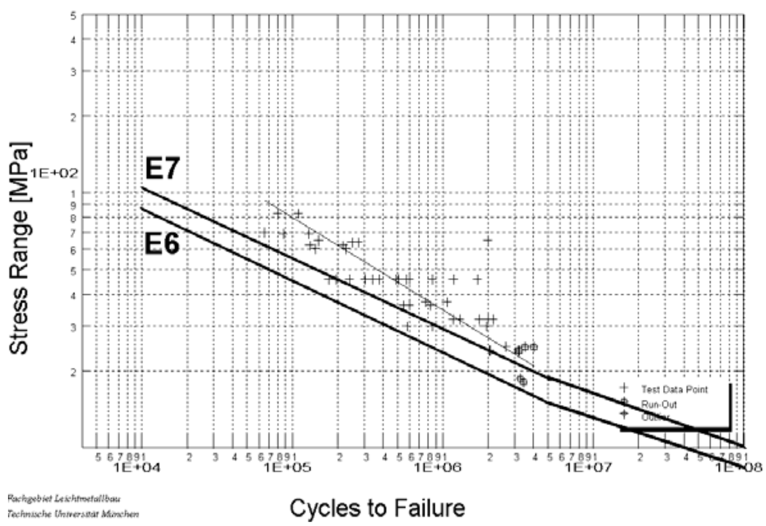

Figure 21 Vertical Attachment (Long'l) - Flange of Built-up/Extruded Beam, no transition radius

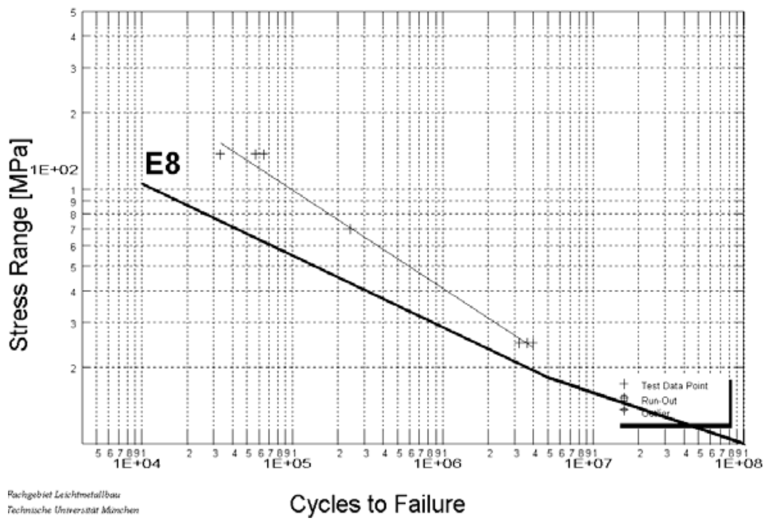

Figure 22 Transverse Attachment Vertical on Flange, Built-up Beams

4.1.3.8 Cruciform Joint

ERAAS detail class F1, transverse load-carrying fillet weld/cruciform joint (toe crack failure). The design curve is based on TUM beam tests from 1986 indicating values of 35 to 40 N/mm² for R=-1 at 2×10^6 cycles for the alloy 5083. Grouping all alloys for different R values at 30 N/mm² was proposed. This value is true for full penetration, butt-weld-like joints or for double fillet welds with failures at toe cracks. This pattern of behavior is supported in a satisfactory manner also by the TUM small specimen tests of 1991 [7]. ERAAS detail class F2, transverse load-carrying fillet weld/cruciform joint (throat crack failure). The design curve is based on Alusuisse data with small specimens supports 35 N/mm² at 2×10^6 cycles for R=0. There are also similar TUM beam test results from 1986. Other test results from TUM small specimens on cruciform joints from 1991 give a value of 28 N/mm² for R=+0.1. For design purposes a value of 25 N/mm² at 2×10^6 cycles with a slope of 4.32 was defined, **Figure 23**.

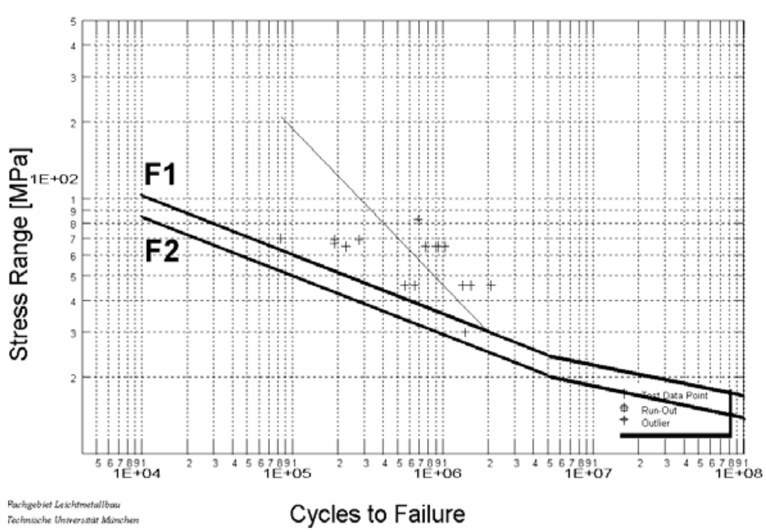

Figure 23 Cruciform Joint, Built-up Beams

4.1.3.9 Cover Plate

ERAAS detail class F3, transverse load-carrying fillet weld/cover plate. Analysis of both TUM beam test results on the 7020 alloy, taking into account reduction factors for fatigue strength values at R=+0.6, indicate a value of 20 N/mm² at 2×10^6 cycles, being adopted for design purposes with a slope of m=4.32, **Figure 24**.

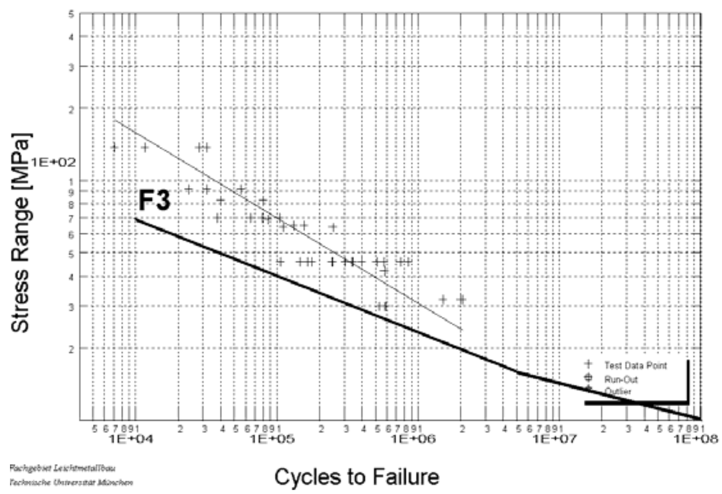

Figure 24 Cover plate, Built-up Beam, TUM Test Results

Further data were provided by Fisher/Menzemer, Lehigh University [8], **Figure 25**. Data points were generated up to 1×10^7 cycles, verifying and completing the existing TUM results and establishing the fatigue behavior of this detail, especially for the long life range, **Figure 26**.

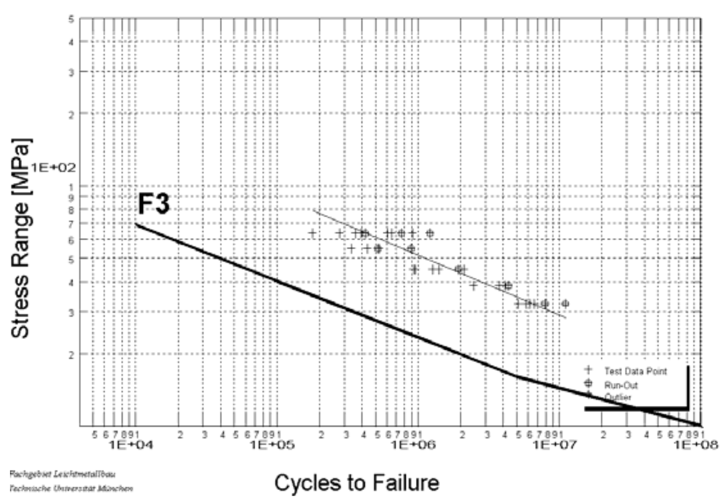

Figure 25 Cover plate, Built-up Beam, Lehigh Test Results

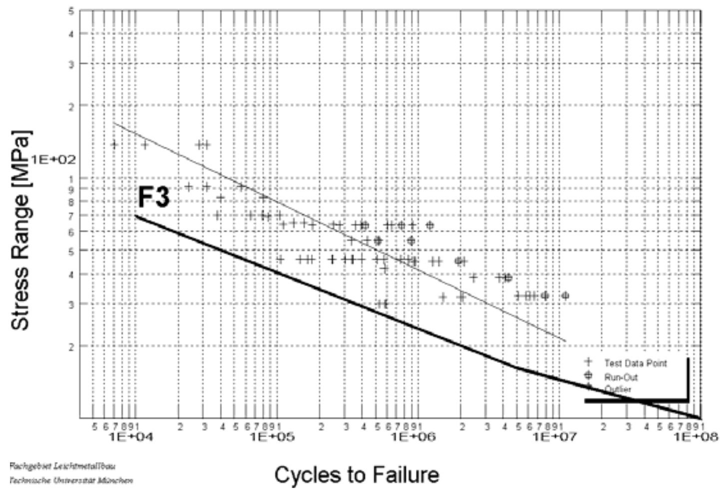

Figure 26 Cover plate, Built-up Beam, Lehigh and TUM Test Results

5. COMPARISON BETWEEN ERAAS AND OTHER CODES

This section of the report presents a brief comparison of the data in ERAAS and various other aluminum codes. Of particular note are:

- Aluminum Association Specification for Aluminum Structures
- British Standard BS 8118 Structural use of Aluminum
- Association of American Railroads
- Ontario Highway Bridge Code

Discussion is also presented for various steel codes to help compare the behavior of steel and aluminum in the fatigue environment.

5.1 Comparison to Aluminum Codes

Several Aluminum Codes [9, 10, 11, 12, 13] were compared to the ERAAS-Fatigue document. The following diagrams in **Figure 27** show the design values at $2{\times}10^6$ cycles. This comparison indicates the historical development of respective recommendations, but, except for the recent edition of the British document BS 8118-1992, it is pointed out that ERAAS has been based on the evaluation of well documented data on full-size components after a homogeneous statistical-regression evaluation.

The comparison between the design values of ERAAS and BS 8118, for instance at $2{\times}10^6$ cycles, for the different structural details in both codes is demonstrated in **Figure 28**.

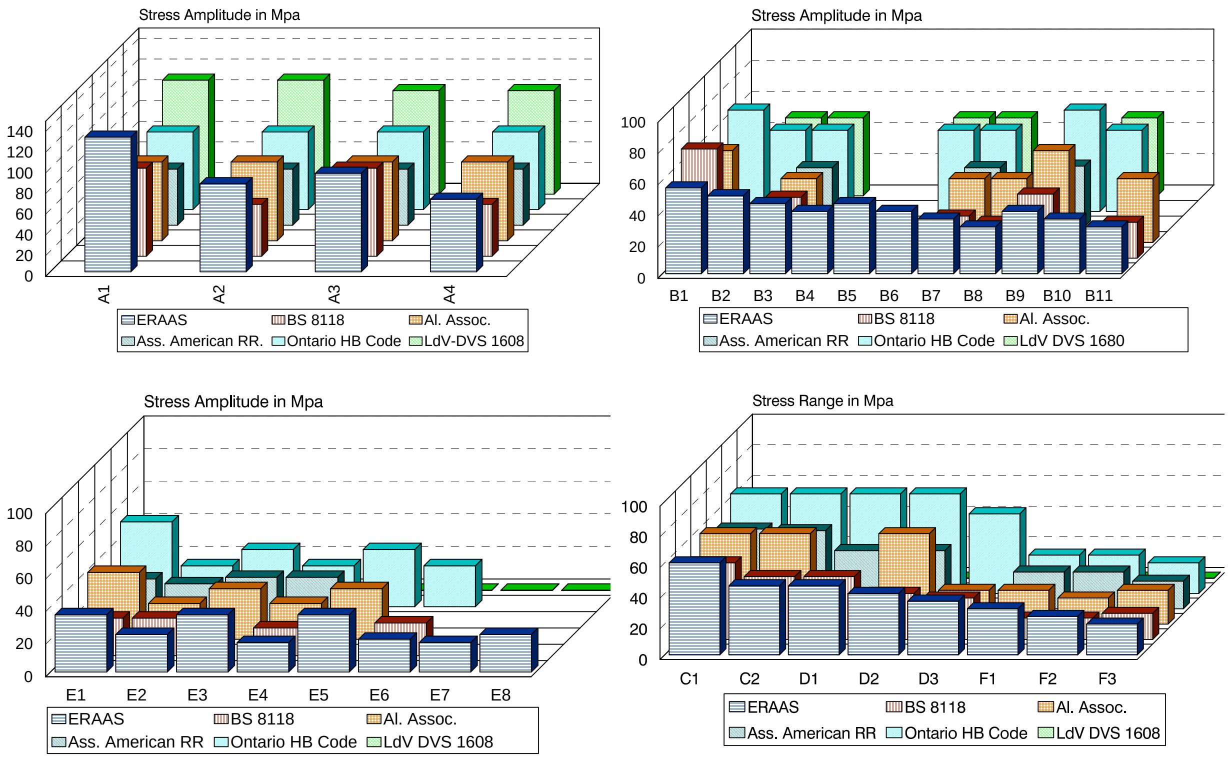

Figure 27 Comparison of ERAAS Fatigue to Various Aluminum Codes

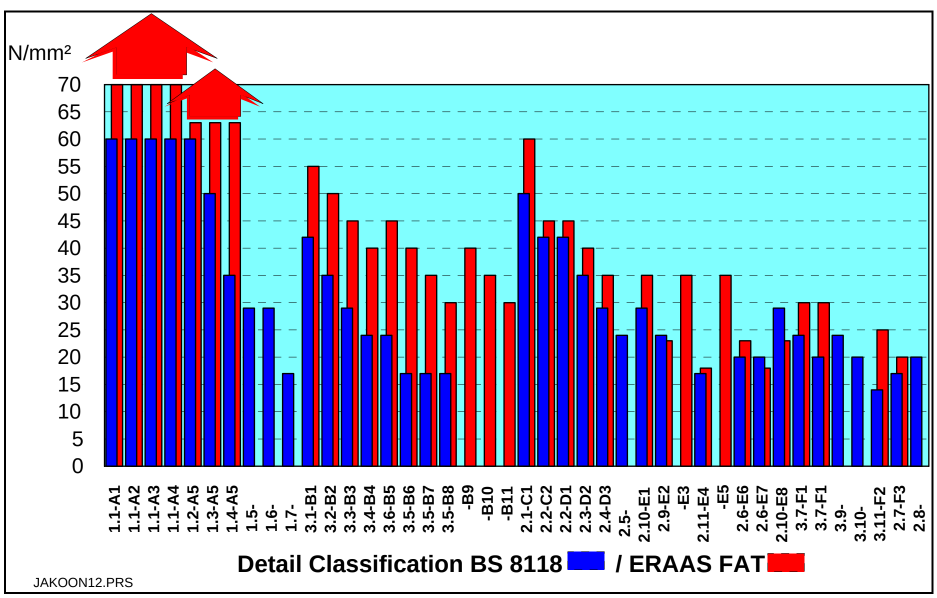

Figure 28 Comparison of ERAAS Fatigue to BS 8118

5.2 Comparison of ERAAS Fatigue 1992 & Aluminum Association Design Manual

The information in **Figure 29** and **Figure 30** focuses on the comparison between ERAAS and the Aluminum Association for fatigue life of detail classes as 2 x 10^6 cycles. **Table 3** provides the description of the various detail classes between the two standards.

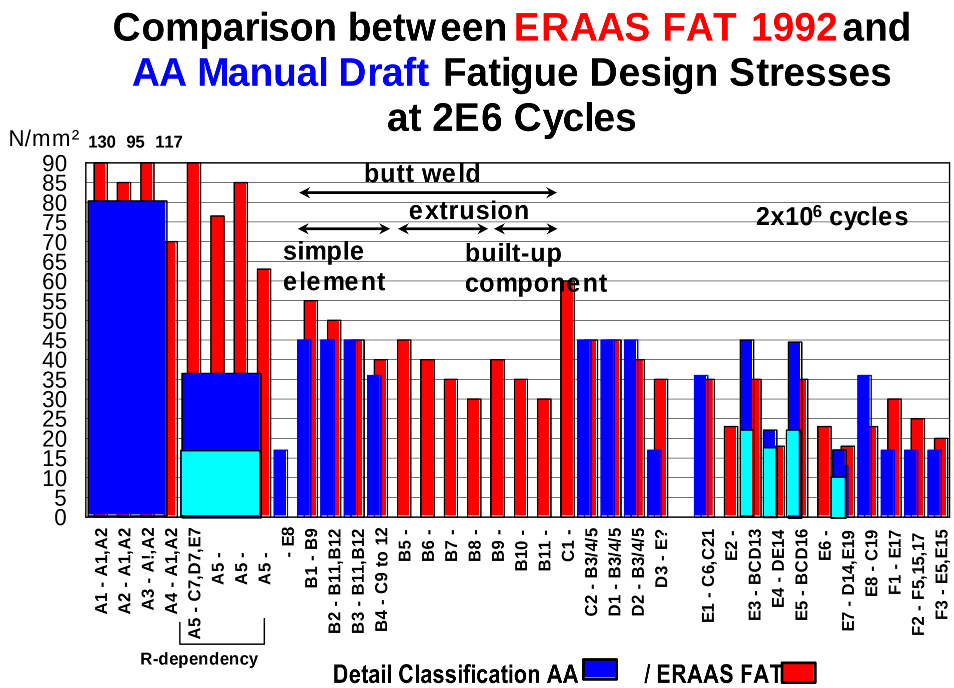

Figure 29 Comparison of ERAAS & Aluminum Association Fatigue @ 2x10^6 Cycles

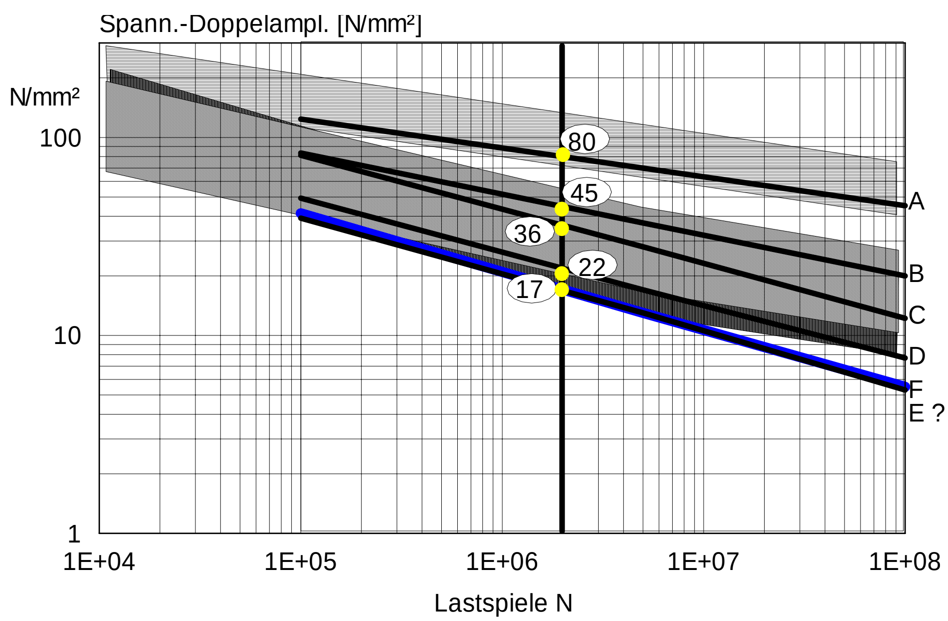

Figure 30 Comparison of ERAAS & Aluminum Association S/N Curves

Table 3 Correlation between ERAAS and Aluminum Association Details

Detail		ERAAS	AA
Base Metal 5000/6000	Elements	A3	A1,A2
	Components	A4	A3,A4
Notches, Holes		A5	CDE7,E8
Butt Weld Transverse Simple Element	flush	B1	B9
	> 150°	B2	B11/12
	> 130°	B3	B11/12 ?
	backing	B4	C9 to 12
Butt Weld Transverse Extruded	flush	B5	
	> 150°	B6	
	> 130°	B7	
		B8	
Butt Weld Transverse Built-Up	flush	B9	
	> 150°	B10	
		B11	
Butt Weld Longitudinal	flush	C1	
	> 150°	C2	B3/4/5
Fillet Weld Longitudinal	no interruptions	D1	B3/4/5
	stop-starts	D2	B3/4/5 ?
	intermittent	D3	E?
Web Stiffener	fillet transverse	E1	C6/21
Web Attachment		E2	
Attachment at Flange Edge	transition ∅	E3	BCD13
	no transition ∅	E4	DE14
Attachment on Flange - Vertical & Longitudinal	extruded transition ∅	E5	BCD16
	extruded no transition ∅	E6	
	built-up no transition ∅	E7	E19
Attachment on Flange - Vertical Transverse	built-up	E8	C19
Fillet-Transverse Cruciform	toe crack	F1	E17
	throat crack	F2	F5/15/18
Cover plate		F3	E5/15/20

5.3 Comparison of ERAAS to Various Steel Codes

Several Steel Codes [14, 15, 16, 17] were also compared to the ERAAS Fatigue document. The diagrams in **Figure 31** show the comparison of design values at 2×10^6 cycles.

Steel codes have been based entirely on small specimen data. The Eurocode 3: Steel Design presents a design concept based on stress range $\Delta\sigma$ with no R-ratio dependency. All other cited steel codes give maximum stress amplitude maxσ_a value with an R-ratio dependency. These values had to be transformed accordingly for an R-ratio of R=+0.5 (as given in ERAAS Fatigue for the basic design curve).

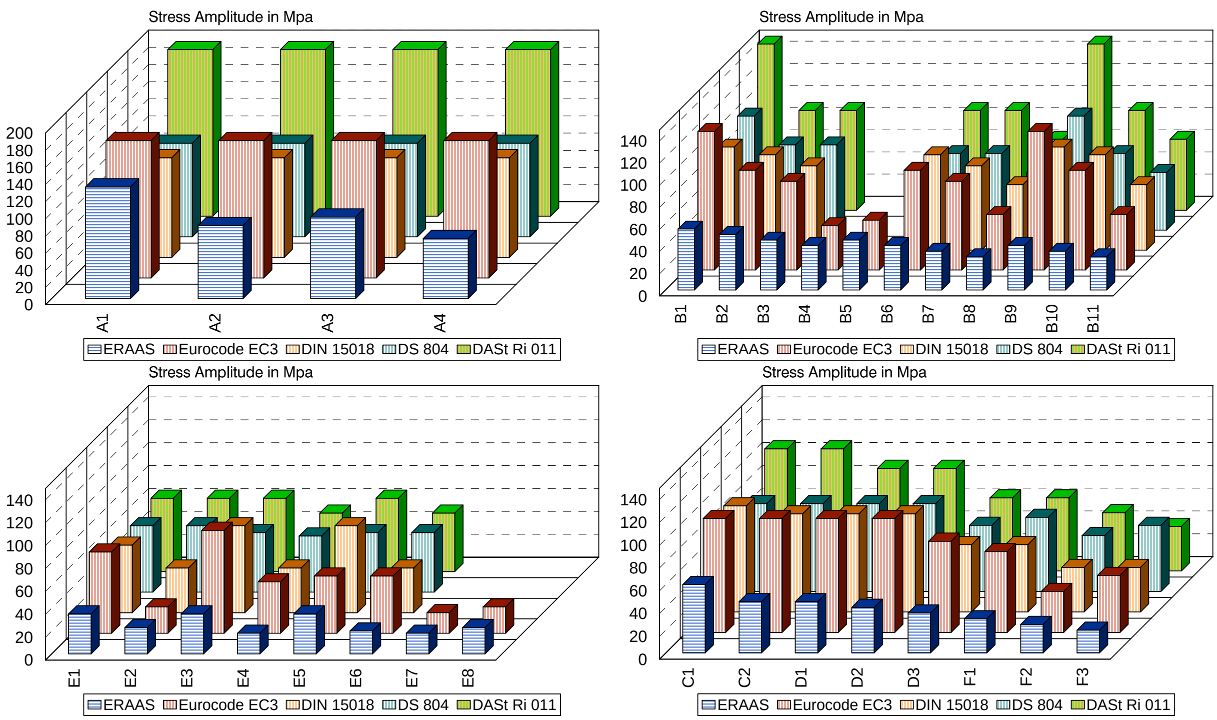

Figure 31 Comparison of ERAAS Fatigue to Various Steel Codes

It is interesting to observe the ratio between design values for aluminum and steel as given in different documents. A ratio of 3:1 (based on the ratio of the modulus of elasticity of the two materials) between steel and aluminum has been previously stated. A direct comparison of fatigue design values at 2×10^6 cycles between the Eurocode 3: Steel Design and ERAAS Fatigue (Aluminum), **Figure 32**, shows that for a majority of structural details a value at or below 2.3:1 appears. Only in a single case is a value above 3:1 observed.

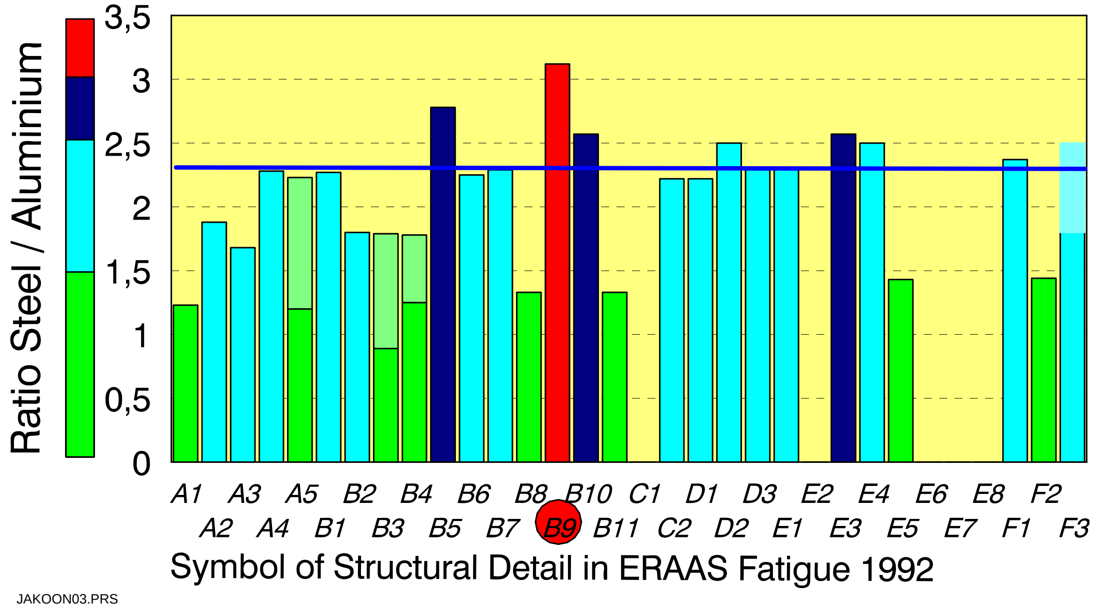

Figure 32 Ratio of Fatigue Design Values (2×10^6 Cycles)-ERAAS (Al) & Eurocode 3 (Steel)

6. TABLES FOR DETAIL CATEGORIES AFTER ERAAS FATIGUE 1992 DECISIONS LEADING TO FATIGUE STRENGTH DESIGN VALUES

The tables in this section of the report present a brief summary, discussion and justification for using the fatigue strength design values relative to ERAAS.

Table 4 Butt Weld Transverse - Simple Specimen & Extruded Component (ERAAS B1-B8)

Detail	ERAAS	Further Data	Final Remarks
B1 - 55 N/mm² Butt weld, transverse overfill dressed flush from both sides *simple element*	TUM small specimens 1991 & ALS small specimens. See TUM / A-L study 1991 Part 6, Doc. A1 and Doc. Z61 to Z92		ERAAS design curve is maintained.
B2 - 50 N/mm² Butt weld, transverse overfill >150° from both sides *simple element*	Conceived as an interpolation between B1 and B3, based mainly on ALS small specimens.		ERAAS design curve is maintained.
B3 - 45 N/mm² Butt weld, transverse overfill > 130° from one or both sides *simple element*	Based on ALS small specimens. See TUM / A-L study 1991 Parts 2, 3 & 6, Doc. Z61 to Z92 and Doc. M34 to M40.		ERAAS design curve is maintained.
B4 - 40 N/mm² Butt weld, transverse from one side only on permanent backing bar *simple element*	TUM small specimens. See TUM / A-L study 1991 Part 6, Doc. A2-A3-A4.	<u>TNO small specimens</u> V-weld from one side, 6 + 12 mm. EU 269 1994, AlDaBa data set no. T0004.0 and T0005.0. <u>INEGI small specimen</u> 12 + 24 mm. EU 269 1994, AlDaBa data set no. T0006.0 and T0007.0. *compare to jakoonI-08.prs*	ERAAS design curve is maintained although data on 24 mm falls on or slightly below line. All TNO 6 & 12 mm welds as well all INEGI 12 mm welds may be pooled & belong to the same scatter band which allows sufficient safety margin to design curve. INEGI 24 mm welds are significantly lower than all other. This may indicate a different type of imperfection.
B5 - 45 N/mm² Butt weld, transverse overfill dressed flush from both sides *extruded components*	ALS beams, Doc. M44 to M46 or Doc. A7-A8. TUM / A-L study 1991, Parts 2 and 6.		New ERAAS design curve proposed - with designation B12 - 45 N/mm² & m = 7.00.
B6 - 40 N/mm² Butt weld, transverse overfill > 150°	ALS beams (Cosandey short beams). TUM / A-L study 1991,		ERAAS design curve is maintained.

from one or both sides *extruded components*	Parts 2 and 6, Doc. M31 to M33.		
B7 - 35 N/mm² Butt weld, transverse overfill > 130° from one or both sides *extruded components*	ALS beams. TUM / A-L study 1991, Parts 2 and 6, Doc. M29-M30.		ERAAS design curve is maintained.
B8 - 30 N/mm² from one side only without perman. backing *extruded components*	ALS data sets no. 7184, 7186, 7188 in TUM analysis of EAA-COST 506 project 1989.		ERAAS design curve is maintained.

Table 5 Butt Weld Transverse – Built up Components (ERAAS B9 to B11)

Detail	ERAAS	Further Data	Final Remarks
B9 - 40 N/mm² Butt weld, transverse overfill dressed flush from both sides *built-up components*	TUM beams 1991. TUM / A-L study 1991, Parts 2 and 6, Doc. M41-M42 or A5-A6.		New ERAAS design curve proposed - with designation B12 - 45 N/mm² & m = 7.00.
B10 - 35 N/mm² Butt weld, transverse overfill > 150° from both sides *built-up components*	TUM beams 1986. Data sets no. B8001, B8002, B8003 and B8028, B8029, B8030. TUM / A-L Study 1991, Parts 2 and 6, Doc. M24 + M27.	TNO beam data. EU 269 1994 program, AlDaBa data set no. T0008.0. Only 3 data points generated fitting into the general pattern of existing data. Exact description of weld quality not available, detail classification taken as mentioned in report. *compare to jakoonI-07.prs*	ERAAS design curve is maintained.
B11 - 30 N/mm² Butt weld, transverse from one side only without perman. backing *built-up components*	TUM beams. Data sets no. B8031, B8032, B8033, B8034, B8035, B8036, B8037. TUM / A-L study 1991, Parts 2 and 6, Doc. M25 + M26.		ERAAS design curve is maintained.

Table 6 Butt Weld – Longitudinal (ERAAS C1 & C2)

Detail	ERAAS	Further Data	Final Remarks
C1 - 60 N/mm² Butt weld, *longitudinal* overfill ground flush	Design curve based on ALS beam data (Cosandey) taking into account as an upper limit the fact that a minimum design value of 60 N/mm² has been fixed for base material. TUM / A-L study 1991, Parts 2 and 5, Doc. M47b. The above are also in accordance to values proposed in the EAA-COST 506, March 1989 document.		ERAAS design curve is maintained.
C2 - 45 N/mm² Butt weld, *longitudinal* overfill > 130°	Design curve values based on ALS beam data (Cosandey) as proposed in TUM / A-L study 1991, Parts 2 and 5, Doc. M47b. Also in accordance with values proposed in the EAA-COST 506, March 1989 document.		ERAAS design curve is maintained.

Table 7 Fillet Weld – Longitudinal (ERAAS D1, D2 & D3)

Detail	ERAAS	Further Data	Final Remarks
D1 - 45 N/mm² Fillet weld, longitudinal no interruptions, no stop-start positions, no tack welds	Design curve based on TUM beams 1991.		ERAAS design curve is maintained
D2 - 40 N/mm² Fillet weld, longitudinal with stop-start positions or tack welds	Design curve based on TUM beams 1986 1991.		ERAAS design curve is maintained, although a few data points fall below it. These should be checked as outliers.
D3 - 35 N/mm² Fillet weld, longitudinal intermittent	Design curve based on TUM beams 1991.		ERAAS design curve is maintained.

Table 8 Fillet Weld – Transverse (non-load carrying), Web Stiffeners & Attachments (ERAAS Design Curves E1 & E2)

Detail	ERAAS	Further Data	Final remark
E1 - 35 N/mm² Fillet weld, transverse, *web stiffener* extruded / built-up beam	ALS Beams TUM/A-L Doc M.48 and M.49 support values up to 45 N/mm² for $2*10^6$, esp. if the raise of 10% for stresses at inner flange side and a levelling-off of the S-N curve is assumed. ALS small specimens TUM/A-L Doc Z.105 and Z.114 give min value of 63 N/mm² at R=0 resulting in 50 N/mm² at R=+0.5. TUM Beams 1986 7020 & 5083 lie in the scatter band at tested life range between 10^5 to $5*10^5$ TUM beams 1991 somewhat lower stresses than ALS beams, but fact should be considered that web stiffeners were loaded. Beam data with transverse flange attachment fits in at 10^5 (accounting for nominal stress at crack site), but no more at longer lives. Data from both TUM programs show R-dependency, i.e. longer lives at R=-1, for higher stress levels.	Fisher/Menzemer Lehigh beams 1993 Results complete and verify existing TUM test data and establish especially for the long life range the fatigue behavior of the detail.	Due to scant data at longer lives a value of 35 N/mm² was adopted. No significant difference in behavior between full stiffeners welded on both flanges and half stiffeners welded only on the compression (due to external loading) flange has been observed. Lehigh data verifies behavior in the long life range. Two data points have not been taken into account in fixing the design line as they seem to be outliers (also in the sense of regression evaluation) and their fracture surfaces should be analyzed for any imperfections before final classification. The ERAAS design curve is maintained.
E2 - 23 N/mm² Web attachments, round or rectangular shapes	Based on ALS beam tests supporting values both for rectangular shapes and round tubes.		ERAAS design curve is maintained.

Table 9 Attachment at Flange Edge (ERAAS E3 &E4)

Detail	ERAAS	Further Data	Final Remarks
E3 - 35 N/mm² Attachment at flange edge with transition radius R>50 mm	Based on ALS beam data. A best-fit proposal according to Design Proposal EAA as of 26.07.89 gave values up to 41 N/mm² at $2*10^6$. A final curve near to the COST 506-EAA study was adopted.		ERAAS design curve is maintained. Two data points have not been taken into account in fixing the design line as they seem to be outliers (also in the sense of regression evaluation) and their fracture surfaces should be analyzed for any imperfections before final classification.
E4 - 18 N/mm² Attachment at flange edge no transition radius	Based on ALS beam data. Best-fit proposal after Design Proposal EAA as of 26.07.89 was reconsidered and values nearer the COST 506-EAA analysis adopted.		There seems to be a certain problem at the lowest tested level with data points on the assumed design curve E4, one point being also lower but another point on the same level and at same lives appearing as a run-out. A fracture surface analysis could provide an answer for unusual imperfections. Either careful design and manufacturing of this detail should be required or the design curve has to be **lowered to approx. 16 N/mm².** Such a detail should not be allowed. It is bad design and the significant enhancement in strength is demonstrated by detail E3.

Table 10 Vertical Attachment on Flange – Longitudinal (ERAAS E5, E6 &E7)

Detail	ERAAS	Further Data	Final remark
E5 - 35 N/mm² Attachment on flange, vertical, *longitudinal* transition radius ≥ 50 mm extruded beam	No data available. Design curve in accordance to attachment at flange edge, at first for extruded beam only.		ERAAS design curve maintained. Experimental verification desirable, for extruded and/or built-up beam.
E6 - 23 N/mm² Attachment on flange, vertical, *longitudinal* no transition radius extruded beam	ALS beam test results with slope m=3.00 (Doc Z-104 A-L/TUM)	<u>EPFLausanne/ Beam Data INALCO´92</u> all constant amplitude data with run-outs at 10^8 (including variable ampl. data up to $5*10^6$) falls within scatter band of data of Doc Z-104 - variable amplitude data from $5*10^6$ to $5*10^7$ though, falling on or slightly below ERAAS E6 line. <u>Maddox / INALCO ´82</u> small specimen data Values slightly below ERAAS curve at $2*10^6$ <u>Kosteas / VA H5 1971</u> 6 mm 7020 small specimen data at P_S=90% (slope 3.60) approx. 3-fold safety margin to ERAAS curve at lower and medium life range	ERAAS design curve E6 has to be corrected by assuming (3 options) Either: new E6 - 20.0 N/mm² with slope m=3.37 or E6=F3 - 20.0 N/mm² with slope m=4.32 or E6=E7 - 18.0 N/mm² and slope m=3.37 The latter being proposed, abandoning the original distinction between extruded and built-up beams. Classification on the basis of nominal stresses calculated at crack site, i.e. on outer flange side, but without taking into account geometrical effect of attachment on cross-section values (moment of inertia, relocation of center of gravity). The respective stress reduction would be in the order of 50% in the case of TUM beams, or 80% in the case of EPFL beams.
E7 - 18 N/mm² Attachment on flange, vertical, *longitudinal* no transition radius built-up beam	TUM beam test results with slope m=3.27.		ERAAS design curve maintained

Table 11 Vertical Attachment on Flange – Transverse (ERAAS E8)

Detail	ERAAS	Further Data	Final remark
E8 - 23 N/mm² Attachment on flange, vertical, *transverse* built-up beam	TUM Beams 1991	TNO/INEGI 1994 small specs. 12 mm, R=+0.1 significantly above ERAAS curve beams, only 3 data points, falling in scatter band of small specs INEGI results higher than TNO results verify former TUM beam tests, with somewhat shallower slope though (3 points only!) Maddox INALCO ´82 small specimens Maddox &Webber 1987 effect of high residual stresses even in small specimens Kosteas 1971 small specimens, all data significantly high strength values, espec. for 6 mm *compare to jakoonI-01.prs*	ERAAS design curve may be maintained. One could even think of proposing a design line at 25 N/mm² with a slope of 4.32

Table 12 Fillet Weld–Transverse (load carrying) Cruciform, Cover plate (ERAAS F2, F3)

Detail	ERAAS	Further Data	Final Remarks
F1 - 30 N/mm² Fillet weld, transverse load-carrying, *cruciform* toe-crack failure	TUM beams 1986 - 35 to 40 N/mm² for R= -1 (5083) at $2*10^6$. Group alloys for various R-ratios indicate values at 30 N/mm², true for full penetration butt-weld-joints or double fillet welds with failures at toe cracks. These results supported by the TUM small specimen, 1991. TUM / A-L study 1991, Parts 5 and 6.		ERAAS design curve is maintained.
F2 - 25 N/mm² Fillet weld, transverse load-carrying, *cruciform* throat-crack failure	ALS data on small specimens support values of 35 N/mm² for R=0 at $2*10^6$. TUM beams 1986. See INALCO ´95 paper by Jaccard/Kosteas/Ondra. TUM small specimen data supports values of 28 N/mm² for R=+0.1 at $2*10^6$. TUM / A-L study 1991, Parts 5 and 6.	TNO small specimens 6+12 mm, constant ampl., AlDaBa data set no. T0012.0 & Z0013.0. TNO/Dutch Rail small specimens 6+12+24 mm, variable ampl., AlDaBa data set nos. T0016.0, T0017.0 and T0018.0. INEGI small specimens 12+24 mm, constant ampl., AlDaBa data set nos. T0014.0 and T0015.0 TNO beams 6+12+24 mm, constant ampl., AlDaBa data set nos. T0019.0, T0020.0 and T0021.0. All EU 269 1994 reports. Kosteas small specs 1971 significantly higher than results for beam details.	ERAAS design curve is maintained. According to the report the characteristic classification is under detail F2 there seem to be no problems in relation to the existing ERAAS design curve values.
F3 - 20 N/mm² Fillet weld, transverse load-carrying *cover plate*	TUM beams 1986 and TUM beams 1991	Fisher/Menzemer, Lehigh 1993 Results complete and verify TUM results and establish the fatigue behavior for long life.	ERAAS design curve is maintained.

7. COMPARISON OF FATIGUE STRENGTH VALUES FOR STRUCTURAL DETAILS

The information presented below addresses comparative data from ERAAS FAT, Eurocode 9 ENV 1999-2 (predecessor of current document prEN 1999-1-3) and assumptions for the International Institute of Welding, IIW, fatigue design rules.

Table 13 Comparison of Design Curve Fatigue Strength Values for Transverse Butt Welds to Experimental Data (at 2*10^6 cycles)

Detail	$\Delta\sigma_C$-m_1	Detail	$\Delta\sigma_C$-m_1	$\Delta\sigma_C$-m_1	Detail	$\Delta\sigma_C$-m_1	$\Delta\sigma_C$-m_1	See Fig.*
ERAAS 1992		Eurocode 9			IIW Recomm. 1996			
Bead ground off, welded from both sides								
B1	55-7	3.1	55-6	44-5	211	50-3		
B5/12	45-7	3.1	44-5	28-4				**a)**
B9/12	45-7							
Bead angle >150°, welded from both sides								
B2	50-4.32	3.2	39-4	35-4	212	40-3		
B6*	35-3.37	3.2	35-4	28-4				**b)**
B10	35-3.37							
Bead >130°, welded from (one or) both sides								
B3	45-4.32	3.2	29-3.2	18-3.2	212	40-3		
					213		32-3	**c)**
B7	35-3.37							
Welded from one side only, with or without permanent backing								
B4	40-4.32	3.3	35-4	25-3.2	215	25-3		
					225		22-3	
					216	28-3		**d)**
B8	30-3.37	3.4	29-3.	18-3.2				
B11	30-3.37							
Welded from one side only, lack of penetration (LOP), root defect								
		3.5	14-3.2		(216)	18-3		

ERAAS: bold lines / *EC9: fine lines* / *IIW: dash-dot lines*

* Please note that all Figures in this section of the report are referenced by the letters "a" through "e", with various letters used more than once. Each figure is related to the specific table that cites the reference and the letters can be found in the lower left hand corner of each figure.

ERAAS / IIW Doc. XIII-1588-95 Transverse Butt, Overfill Dressed Flush Both Sides
B1 (55-7) Simple Element or B5/12 (45-7) Extrusion and B9/12 (45-7) Built-Up Component
EC 9 Welded Butt Joint Ground Flush Cat. 3.1 (55-6) or (44-5) for flats and solids
(44-5) or (28-4) for open shapes
not applicable for hollow sections
IIW Recom 96 Det. No. 211 (50-3,0) Transverse Butt (X or V) Ground Flush

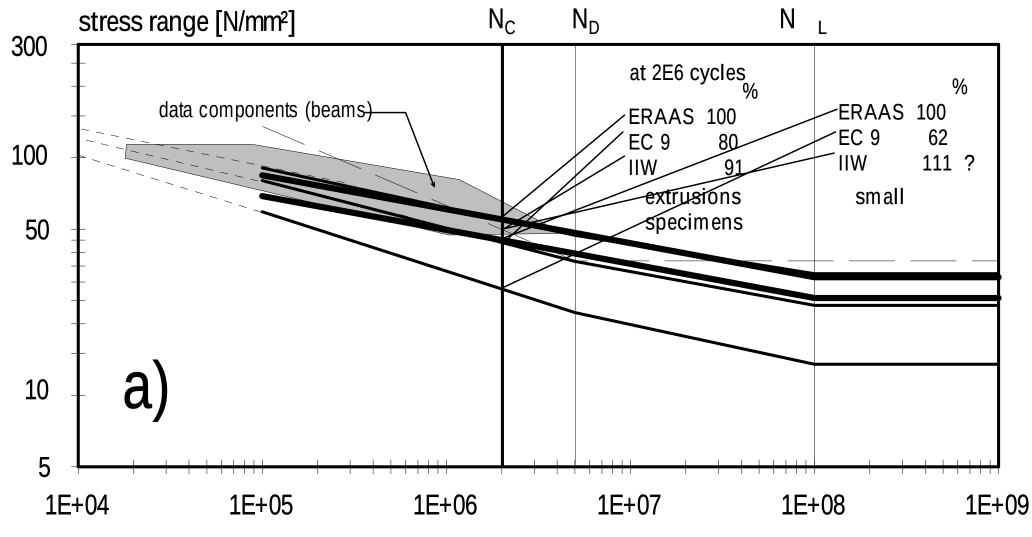

ms.dos_6/(eigene)
daten/praes/inalco98/inalco.pr4-no11

FINAL DRAFT prENV 1999-2 April 1997

ERAAS / IIW Doc. XIII-1588-95 Transverse Butt Overfill>150°, Both Sides
Simple Element B2 (50-4,32);Extruded Component B6 (35-3,37);
Built-Up Component B10 (35-3,37)
EC 9 Welded Butt Joint Double Sided Cat. 3.2 (39-4) or (35-4) for flats and solids
(35-4) or (28-4) for open shapes
not applicable for hollow sections
IIW Recom 96 Transverse Butt, Both Sides Det. No. 212 (40-3,0) >150°

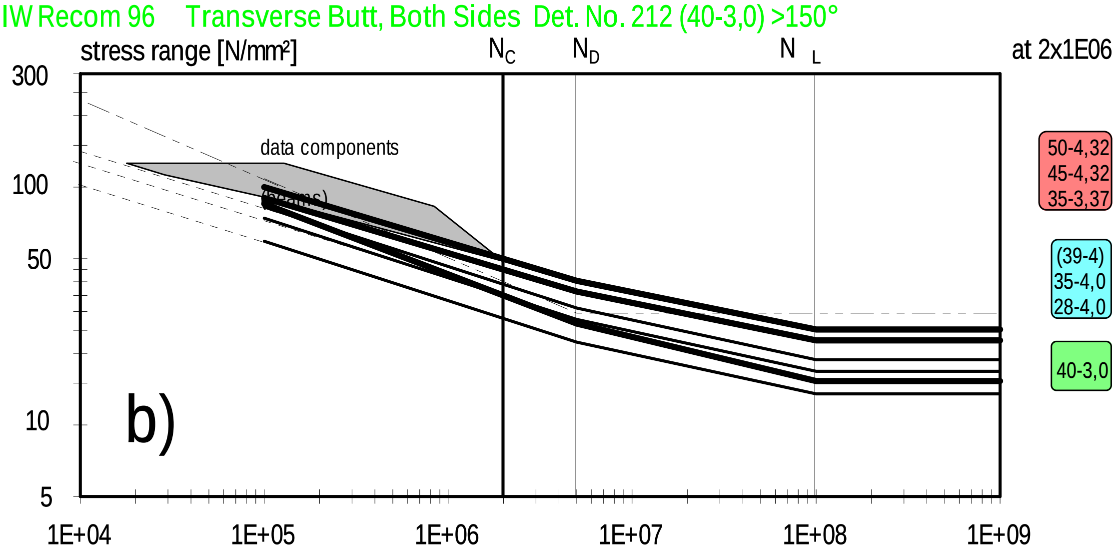

FINAL DRAFT prENV 1999-2 April 1997

ms.dos_6/(eigene)
daten/praes/inalco98/inalco.pr4-no12

ERAAS / IIW Doc. XIII-1588-95 Transverse Butt Overfill >130°, Welded from (One) or Both Sides Simple Element B3 (45-4,32); Extruded Component B7 (35-3,37)

EC 9 Welded Butt Joint Double Sided Cat. 3.2 (39-4) or (35-4) for flats and solids
(35-4) or (28-4) for open shapes
not applicable for hollow sections

IIW Recom 96 Transverse Butt Both Sides Det. No. 212 (40-3,0) >150° and No. 213 (32-3,0) >130°

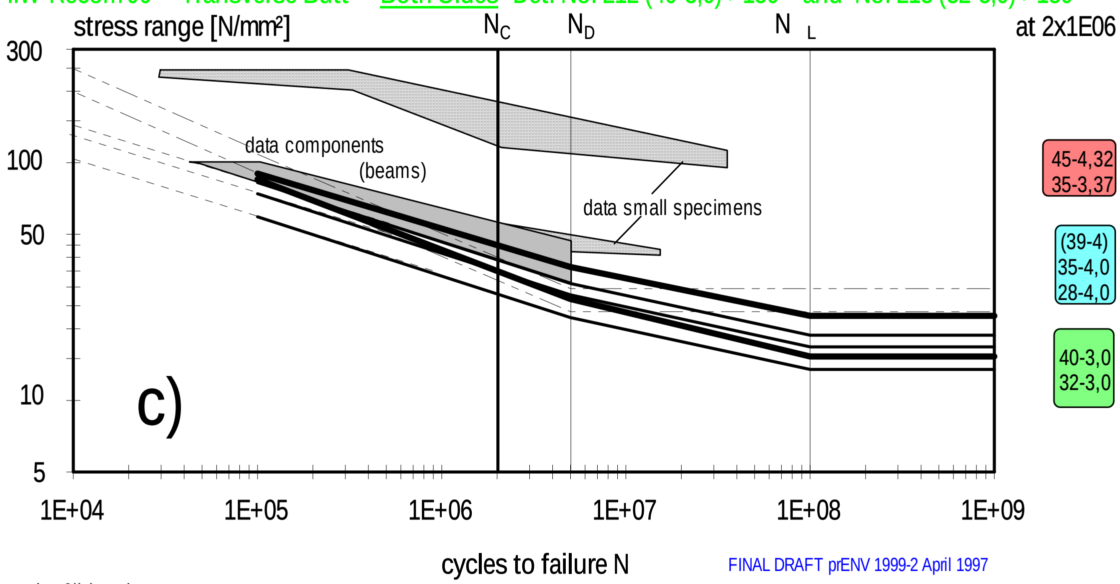

ms.dos_6/(eigene)
daten/praes/inalco98/inalco.pr4-no13

ERAAS / IIW Doc. XIII-1588-95 Transverse Butt / One Side Only
Simple Element B4 (40-4,32) On Permanent Backing Bar
Extruded Component B8 (30-3,37) Without Permanent Backing Bar
Built-Up Component B11 (30-3,37) Without Permanent Backing Bar

EC 9 Welded Butt Joint Single Sided Cat. 3.3 (35-4) or (25-3,2) Backed
or Cat. 3.4 (29-3,2) or (18-3,2) Unbacked

IIW Recom 96 Transverse Butt Det. No. 215 (25-3,0) Perm. Backing and No. 225 (22-3,0)

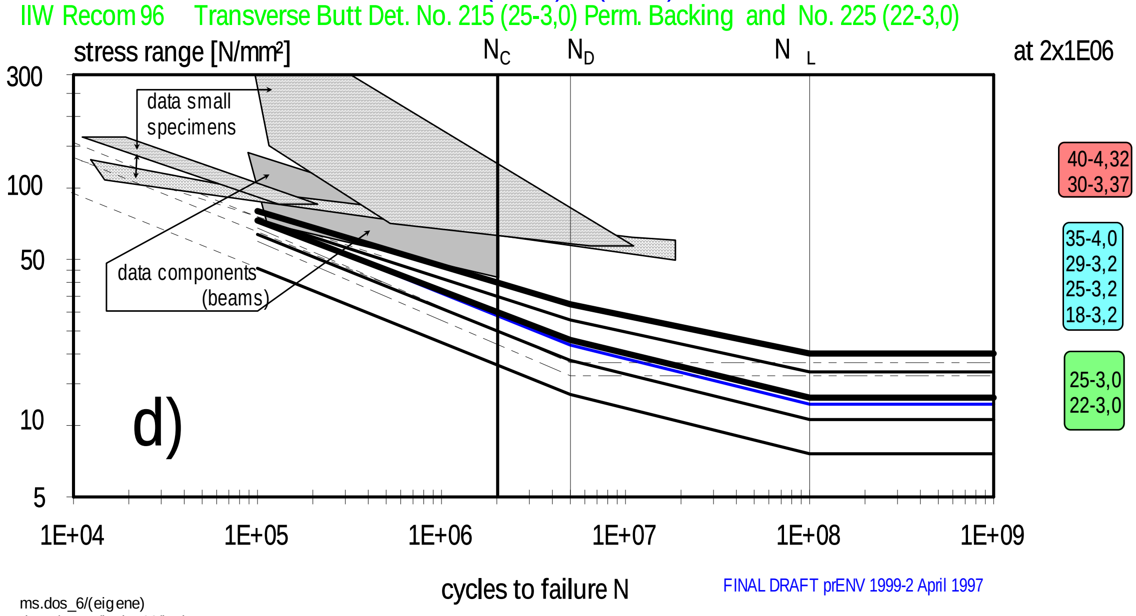

ms.dos_6/(eigene)
daten/praes/inalco98/inalco.pr4-no17

Table 14 Comparison of Design Curve Fatigue Strength Values for Parent Material and Experimental Data (at 2*10^6 cycles)

Detail	$\Delta\sigma_C$-m_1	Detail	$\Delta\sigma_C$-m_1	$\Delta\sigma_C$-m_1	Detail	$\Delta\sigma_C$-m_1	$\Delta\sigma_C$-m_1
ERAAS 1992		Eurocode 9			IIW Recomm. 1996		
Parent material							
7020 – simple extrusions, mechanically formed parts, components							
A1	130-7	1.1	121-7				
A2	85-7	1.3	96-7		111	80-5	
					122 ?		40-3
5000/6000 - simple extrusions, mechanically formed parts, components							
A3	95-7	1.2	86-7				
A4	70-7	1.4	69-7		111	71-5	
					122 ?		40-3

ERAAS: bold lines / *EC9: fine lines* / *IIW: dash-dot lines*

Table 15 Comparison of Design Curve Fatigue Strength Values for Longitudinal Butt and Longitudinal Fillet Welds and Experimental Data (at 2*10^6 cycles)

Detail	$\Delta\sigma_C$-m_1	Detail	$\Delta\sigma_C$-m_1	$\Delta\sigma_C$-m_1	Detail	$\Delta\sigma_C$-m_1	$\Delta\sigma_C$-m_1	See Fig.
ERAAS 1992		Eurocode 9			IIW Recomm. 1996			
Longitudinal butt welds								
Continuous, no stop-starts, bead ground off								
C1	60-4.32	2.14	60-4.5	55-4.5	311	50-3		
					312			
Continuous, no stop-p-starts								
C2	45-4.32	2.15	44-4.5		313	45-3		**a)**
With stop-starts								
		2.16	35-4		311	36-3		
					313			
Longitudinal fillet welds								
On one or both sides, continuous, no stop-starts								
D1	45-4.32	2.15			322	40-3		
With stop-starts								
D2	40-4.32	2.16			323	36-3		**b)**
Intermittent weld								
D3	35-4.32	2.17			324	32 ? -3		
Weld toe at hole (or notch)								
		2.18			325	28 ? -3		

ERAAS: bold lines / *EC9: fine lines* / *IIW: dash-dot lines*

ERAAS / IIW Doc. XIII-1588-95 Longitudinal Butt Weld One Side Only / Continuous, No Stop-Start
Built-Up Component C1 (60-4,32) Ground Flush or C2 (45-4,32) Overfill >130°
EC 9 Longitudinal Weld Single Sided Cat. 2.14 (60-4,5) or (55-4,5) Ground Flash, Continuous
or Cat. 2.15 (44-4,5) Continuous
Cat. 2.16 (35-4) Stop-Start
IIW Recom 96 Longitudinal Butt Weld Det. No. 311/312/313 (50/45-3,0) Continuous
No. 311/313 (36-3) With Stop-Start

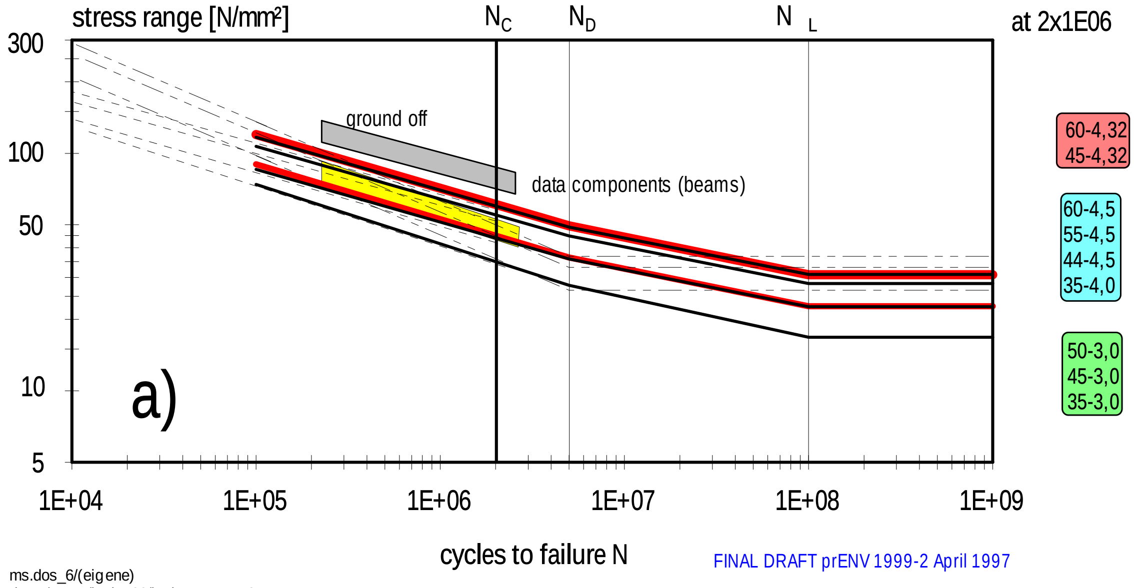

ms.dos_6/(eigene)
daten/praes/inalco98/inalco.pr4-no18

ERAAS / IIW Doc. XIII-1588-95 Fillet Longitudinal / One or Both Sides
D1 (45-4,32) Continuous, No Stop-Start / or D2 (40-4,32) With Stop-Start
D3 (35-4,32) Intermittent
EC 9 Attachment With Fillet Longitudinal Cat. 2.15 (44-4,5) No Stop-Start; Cat. 2.16 (35-4) With Stop-Start; (Weld Toe) Cat. 2.17 (31-3,5) Intermittent or Cat. 2.18 (28-3,5) Cope Hole
IIW Recom 96 Fillet Longitudinal Det. No. 322/323 (40/36-3) Continuous
No. 324 (32 ? -3) With Stop-Start / No. 325 (28 ? -3) Cope Hole

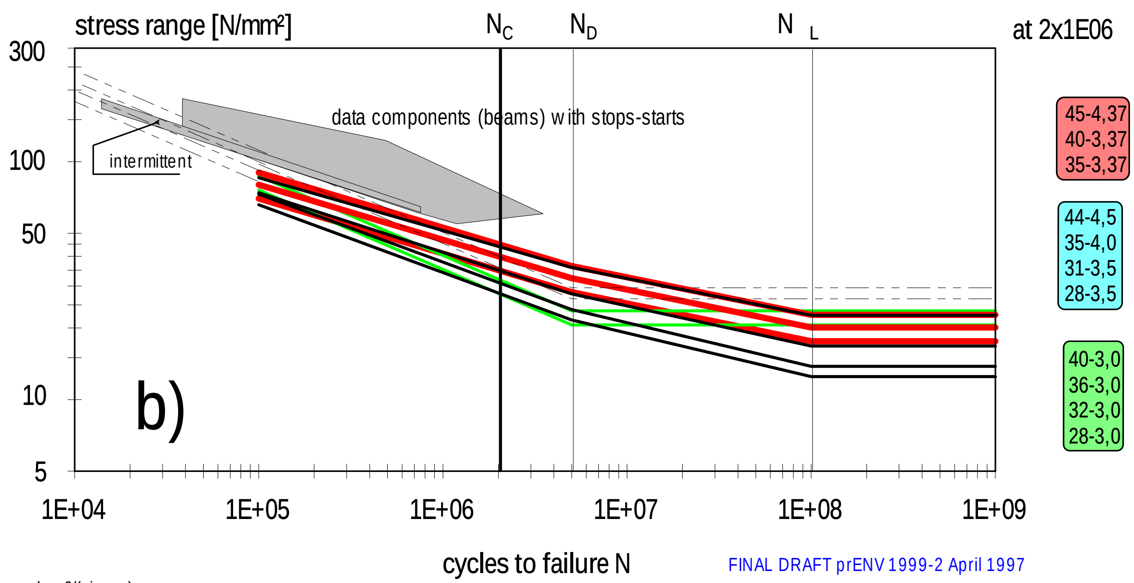

ms.dos_6/(eigene)
daten/praes/inalco98/inalco.pr4-no19

Table 16 Comparison of Design Curve Fatigue Strength Values for Transverse Fillet Welds and Experimental Data (at 2*10⁶ cycles)

Detail	$\Delta\sigma_C$-m_1	Detail	$\Delta\sigma_C$-m_1	$\Delta\sigma_C$-m_1	Detail	$\Delta\sigma_C$-m_1	$\Delta\sigma_C$-m_1	See Fig.
ERAAS 1992		Eurocode 9			IIW Recomm. 1996			
Transverse Fillet Weld								
Cruciform, load-carrying fillet, crack at weld toe								
F1	30-4.32	(3.6)			412	25-3		
		(3.7)						
		2.3	25-3.2					
		(2.9)						**a)**
		2.4	22-3.2					
Cruciform, load-carrying fillet, crack through weld (root)								
F2	25-4.32	3.8	18-3.2		414	16-3		
Cover plate, transverse fillet load-carrying								
F3	20-4.32	2.8	22-3.2		711	20-3		**b)**
		2.9	20-3.2					

ERAAS: bold lines / *EC9: fine lines* / *IIW: dash-dot lines*

ERAAS / IIW Doc. XIII-1588-95 Transverse Fillet Load-Carrying F1 (30-4.32) Toe
"Cruciform" or F2 (25-4.32) Throat/Root

EC 9 Member Joint Transeverse Fillet Toe Cat. 3.6/3.7 ➞ 2.3 (25-3.2) for L=30 mm, T=15 mm
away from edge
or Cat. 2.9 2.4 ➞ minus 1 cat. (22-3.2) at corner
Throat/Root Cat. 3.8 (18-3.2)

IIW Recom Det. No. 412 (25-3.0) Toe or Det. 414 (16-3.0) Throat

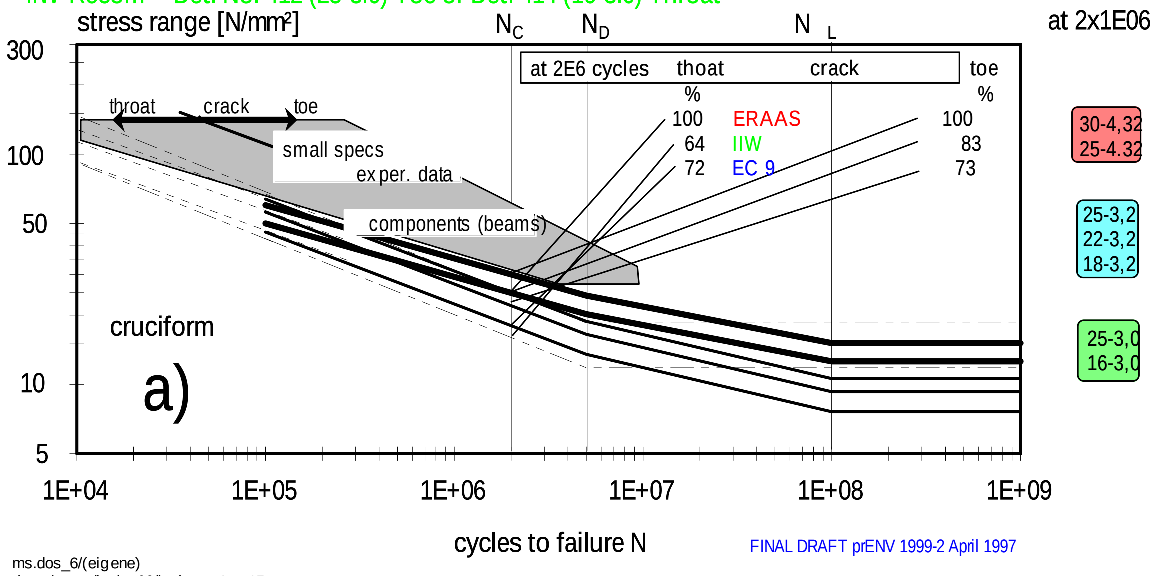

ms.dos_6/(eigene)
daten/praes/inalco98/inalco.pr4-no15

ERAAS / IIW Doc. XIII-1588-95 Transverse Fillet Load-Carrying F3 (20-4.32) "Coverplate"

EC 9 Transverse Fillet, Toe, Cat. 2.8 (22-3.2) for L>200 mm, T=15 mm
away from edge
Cat. 2.9 ➞ 2.8 minus 1 cat. (20-3,2) if on edge

IIW recom Det. 711 (20-3,0) Transverse Fillet Toe, Reinforcement t_D < 0,8t

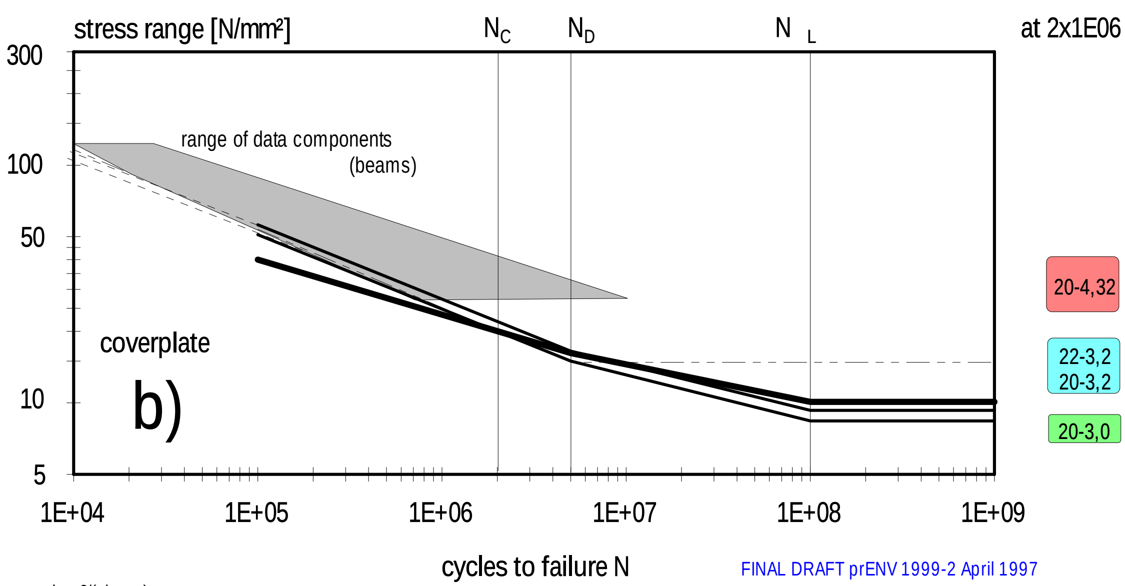

ms.dos_6/(eigene)
daten/praes/inalco98/inalco.pr4-no16

Table 17 Comparison of Design Curve Fatigue Strength Values for Welded Transverse or Longitudinal Attachments on Load-Carrying Structural Components and Experimental Data (at $2*10^6$ cycles)

Detail	$\Delta\sigma_C$-m_1	Detail	$\Delta\sigma_C$-m_1	$\Delta\sigma_C$-m_1	Detail	$\Delta\sigma_C$-m_1	$\Delta\sigma_C$-m_1	See Fig.
ERAAS 1992		Eurocode 9			IIW Recomm. 1996			
Attachments								
Weld toe transverse to stress (longitudinal or transverse butt/fillet weld)								
Web stiffener								
E1	35-3.37	2.1	31-3.2		511	28-3		**a)**
		2.9		28-3.2	512		25-3	
Web attachment								
E2	23-3.37	2.6	20-3.2		512	36-3		**b)**
		2.17	31-3.5		513	28-3		
Longitudinal attachment at flange edge, with/without transition radius								
E3	35-3.37	2.11	25-3.2		526	36-3		
		2.12	28-3.2			28-3		
		2.13	31-3.2			22-3		**c)**
E4	18-3.37	2.10	18-3.2		525		18-3	
E4*	(16-3.37)						16-3	
							14-3	
Vertical longitudinal attachment on flange, with/without transition radius								
E5	35-3.37	2.13	31-3.2	approx.	522	32-3		
					(523)	25/20-3		
					(524)	18/16-3		**d)**
E6*	18-3.37	2.8	22-3.2	No corresp. category	521	(28/25/20) / 18-3		
E7	18-3.37	?		No corresp. category	521	(28/25/20) / 18-3		
Vertical transverse attachment on flange								
E8	23-3.37	2.2	28-3.2	No corresp. category	511	36/28/25-3	approx.	**e)**

ERAAS: bold lines / *EC9: fine lines* / *IIW: dash-dot lines*

ERAAS / IIW Doc. XIII-1588-95 Attachment With Transverse Fillet, E1 (35-3.37) Web Stiffener, Extruded/Built-Up Beam

EC 9 Welded Attachment, Transverse Weld Toe Cat. 2.1 (31-3.2) or actually Cat. 2.9 (28-3.2)

IIW Recom 96 Det. No. 511 or 512 (28/25-3) Transverse Fillet, As Welded

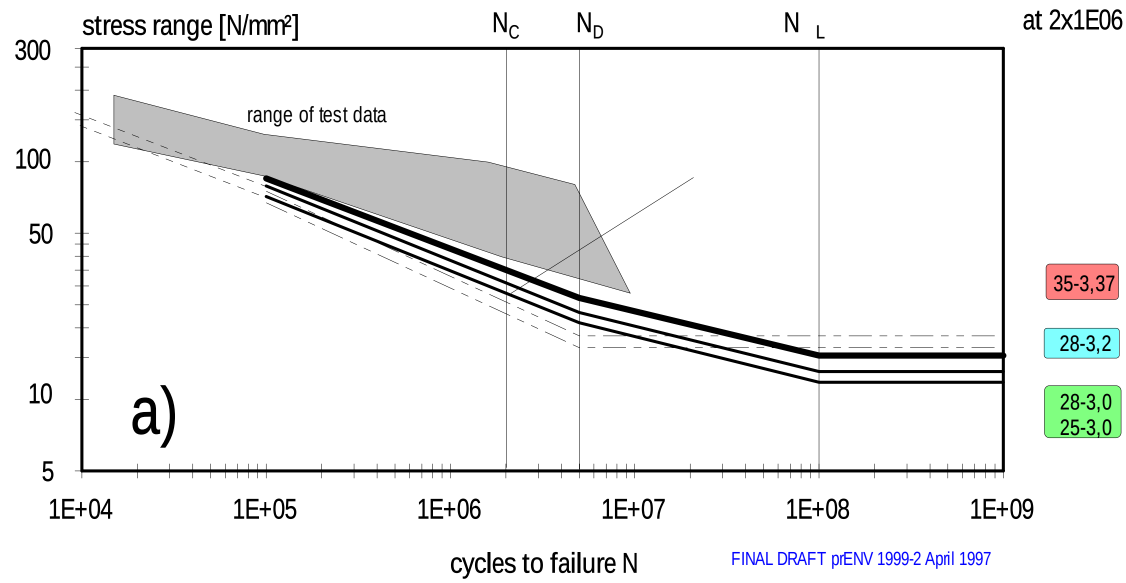

ms.dos_6/(eigene)
daten/praes/inalco98/inalco.pr4-no14

ERAAS / IIW Doc. XIII-1588-95 Web Attachment With Transverse Fillet, E2 (23-3.37)

EC 9 Welded Attachment, Transverse Weld Toe Cat. 2.6 (20-3.2) for L=100 mm, T=15 mm or Cat. 2.17 (31-3,5)

IIW Recom 96 Transverse Fillet, As Welded Det. No. 512 (28/25-3) or No. 513 (28-3)

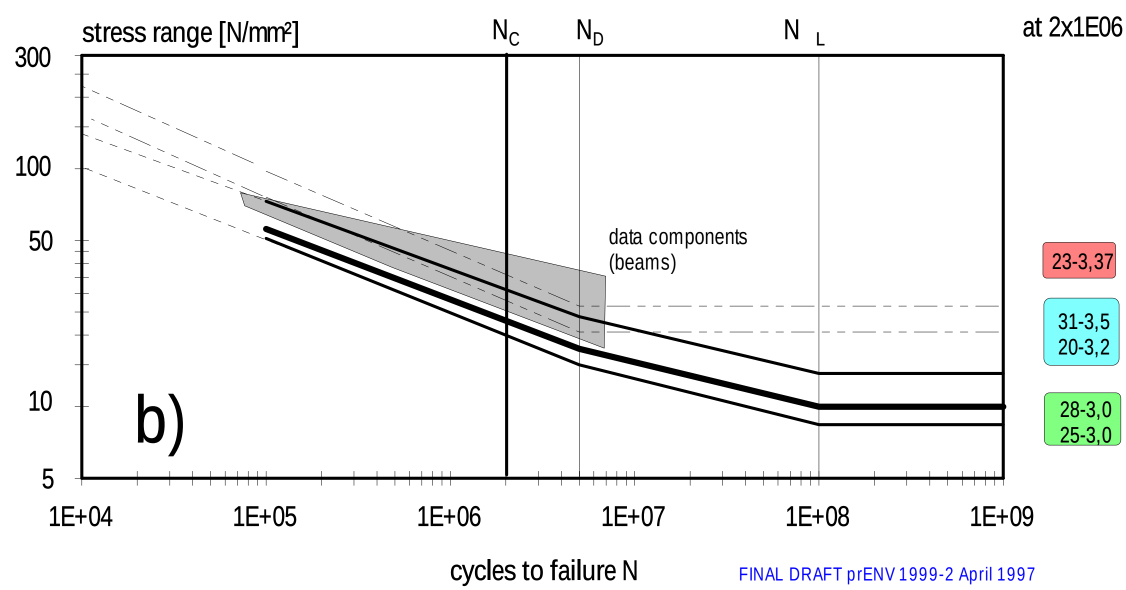

ms.dos_6/(eigene)
daten/praes/inalco98/inalco.pr4-no20

ERAAS / IIW Doc. XIII-1588-95 Flange Edge Attachment E3 (35-3.37) or E4 (18-3,37)

EC 9 Flange Edge Welded Attachment Cat. 2.11/2.12/2.13 (31/28/25/-3.2) or Cat. 2.10 (18-3,2)

IIW Recom 96 Transverse Fillet, As Welded Det. No. 526 (36/28/22-3) or No. 525 (18/16/14-3)

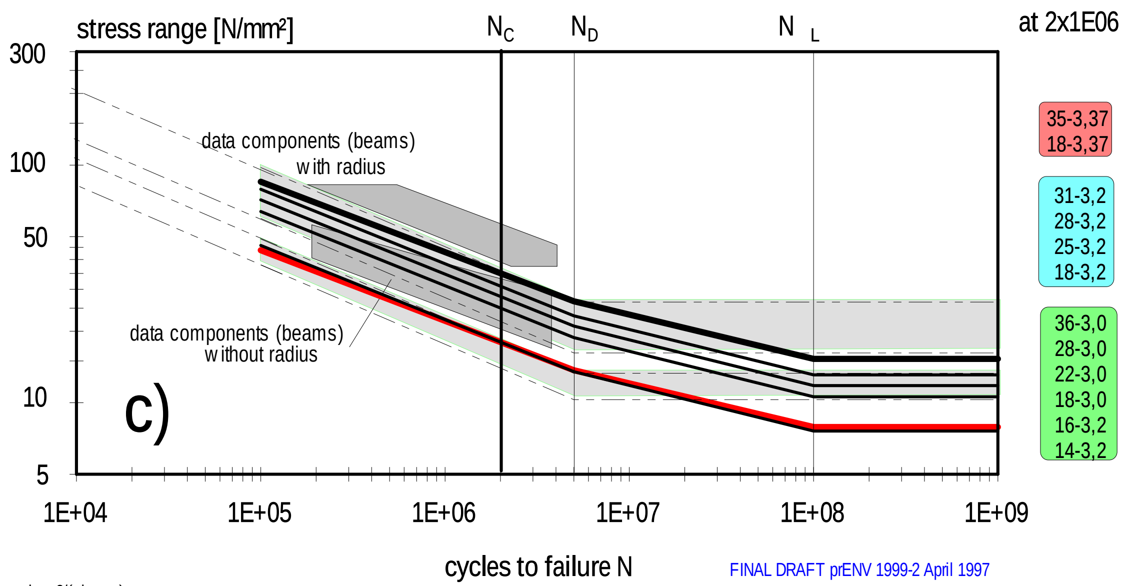

ms.dos_6/(eigene)
daten/praes/inalco98/inalco.pr4-no21

ERAAS / IIW Doc. XIII-1588-95
Vertical-Long. Flange Attachment E5 (35-3.37) or E6 = E7 (18-3,37)
trans. radius extruded or built-up beam

EC 9 Flange Attachment Cat. 2.13 (31-3.2) and Cat. 2.8 (22-3,2)

IIW Recom 96 Det. No. 522 (32-3) or No. 521 (28/25/20/18-3)

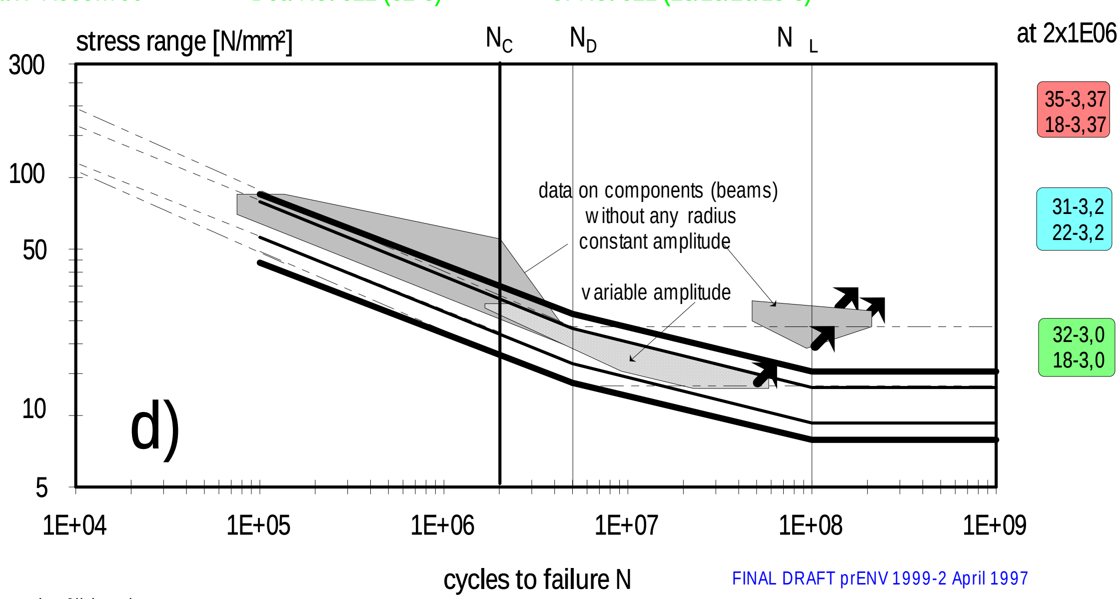

ms.dos_6/(eigene)
daten/praes/inalco98/inalco.pr4-no22

➚ **runout**

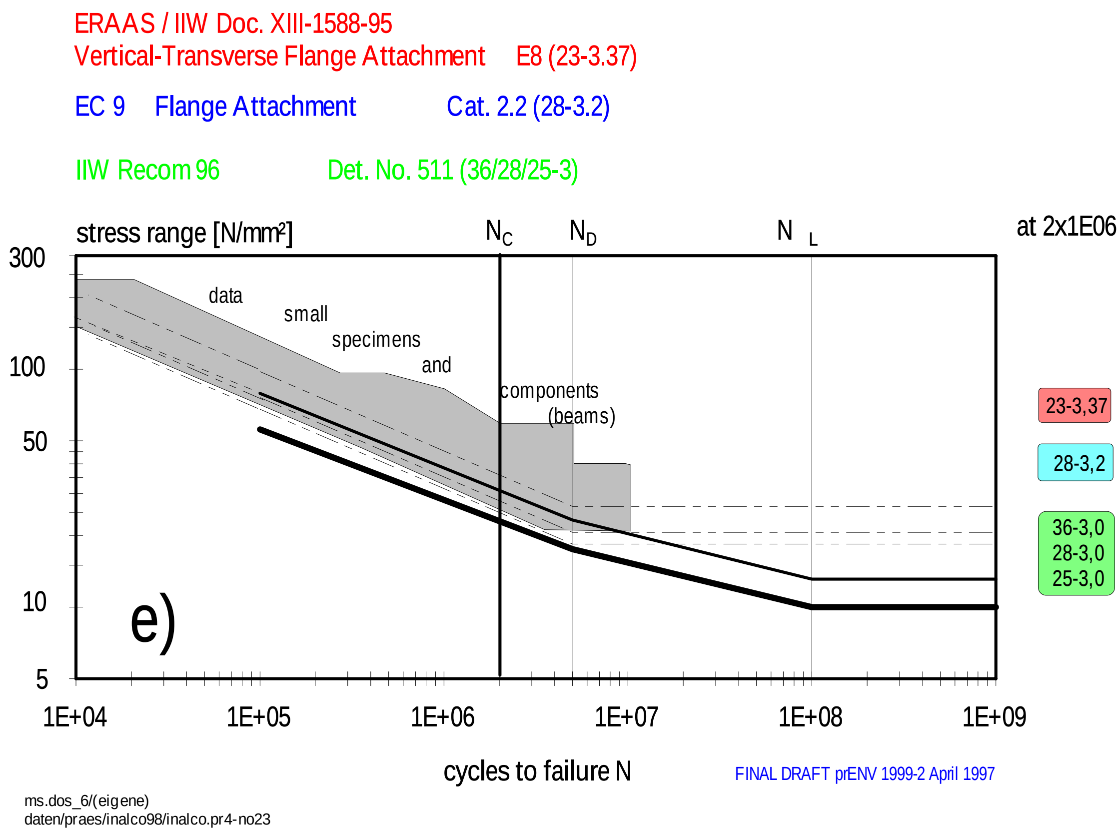

A general comment: in the initial classification according to the European recommendations ERAAS allowed for somewhat higher values, i.e. higher utilization of the detail capacity. It is noted that attention had been drawn from the very beginning to the fact that these values are attainable only under specific manufacturing and quality control procedures stated in the document. Extrapolations to other conditions of manufacturing and service shall be handled with care.

To this purpose the current documents (European codes for design and manufacturing/quality for aluminum structures) give more information.

In the diagrams above a cut-off limit at $5x10^6$, N_D, cycles for the IIW assumption of the design S-N line, contrary to the definition of 10^8 cycles, N_L, for the Eurocode. There is some indication that the first limit could be true if considering the limited information of runouts in spectrum loaded and random tests performed in this life region. The Eurocode is more conservative in this high cycle fatigue region and more information will be necessary under different loading conditions and patterns to confirm results.

8. FRICTION STIR WELDING

This section of the report provides introductory material on Friction Stir Welding, FSW. It describes the physical processes occurring in the joined members and provides an understanding of the differences between FSW and traditional fusion welding.

Another important source of information on the subject of FSW is the currently evolving document ISO TC/ SC N "Welding – Friction Stir Welding of Aluminum – General Requirements". The document handles issues of Specification and qualification of welding procedures, Welding operator qualification, Fabrication, Inspection and testing. It will serve as an intermediate step toward the integration of FSW in design and execution codes, the Eurocode or respective specifications, although considerable work has to be performed on data accumulation and evaluation especially in the area of fatigue behavior.

Friction Stir Welding of aluminum is used in limited applications by various European shipbuilders for high speed aluminum craft and the discussion presented herein includes the mechanics of the FSW process as well as some of the reasons why the finished product has higher static and fatigue design properties than their fusion welded counterparts. It also presents a summary of the continuing studies into the use and application of friction stir welding.

8.1 General Information on Friction Stir Welding

8.1.1 The Process

Friction Stir Welding is a solid state joining process invented by The Welding Institute (TWI) in 1991 and is rapidly emerging as a viable alternative to fusion welding for joining a variety of structural alloys. FSW can best be described as a combination of extrusion and forging of metals at elevated temperatures. It is considered a solid state process, and it does not normally require any edge preparation of the joint, shielding gases or consumable filler metals.

The process is suitable for welding butt joints, corner sections, T-sections and different lap-joint configurations, and offers new possibilities for fabrication of large aluminum sections.

Among the benefits of FSW are the ability to weld difficult-to-weld aluminum alloys such as 7xxx series, better retention of baseline material properties and improved dimensional stability of the welded structure. Since it is essentially solid-state, i.e. without melting in the Heat Affected Zone HAZ, high quality weld can generally be fabricated with fewer weld defects, low residual stresses, absence of solidification cracking, porosity and oxidation.

The process is attractive for several other reasons. First, the friction heating is generated locally, so there is no widespread softening of the assembly. The weld is formed across the entire cross-sectional area of the interface in a single shot process. The technique is capable of joining dissimilar materials. Finally, the process is completed in a few seconds with very high reproducibility – an essential requirement for a mass production industry.

8.1.2 The Principle of Operation

In Friction Stir Welding, **Figure 33** & **Figure 34**, the plates to be joined are clamped on a backing plate to resist the vertical, longitudinal and lateral forces, trying to lift and push them apart. A cylindrical shoulder tool with a specially designed and profiled probe, **Figure 35**, made from a hard, wear resistant material relative to the material being welded, is rotated at a high speed and slowly plunged into the abutting edges of the parts to be joined.

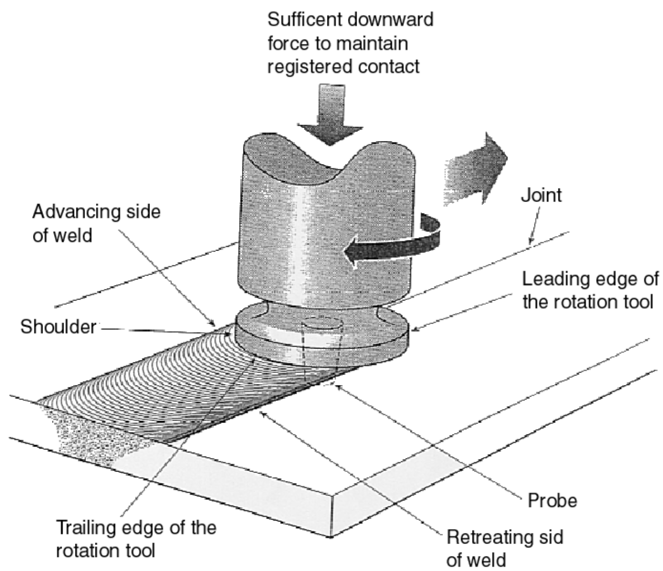

Figure 33 Schematic Illustration of Friction Stir Welding

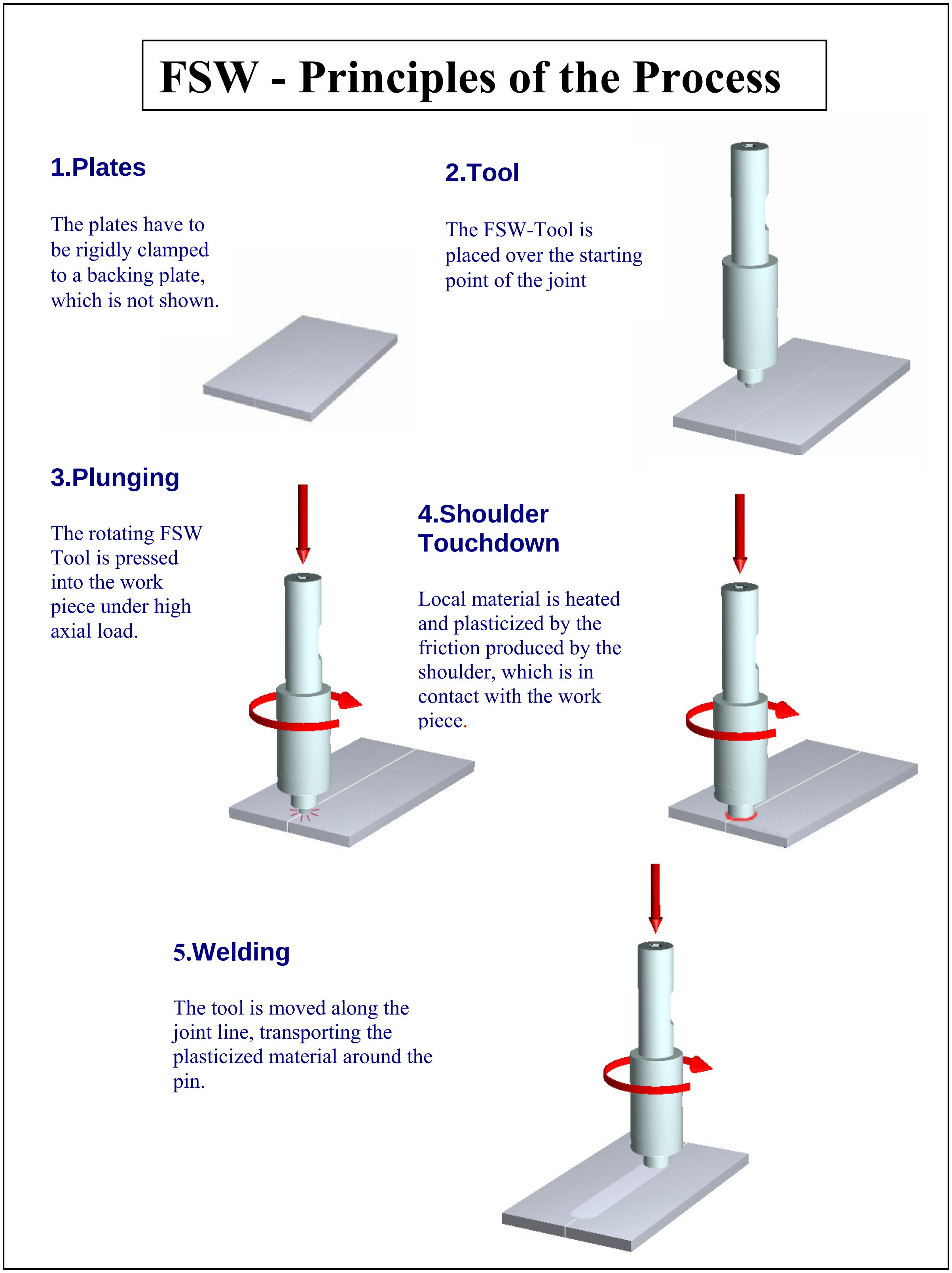

Figure 34 FSW – Principles of the Friction Stir Weld Process

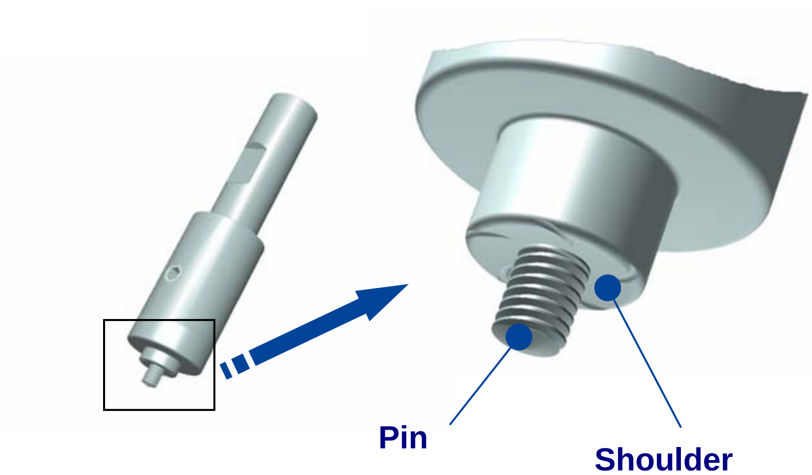

Figure 35 Schematic for the Tip of the FSW Tool

The rotating pin produces the stirring action in the material along the bond line and produces the required thermo-mechanical deformation. During welding, the probe first makes contact as it is plunged into the joint region. This initial plunging friction heats a cylindrical column of metal underneath the probe: the material softens without reaching the melting point and allows traversing of the tool along the welding line. The depth of penetration is controlled by the length of the probe below the shoulder of the tool. The contacting shoulder applies additional frictional heat to the weld region and prevents highly plasticized material from being expelled during the welding operation. Once the shoulder makes contact the adjacent thermally softened region takes up a frustum shape corresponding to that of the overall tool geometry, **Figure 36**.

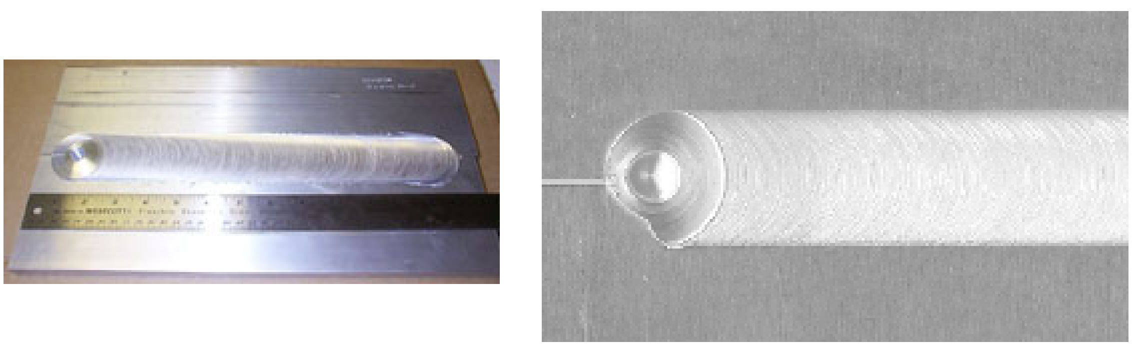

Figure 36 Samples of FSW Welds

Typically, the surface appearance is a regular series of partial circular ripples, which point towards the start of the weld. These ripples are essentially cycloidal and are produced by the final sweep of the trailing circumferential edge of the shoulder. The combined frictional heat from the probe and the shoulder creates a plasticized, almost hydrostatic condition, around the immersed probe and the contacting surface of the shouldered region of the work piece top surface. The soft material is mashed by the leading face of the pin profile and transported to the trailing face of the pin where it consolidates and cools to produce a high integrity weld. The process can be regarded as a solid phase keyhole welding technique since a hole to accommodate the probe is generated, then filled during the welding sequence. The consolidated welds are solid-phase in nature and do not show fusion welding defects. The distortion is significantly less than that caused by any fusion welding technique. The properties of the weld are closely related to the tool technology. The tool bit shape and material determines the heating, plastic flow and forging pattern. Usually, the pin is almost brought into contact with the backing plate, as close as a few tenths of a millimeter. The stronger the base material, the closer the pin to the backing plate, in order to ensure complete penetration of the weld through the thickness.

Friction stir welds are not symmetric about the weld centreline due to the tool rotation: the side of the weld on which the rotational velocity of the tool has the same direction as the welding velocity is designated the *advancing side of the weld*; the side of the weld on which the two velocities have opposite direction is the *retreating side of the weld*, **Figure 37**.

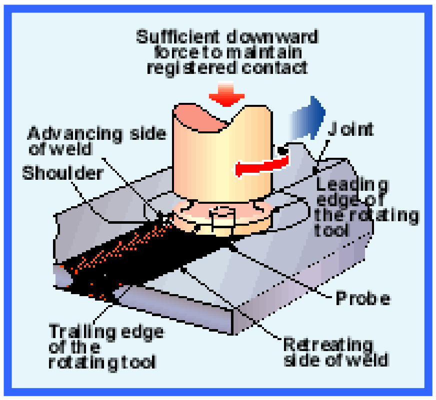

Figure 37 Definitions of FSW terminology

The use of an effective fixture, **Figure 38**, is vital for the success of the process: if the clamping is not firm enough, a lack of material is experienced in the weld zone.

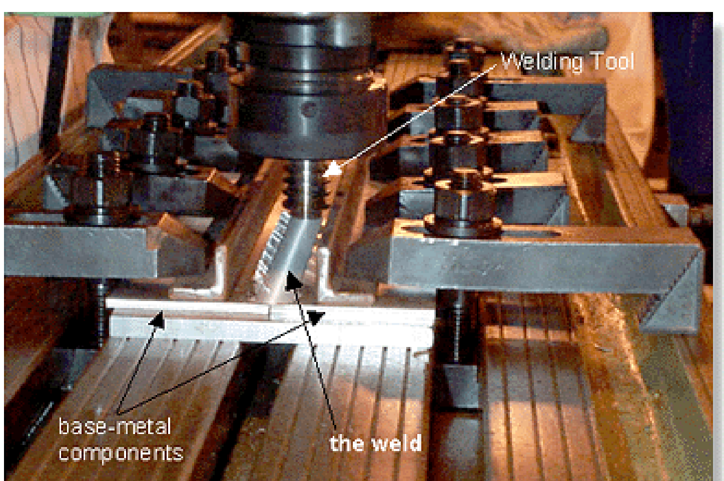

Figure 38 FSW Setup

The forces associated with such softening and mass transfer are significant and will act to push the softened material out of the joint line. Special care must be taken not to set the tool too deep which can result in mixing and joining of the backing bar and aluminum plate materials. This would be unacceptable to the joint and would also damage the probe.

8.1.3 Friction Stir Welding Process Advantages

The process advantages result essentially from the fact that the FSW takes place in the solid phase, below the melting point of the material to be joined. The benefits include the ability to join materials that are difficult to fusion weld, for example 2000 and 7000 aluminum alloys. Friction Stir Welding can use existing available machine tool technology and is also suitable for automation and adaptable for robotic use. Among its main advantages are:

- Low distortion and shrinkage, even in long welds;
- Excellent mechanical properties as proven by fatigue, tensile and bend tests;
- No fumes, sparks, porosity or spatter;
- Environmentally friendly;
- Can operate in all positions and is energy efficient.
- Non-consumable tool;
- One tool can typically be used for up to 1000m of weld in 6000 series aluminum alloys;
- No need for shielding gas or filler wire;
- No welder certification required;
- Some tolerance to imperfect weld preparations – thin oxide layers can be accepted;
- No grinding, brushing or pickling required in mass production.
- Weight savings compared to fusion welding due to the lack of any required consumables to complete the weld.

The main limitations of the FSW process are at present:

- Keyhole at the end of each weld;
- Welding speeds are moderately slower than those of some fusion welding processes (up to 750mm/min for welding 5mm thick 6000 series aluminum alloy on commercially available machines);
- High axial and transverse loads applied: need for stable backing and clamping elements;
- High degree of stiffness required from the handling system used;
- Limited flexibility when compared to fusion welding processes.
- Too complex for repair welds in the field.

8.1.4 Materials and Thickness

Friction stir welding can be used for joining many types of materials and material combinations, if tool materials and designs can be found which operate at the forging temperature of the pieces. It can weld all aluminum alloys, including those that cannot normally be joined by conventional fusion techniques. Up to the present day, TWI has concentrated most of its efforts on optimizing the process for the joining of aluminum and its alloys. A major Group Sponsored Project undertaken for TWI's Industrial Members demonstrated that the following aluminum alloys could be successfully welded to yield reproducible, high integrity welds within defined parametric tolerances:

- 2000 series aluminum (Al-Cu)
- 5000 series aluminum (Al-Mg)
- 6000 series aluminum (Al-Mg-Si)
- 7000 series aluminum (Al-Zn)
- 8000 series aluminum (Al-Li)

This work primarily investigated welding of wrought and extruded alloys. However, subsequent studies have shown that cast to cast, and cast to extruded (wrought) combinations in similar and dissimilar aluminum alloys are equally possible.

The stirring effect of the tool is clearly visible in transverse macrosections if different types of materials have been welded such as wrought aluminum sheets to cast aluminium, **Figure 39**, or extrusions to wrought sheets. The onion ring like structure of the nugget is typical of high quality stir welds in which no porosity or internal voids are detectable.

Figure 39 Transverse Section of 6mm Wrought Aluminum Welded to Cast Aluminum

Continuing development of the FSW tool, its design and materials have allowed preliminary welds to be successfully produced in:

- Copper and its alloys
- Lead
- Titanium and its alloys
- Magnesium alloys

- Zinc
- Aluminum alloys of the 1000 (commercially pure), 3000 (Al-Mn) and 4000 (Al-Si) series
- Plastics
- Mild steel

Preliminary trials have also yielded encouraging results when FSW was used to join aluminum based metal matrix composites (MMCs), and when the process was applied to dissimilar materials such as cast magnesium alloy to extruded aluminum alloy.

Single pass butt joints with aluminum alloys have been made in thicknesses ranging from 1.2 to 50 mm without the need for edge preparation. Parameters for butt welding of most aluminum alloys have been optimized in a thickness range from 1.6 to 10 mm. Special lap joining tools have been developed for aluminum with thicknesses of 1.2 - 6.4 mm. Thicknesses of up to 100 mm can be welded using two passes, one from each side, with 6082 aluminum alloy, **Figure 40**.

Figure 40 Double Sided Friction Stir Weld in 75 mm Thick Aluminum Extrusion

8.1.5 Weld Properties and Characteristics

Since traditional heating methods are not employed, the properties of the metal in the joined area are higher than those from any other known welding process and distortion is virtually eliminated. The repeatable quality of the solid-phase welds can improve existing products and lead to a number of new product designs previously not possible. The crushing, stirring and forging action of the FSW tool produces a weld with a finer microstructure than the parent material.

The first attempt at classifying microstructures was made by P L Threadgrill (Bulletin, March 1997). This work was based solely on information available from aluminum alloys. However, it has become evident from work on other materials that the behaviour of aluminum alloys is not typical of most metallic materials, and therefore the scheme cannot be broadened to encompass all materials. It has been proposed to use the following scheme:

When a cross-section is taken through a friction stir weld, a unique structure is seen that is comprised of four characteristic regions, **Figure 41**. The region far from the weld center is *Parent material* (*base material*), which is unaffected by heat or mechanical deformation. The grains are elongated as a consequence of the earlier rolling operation. In the *Heat affected zone* (HAZ), which is closer to the weld center, the material has experienced a thermal cycle, which has modified the microstructure and the mechanical properties. However, there is no plastic deformation occurring in this area. This region is similar to the heat-affected zone in a fusion weld but the peak temperatures are lower. In this zone optical microscopy shows no apparent difference from the parent material but in age hardened alloys and mechanically hardened alloys, the hardness is lower in this area: this shows that heat from the welding process either causes over aging, or lowering of dislocation density, and probably both in fully aged alloys.

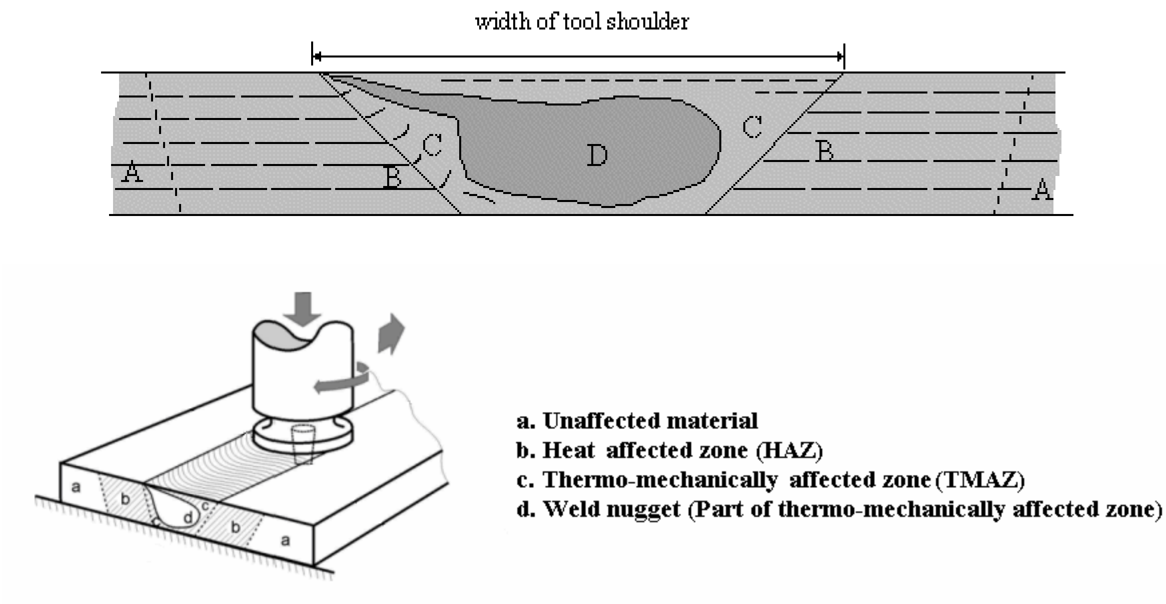

Figure 41 Illustration of the Regions Associated with a Friction Stir Weld

In the *Thermo-mechanically affected zone* (TMAZ) the material has been plastically deformed by the FSW tool, and the heat from the process will also exert some influence on the material. In the case of aluminum, it is possible to get significant plastic strain without recrystallization in this region, and there is generally a distinct boundary between the recrystallized zone and the deformed zones of the TMAZ. In the earlier classification, these two sub-zones were treated as distinct regions of microstructure. However, subsequent work on other materials has shown that aluminum behaves in a different manner to most other materials, in that it can be extensively deformed at high temperature without recrystallization. In other materials, the distinct recrystallized region (the nugget) is absent, and the whole TMAZ appears to be recrystallized.

The center of the weld experiences plastic flow and recrystallization: this zone is known as the *nugget*, **Figure 42**. The nugget has an asymmetric shape caused by material being preferentially sheared from one side of the tool and drawn into the centre. The diameter is usually slightly greater than the diameter of the pin. The weld nugget is the region where full dynamic recrystallization occurs and is comprised of a fine equi-axed grain structure. Grain size depends on the alloy and the welding procedure. Typically, it is less than about ten microns (10 µm). For example, fine equiaxed grains of 2-4 µm in diameter are reported for 7075-T6 alloy while grains of 10 µm are reported in the weld zone of 6061-T6 Al, in contrast with an average grain size of 100 µm in the base material. In addition, the dislocation density can be significantly reduced. Electron diffraction indicates that the grain boundaries are of the high angle type, which means the structure is really formed by grains, not by subgrains, characterized by low-angle boundaries. Typically, the parent metal chemistry is retained, without any segregation of alloying elements.

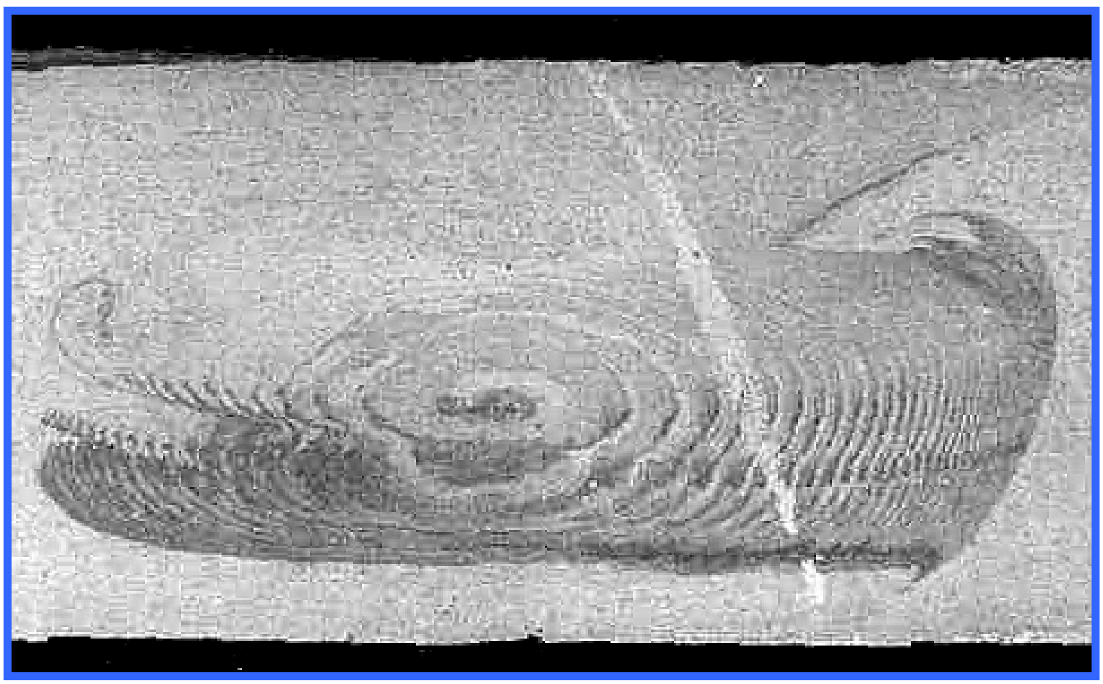

Figure 42 Nugget at Center of Friction Stir Weld

Each region has different mechanical properties resulting from the local thermal and mechanical processing cycles.

The weld nugget strength in the as-welded condition can be in excess of that in the heat affected zone. In the case of annealed materials, tensile tests usually fail in the unaffected material well away from the weld and heat affected zone. The welding properties of fully hardened (cold worked or heat treated) alloys can be further improved by controlling the thermal cycle, in particular by reducing the annealing and over aging effects in the thermo-mechanically affected zone, where the lowest hardness and strength are found after welding. For optimum properties, it would seem that, for the latter, a heat treatment after welding is the best choice, although it is recognised that this will not be a practical solution for many applications.

Typical tensile properties of friction stir welded 5000, 6000 and 7000 series alloys are given in **Table 18**. The studies have been conducted by TWI [46], Granges technology [36], Finspång, Sweden and Hidro Aluminum [47] in Håvik, Norway. They show that for solution treated plus artificially aged 6082-T6 aluminum by post weld heat treatment a tensile strength similar to that of the parent material could be achieved, although the ductility was not fully restored. A further improvement was possible when weld specimens where made from solution treated and naturally aged 6082 base metal in the T4 condition and then after welding subjected to normal aging. Natural aging at room temperature led, in the recently developed 7108 aluminum alloy, to a similar effect which resulted in a tensile strength of 95% of that of the base material.

Table 18 Typical Mechanical Properties of Friction Stir Welded Aluminum Specimens

Material	0.2% Proof strength Mpa	Tensile strength Mpa	Elongation %	Welding factor UTS_{FSW}/UTS_{PARENT}
5083-0 Parent	148	298	23,5	N/A
5083-0 FSWed	141	298	23	(1.00)
5083-H321 Parent	249	336	16,5	N/A
5083-H321FSWed	153	305	22,5	0.91
6082-T6 Parent	286	301	10,4	N/A
6082-T6 FSWed	160	254	4,85	0.83
6082-T6 FSWed and aged	274	300	6,4	(1.00)
6082-T4 Parent	149	260	22,9	N/A
6082-T4 FSWed	138	244	18,8	(0.93)
6082-T4 FSWed and aged	285	310	9,9	(1.19)
7108-T79 Parent	295	370	14	N/A
7108-T79 FSWed	210	320	12	(0.86)
7108-T79 FSWed naturally aged	245	350	11	(0.95)

Fatigue tests on friction stir welds made from 6 mm thick 5083-0 and 2014-T6 have been conducted [46]. The fatigue performance of friction stir butt welds in alloy 5083-0 was comparable to that of the parent material when tested using a stress ratio of R=0.1. Despite the fact that the fatigue tested friction stir welds were produced by a single pass from one side, the results have substantially exceeded design recommendations for fusion welded joints [1]. Analysis of the available fatigue data has shown that the performance of friction stir welds is comparable with that of fusion welds, and in most cases substantially better.

The outstanding fatigue results can only be achieved if the root of butt welds is fully bonded. As known from other welding processes, it is also essential in FSW to avoid root flaws. If the pin is too short for the actual material thickness, the work pieces are only forged together without stirring up the oxide layers. These flaws are difficult to detect by non-destructive testing. In case of large variations in sheet thickness, it could be necessary to have extendible pins, which can be adjusted depending on the actual sheet thickness.

8.1.6 Welding Parameters

There are a number of variables that need to be controlled when performing friction stir welds:

- *Tool plunge depth*: the tool probe is kept at a small distance above the backing bar (typically 0.2 mm). If the distance is greater than 0.2 mm the stirring action will not proceed down to the backing bar. High pressures will be transmitted to the backing bar and cause the root area to be pressure bonded. Pressure bonds are weaker than both stirred material and parent plate. The tool plunge depth may be influenced by the thickness of material. If the material is thinner than expected, the probe may gouge into the backing bar. If the material is thicker than expected then pressure bonds will result.

- *Machine parameters*: the speed of rotation and tool movement along the weld has an important effect on weld quality. Tools travelling too fast may not allow consolidation of plasticized material and the tool could rise similar to a hydrofoil. If speed is too slow, then material may not become plasticized or be heated to sufficiently high temperatures.

- *Plate positioning*: the positioning of the plates relative to each other and the tool is significant. First, the tool probe is of a small diameter and must be positioned over the center of the joint line. If this is offset then the amount of plasticized material on one side of the joint will be too small. This leads to weaker joints with the possibility of only pressure bonding the plates together in extreme circumstances. The plates need to be in contact: small gaps between the plates are closed by the tool, appearing to zip the plates together. However, if the gap between the plates is greater than 10% of the tool diameter the joint strength and elongation will be reduced. As the gap between plates increases there will be insufficient material to fill the gap resulting in void formation.

Care should be taken during the set-up to ensure optimum positioning of the tool and plates.

8.1.7 Joint Geometries

The process has been used for the manufacture of different kind of welds, **Figure 43**, i.e. butt welds, overlap welds, T-sections, fillet and corner welds.

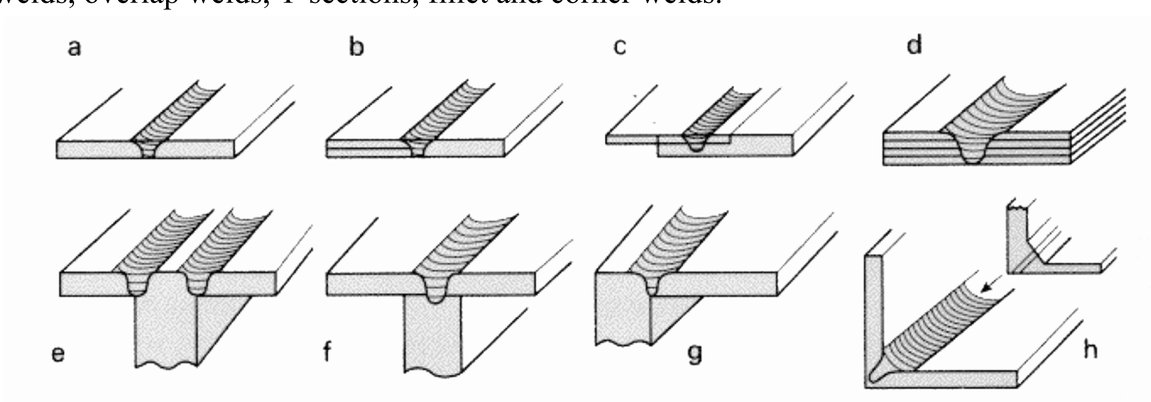

Figure 43 Typical Joint Configurations for Friction Stir Welds

The joint configurations shown in **Figure 43** correspond to:

a. Square butt
b. Combined butt and lap
c. Single lap
d. Multiple lap
e. 3 piece T butt
f. 2 piece T butt
g. Edge butt
h. Corner Fillet

For each of these joint geometries specific tool designs are required which are being further developed and optimized.

The Friction Stir Welding process can also be used for circumferential, angular, non-linear, and three-dimensional welds, **Figure 44**.

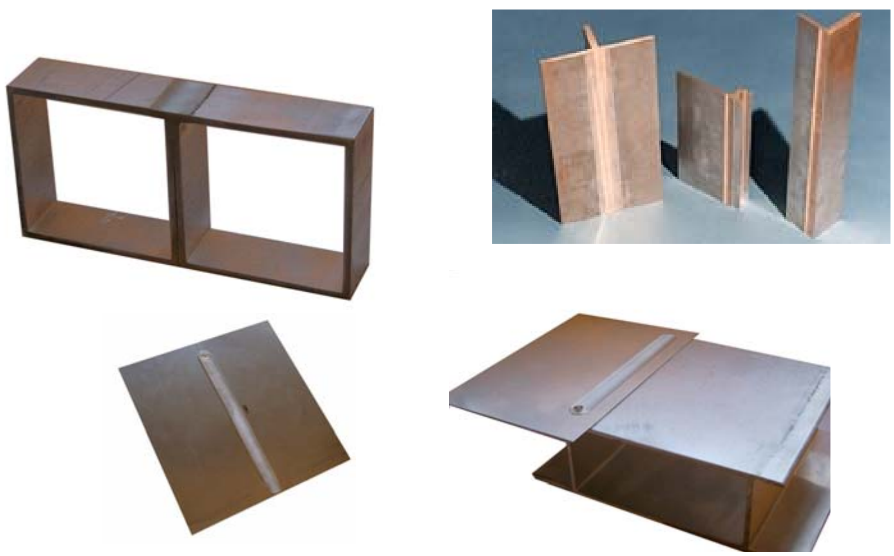

Figure 44 Samples of FSW Components

Since gravity has no influence on the solid-phase welding process, it can be used in all positions: horizontal, vertical, overhead and orbital.

8.1.8 Applications in Shipbuilding and Marine Industries

The shipbuilding and marine industries are two of the first industry sectors to have adopted the process for commercial applications, **Figure 45**.

Friction stir welding has been used in the construction of fast ferries and cruise ships. Fabricators construct components, which are then delivered to shipyards and fitted directly into place. With component generation being done away from the shipyards and leaving them with final assembly of sections to the main structure; shipyards can have faster turn-around times.

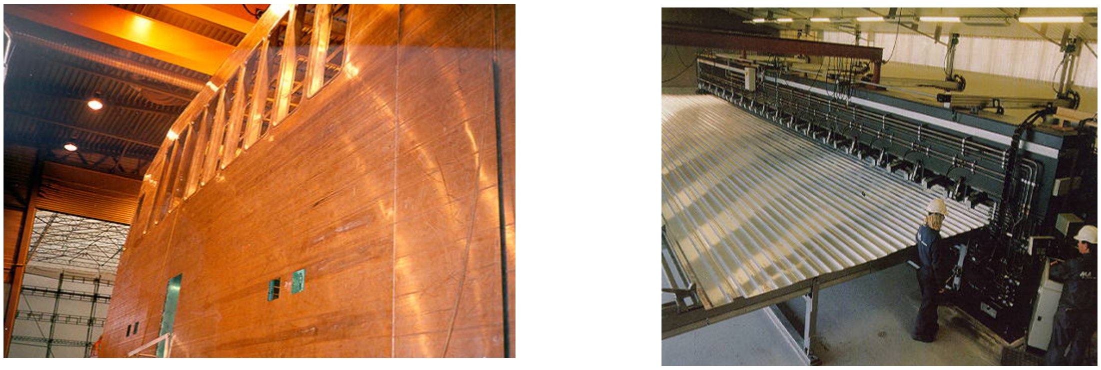

Figure 45 Deck panels made from FSW profiles

The initial commercial application of friction stir welding involved the manufacture of hollow aluminum panels for deep freezing of fish. The minimal distortion and high reproducibility make FSW both technically and economically attractive for production of these stiff panels.

To date, the main application of friction stir welding has been to join extruded sections for deck structures of fast ferries and helo-decks. Another application has been joining extruded sections in cruise ship fabrication. Pre-fabricated wide aluminum panels for high speed ferry boats are already commercially available. The panels are made by joining extrusions which can be produced in standard size extrusion presses: compared to fusion welding, the heat input is very low and this results in low distortion and reduced thermal stresses. However, there may be a number of other applications for friction stir welding in the marine sector. Hull plates may one day be joined by this process. Another application of friction stir welding may be in the repair of fusion welds: defects such as cracks and porosity may be stir welded to give a worked microstructure free from the original imperfections.

8.2 Fatigue Behavior of Friction Stir Welds in 6000 Series Aluminum Alloys

This section presents the literature survey carried out in order to summarize the current state of knowledge on the fatigue behavior of friction stir welds in aluminum alloys 6XXX (Magnesium and Silicon). Using computer analyses of all data, many Wöhler Diagrams have been obtained for different series alloys and different testing parameters. The majority of the data available was from studies on 6082 aluminum alloy. All these collected data were on butt-welded joint tests. In most cases, testing was conducted with an R value equal to 0.1 and a frequency value between 10 and 20 Hz. A comparison between friction stir welds and design curves for conventional welds has been presented in order to highlight the enhancement of fatigue behavior. Finally, a diagram summarizes the bulk of the available data.

8.2.1 Fatigue Behavior of Friction Stir Welds in Aluminum Alloy 6082

8.2.1.1 First experimental data on aluminum alloy 6082-T6

Initial experimental data deals with fatigue tests performed on friction stir butt welds in aluminum alloy 6082-T6. The chemical composition of the parent material is shown in **Table 19**.

Table 19 Chemical Composition of AA6082-T6 in Initial FSW Fatigue Tests

Element	Compositions [wt. %]
Silicon (Si)	0.9
Iron (Fe)	0.50
Copper (Cu)	0.10
Manganese (Mn)	0.40
Magnesium (Mg)	1.0
Chromium (Cr)	0.25
Zinc (Zn)	0.20
Titanium (Ti)	0.10

The mechanical properties of the material are listed in**Table 20**.

Table 20 Mechanical Properties of AA6082-T6

Yield [N/mm^2]	**Ultimate** [N/mm^2]	**Elongation** [%]
140	240	23

The specimen's geometry is shown in **Figure 46**. The plate thickness was 6 mm.

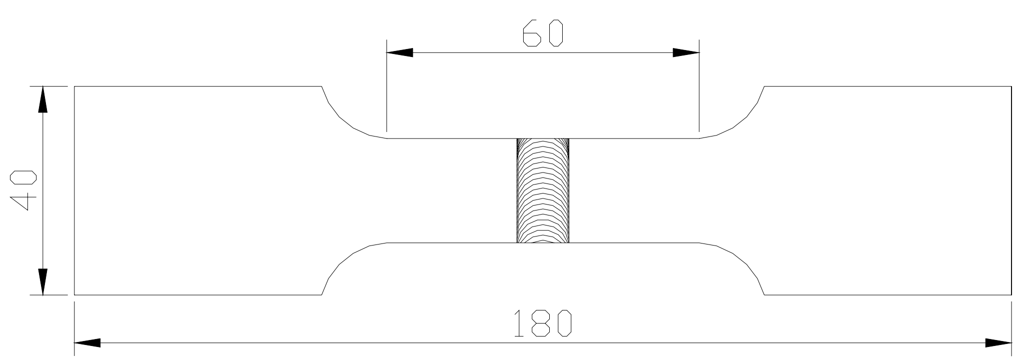

Figure 46 Specimen Geometry

Table 21 Experimental points from FSW-joints fatigue tests

Material: Aluminum alloy 6082-T6 **R = + 0.1**			
Specimen Nr.	**Stress Range, S [N/mm^2]**	**Cycles to Failure, N**	**Remarks**
1	100	275043	Fatigue failure in parent material
2	100	243673	Fatigue failure in parent material
3	100	263799	Fatigue failure in parent material
4	140	60007	Fatigue failure in parent material
5	140	64802	Fatigue failure in parent material
6	150	63440	Fatigue failure in parent material
7	150	46555	Fatigue failure in parent material
8	200	80000	Fatigue failure at the weld toe
9	150	400000	Fatigue failure at the weld toe
10	150	500000	Fatigue failure at the weld toe

The specimens were tested under axial loading in a servo-hydraulic machine at a frequency of 14 Hz. The R value was equal to +0.1. Unfortunately, no information on welding conditions is available. The test results are presented in**Table 21**. The fatigue failures in the first seven specimens initiated in the parent material as a result of grain imperfections on their surfaces. In fact, the heat input caused by friction stir welding had improved the fatigue strength properties in the welding zone. In the last three specimens, flushed to eliminate such imperfections, fatigue failure initiated, as expected, at the weld toe. In the statistical evaluations of results, these last three specimens were considered to obtain information about fatigue strength of the friction stir weld.

The equation of the regression line **(1)** and other information about the regression analysis are presented below, **Table 22**. Broken points were excluded from analysis.

$$LogN = -5.98 \times LogS + 18.67 \quad \textbf{(1)}$$

The Wöhler Diagram is presented in **Figure 47**.

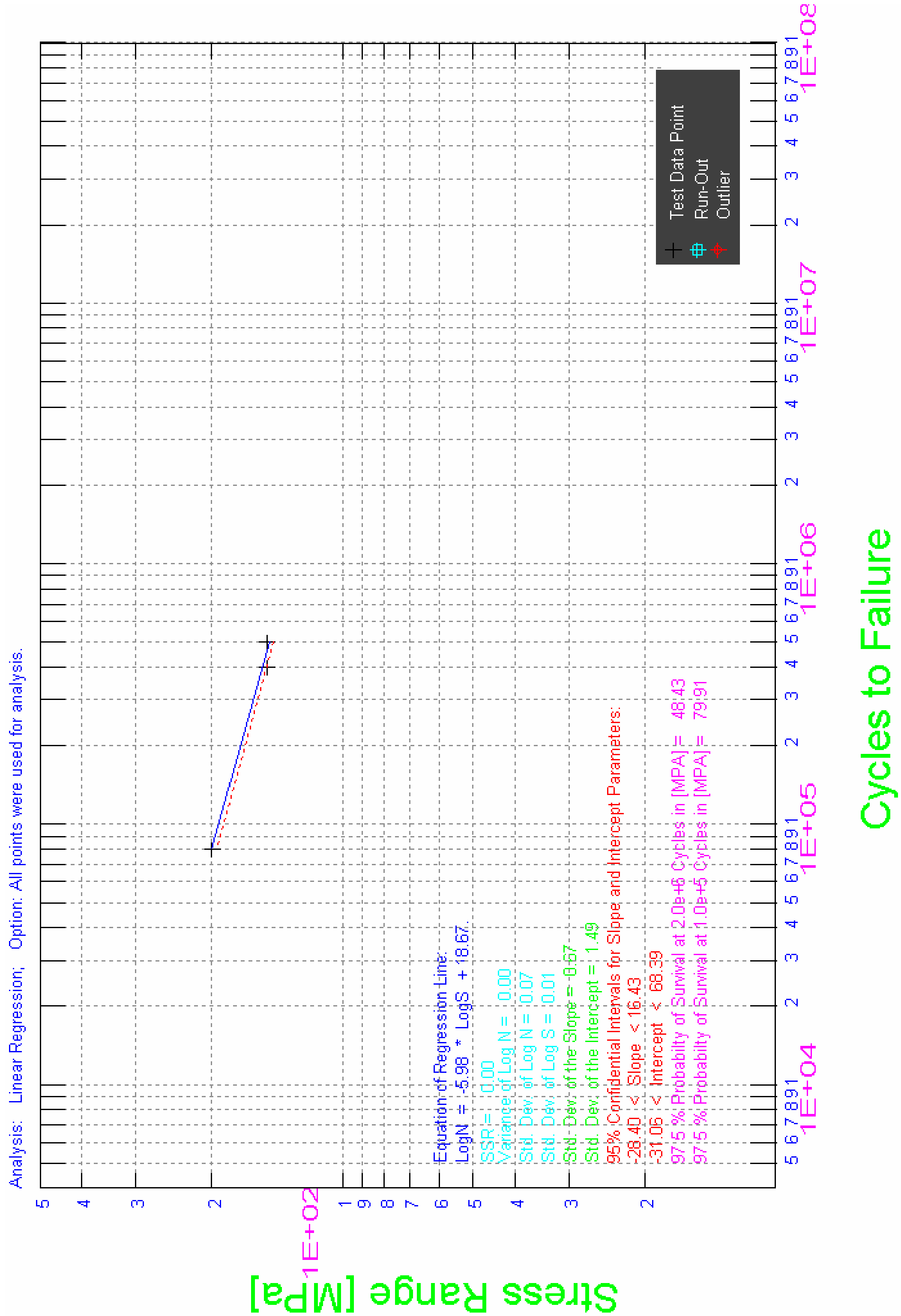

Figure 47 Wöhler Diagram for friction stir butt weld in aluminum alloy 6082-T6

Table 22 Results of Linear Regression Analysis

Average Values:			
Mean Log[Stress]:	2.22	Mean Log[Cycles]:	5.40
Variance and Standard Deviations:			
SSR:	0.00	Std. Dev. Log S:	0.01
Variance of LogN:	0.00	Std. Dev. Slope:	0.67
Std. Dev. LogN:	0.07	Std. Dev. Intercept :	1.49
95% Confidence Intervals for Slope and Intercept Parameters:			
-28.40 < Slope < 16.43		-31.06 < Intercept < 68.39	
Estimated Values:			
Estimated Mean Stress at 2E+06 Cycles to Failure [MPa]:			116.78
Estimated Mean Stress at 1E+05 Cycles to Failure [MPa]:			192.68
Estimated LogN Stress Range at 30 MPa:	LogN: 9.83	Cycles:	6791812235
Estimated LogN Stress Range at 50 MPa:	LogN: 8.50	Cycles:	319751641
Estimated LogN Stress Range at 100 MPa:	LogN: 6.70	Cycles:	5057680
Probability of Survival:			
97.5% Probability of Survival at 2E+06 Cycles in [MPa]:			48.43
97.5% Probability of Survival at 1E+05 Cycles in [MPa]:			79.91

In order to make a comparison with the fatigue strength of the parent material, a regression analysis was developed on the seven points where the failure occurred in the parent material. The equation of the regression line **(2)** and other information about the regression analysis are presented below, **Table 23**. Broken points were excluded from analysis.

$$LogN = -4.00 \times LogS + 13.41 \qquad \textbf{(2)}$$

The Wöhler Diagram is presented in **Figure 48**. The two Wöhler Diagrams are then compared in **Figure 49**, which shows the regression line obtained from the tests on the last three specimens is higher than the other because of the fatigue strength enhancement obtained by flushing. These can be considered only as indicative results because of the low number of specimens.

Table 23 Results of Linear Regression Analysis

Average Values:					
Mean Log[Stress]:	2.09	Mean Log[Cycles]:			5.04
Variance and Standard Deviations:					
SSR:	0.01	Std. Dev. Log S:			0.01
Variance of LogN:	0.00	Std. Dev. Slope:			0.25
Std. Dev. LogN:	0.05	Std. Dev. Intercept :			0.53
95% Confidence Intervals for Slope and Intercept Parameters:					
-4.98 < Slope < -3.01				11.35 < Intercept < 15.47	
Estimated Values:					
Estimated Mean Stress at 2E+06 Cycles to Failure [MPa]:					59.94
Estimated Mean Stress at 1E+05 Cycles to Failure [MPa]:					126.78
Estimated LogN Stress Range at 30 MPa:		LogN:	7.50	Cycles:	31848916
Estimated LogN Stress Range at 50 MPa:		LogN:	6.62	Cycles:	4129725
Estimated LogN Stress Range at 100 MPa:		LogN:	5.41	Cycles:	258286
Probability of Survival:					
97.5% Probability of Survival at 2E+06 Cycles in [MPa]:					53.12
97.5% Probability of Survival at 1E+05 Cycles in [MPa]:					112.36

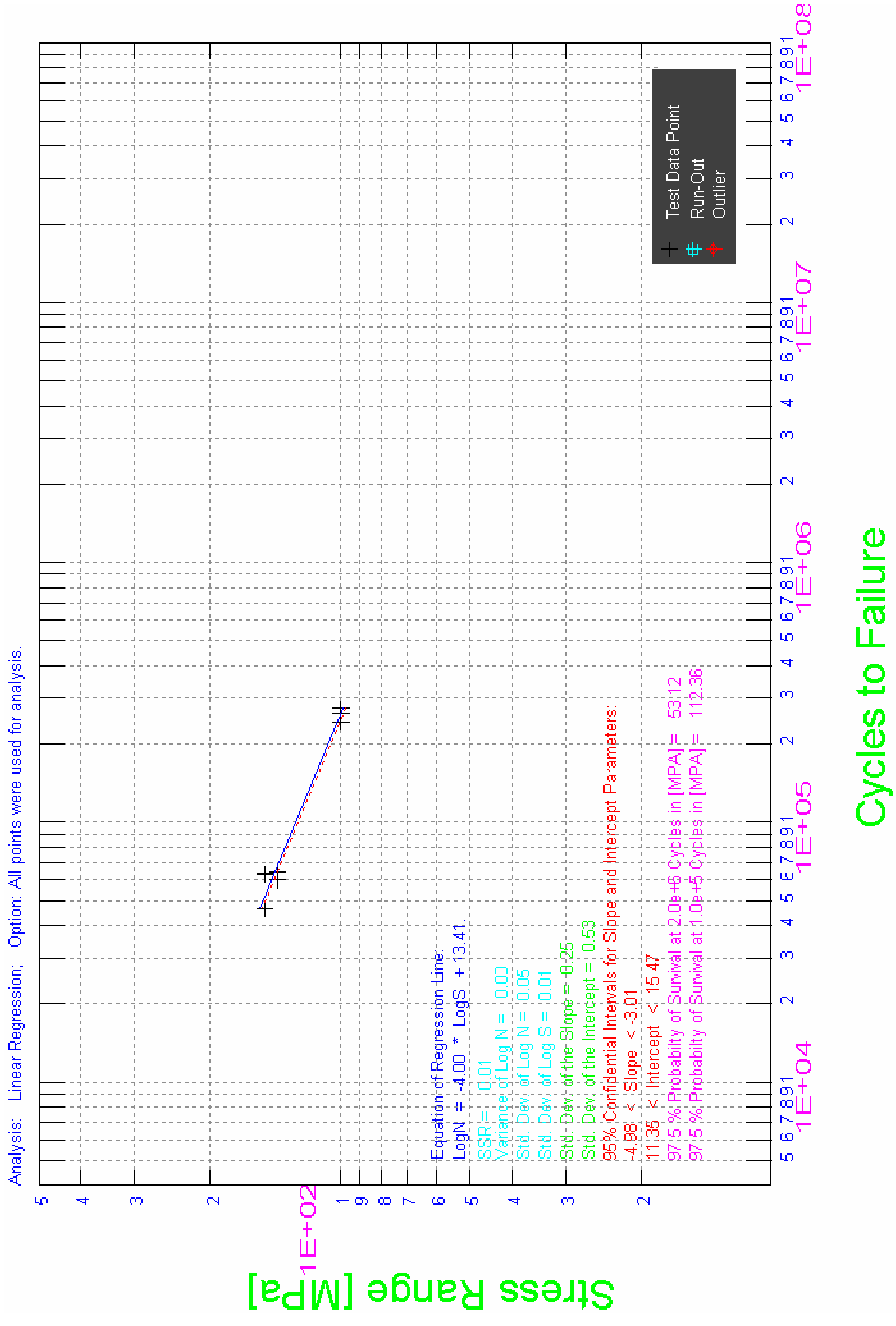

Figure 48 Wöhler Diagram for AA6082-T6 (failure occurred in parent material)

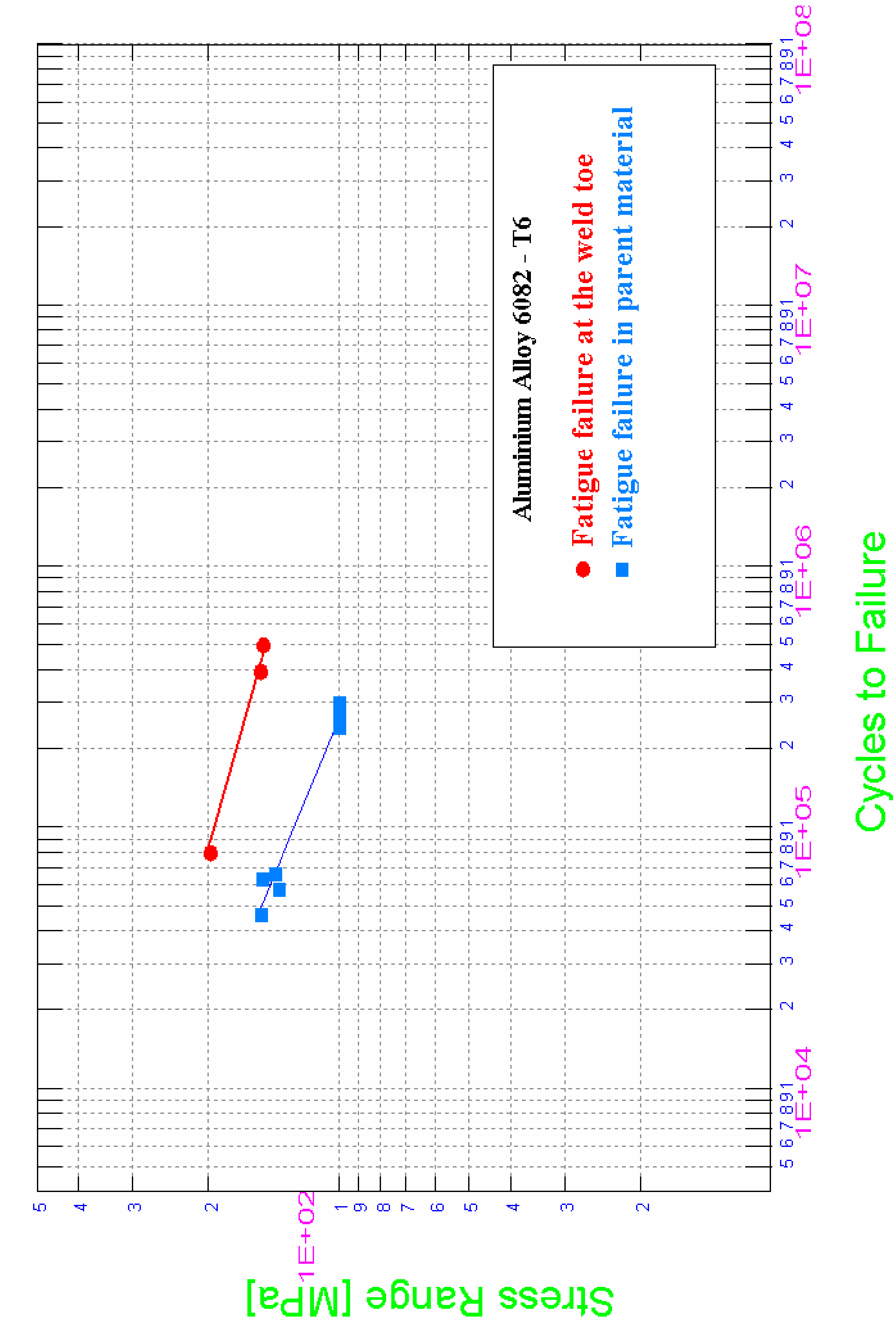

Figure 49 Comparison between the two Wöhler Diagrams

8.2.1.2 Data on Friction Stir Welds in Aluminum 6082 in the T4 and T6 Tempers

Other experimental data on AA6082 are presented in **Table 24** through **Table 28**. In this case AA6082 was friction stir welded in the T4 and T6 tempers. The aim was to determine fatigue properties of friction stir welded aluminum alloy 6082, T4 and T6 tempers when subjected to a post weld aging treatment (PWAT) to improve the static properties. To increase the ductility and toughness of the alloy, small amounts of manganese were added (typically around 0.7wt%). A solution heat treatment was executed at 530-550°C, followed by quenching to room temperature. The solid solution then became supersaturated. The T4 temper is referred to as the condition obtained if the material is allowed to age naturally at room temperature. The T6 condition is obtained through artificial aging at an elevated temperature of 170-200°C. The welds in the T4 alloy were further post weld heat treated (PWAT), which enhances yield- and tensile properties to those of the base material in the T6 condition. The post weld heat treatment consisted of artificially aging at 185°C for 5 hours, which gives re-precipitation of the hardening particles. Through this process about 90% HAZ strength recovery can be achieved, resulting in a considerable increase in the strength of the material. A servo-hydraulic testing machine equipped with an actuator of 250kN load capacity was used to determine the fatigue properties of the welds. The dimensions of the pieces tested were 260 x 70 x 5.8mm (length x width x thickness). The stress ratio R of the sinusoidal curve function was set to +0.5. Average stresses in the range of 105 to 165 MPa were tested. The frequency was adjusted in the range from 9 Hz to 15 Hz.

Table 24 Experimental points from FSW-joints fatigue tests

Material: Aluminum Alloy 6082-T4 **R = + 0.5**			
Specimen Nr.	**Stress Range, S [N/mm^2]**	**Cycles to Failure, N**	**Remarks**
1	70	1400000	Failure
2	70	1500000	Failure
3	80	1000000	Failure
4	80	900000	Failure
5	80	700000	Failure
6	90	500000	Failure
7	90	450000	Failure
8	90	400000	Failure
9	100	400000	Failure
10	100	250000	Failure
11	100	200000	Failure
12	110	120000	Failure

For T4+PWAT the fractures, for more than half of the specimens, were in the weld area. They occurred near the weld center or halfway between the center and the weld/HAZ border on the shear side of the weld. For the rest of the specimens the fracture was located in the thermo-mechanically affected zone, or in some case in the base material, probably as a consequence of

PWAT treatment. The equation of the regression line **(3)** and other information about the regression analysis are presented below, **Table 25**.

$$LogN = -5.18xLogS + 15.76 \qquad \textbf{(3)}$$

The Wöhler Diagram is presented in **Figure 50**.

Table 25 Results of Linear Regression Analysis

Average Values:			
Mean Log[Stress]:	1.94	Mean Log[Cycles]:	5.70
Variance and Standard Deviations:			
SSR:	0.09	Std. Dev. Log S:	0.02
Variance of LogN:	0.01	Std. Dev. Slope:	0.44
Std. Dev. LogN:	0.09	Std. Dev. Intercept :	0.86
95% Confidence Intervals for Slope and Intercept Parameters:			
-6.55 < Slope <-3.80		13.09 < Intercept < 18.42	
Estimated Values:			
Estimated Mean Stress at 2E+06 Cycles to Failure [MPa]:			67.10
Estimated Mean Stress at 1E+05 Cycles to Failure [MPa]:			119.70
Estimated LogN Stress Range at 30 MPa:	LogN: 8.11	Cycles:	129010425
Estimated LogN Stress Range at 50 MPa:	LogN: 6.96	Cycles:	9170064
Estimated LogN Stress Range at 100 MPa:	LogN: 5.40	Cycles:	253683
Probability of Survival:			
97.5% Probability of Survival at 2E+06 Cycles in [MPa]:			59.06
97.5% Probability of Survival at 1E+05 Cycles in [MPa]:			105.35

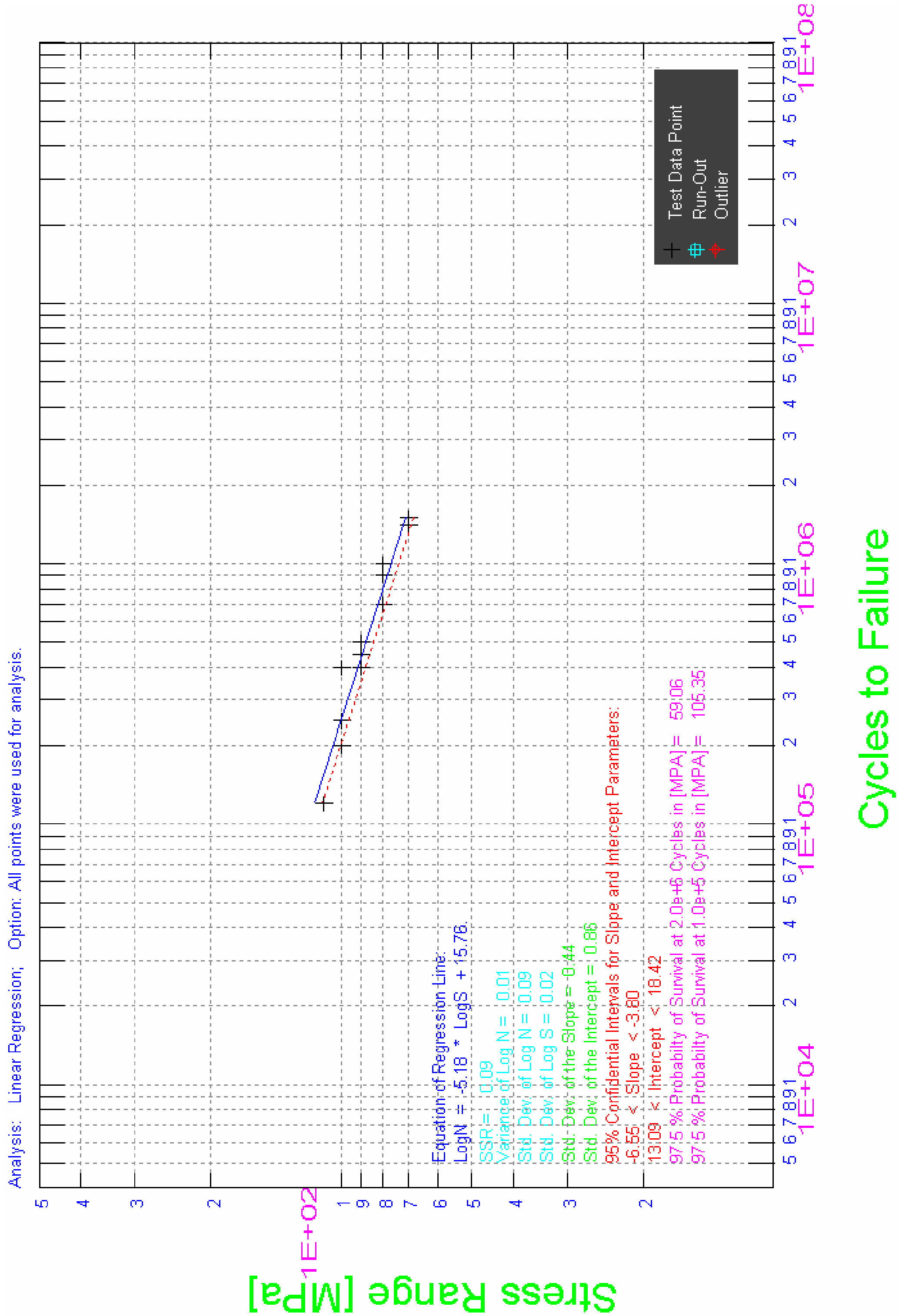

Figure 50 Wöhler Diagram for AA6082-T4 Friction Stir Welds R=0.5

The process parameters concerning the friction stir welding processes are listed in **Table 26**.

Table 26 Friction Stir Welding Process Parameters

FSW Parameters	Value	Description
Travel speed	350 mm/min	Horizontal speed
Rotating speed	1000 rpm	Rotating speed of pin tool
Shoulder Diameter	20 mm	Shoulder diameter of the tool

Table 27 Experimental points from FSW-joints fatigue tests

Material: Aluminum alloy 6082-T6 **R = + 0.5**			
Specimens Nr.	**Stress Range, S [N/mm^2]**	**Cycles to Failure, N**	**Remarks**
1	110	100000	Failure
2	110	180000	Failure
3	110	270000	Failure
4	110	300000	Failure
5	110	350000	Failure
6	100	120000	Failure
7	100	180000	Failure
8	100	200000	Failure
9	100	480000	Failure
10	100	600000	Failure
11	92	800000	Failure
12	90	250000	Failure
13	90	500000	Failure
14	90	700000	Failure
15	90	800000	Failure
16	90	900000	Failure
17	80	480000	Failure
18	80	1400000	Failure
19	80	1500000	Failure
20	80	1800000	Failure
21	80	1850000	Failure
22	80	2100000	Failure
23	70	2000000	Failure
24	68	700000	Failure
25	68	2500000	Failure
26	68	3000000	Failure
27	68	> 4500000	Run Out
28	50	> 3500000	Run Out

For the T6 material all samples went to fracture at the side of the weld that contains the rougher welding edge, resulting from the rotating action of the tool. This is the shear side of the weld, where the relative difference in velocity between tool and work piece is the largest and thereby also the welding induced residual stresses. The fracture is in the border area weld/HAZ, which is the softest area in the material. Fracture has in some cases (high stress) been initiated in the weld, slightly on the inside of the rough edge. The cracks initiated at the top or root edges of the specimens, alternatively grew out to the edge and then went into the material again. The equation of the regression line **(4)** and other information about the regression analysis are presented below, **Table 28**.

$$LogN = -5.06 x LogS + 15.65 \qquad \textbf{(4)}$$

The Wöhler Diagram is presented in **Figure 51**.

Table 28 Results of Linear Regression Analysis

Average Values:					
Mean Log[Stress]:	1.95	Mean Log[Cycles]:			5.78
Variance and Standard Deviations:					
SSR:	1.50	Std. Dev. Log S:			0.05
Variance of LogN:	0.06	Std. Dev. Slope:			0.72
Std. Dev. LogN:	0.25	Std. Dev. Intercept :			1.41
95% Confidence Intervals for Slope and Intercept Parameters:					
-6.55 < Slope <-3.80			13.09 < Intercept < 18.42		
Estimated Values:					
Estimated Mean Stress at 2E+06 Cycles to Failure [MPa]:					70.44
Estimated Mean Stress at 1E+05 Cycles to Failure [MPa]:					127.36
Estimated LogN Stress Range at 30 MPa:		LogN:	8.18	Cycles:	150101110
Estimated LogN Stress Range at 50 MPa:		LogN:	7.05	Cycles:	11327182
Estimated LogN Stress Range at 100 MPa:		LogN:	5.53	Cycles:	339866
Probability of Survival:					
97.5% Probability of Survival at 2E+06 Cycles in [MPa]:					51.57
97.5% Probability of Survival at 1E+05 Cycles in [MPa]:					93.23

The results show that the fatigue strength of T4 + PWAT is lower than for T6. This was not expected since the T4 + PWAT welded material is statically stronger.

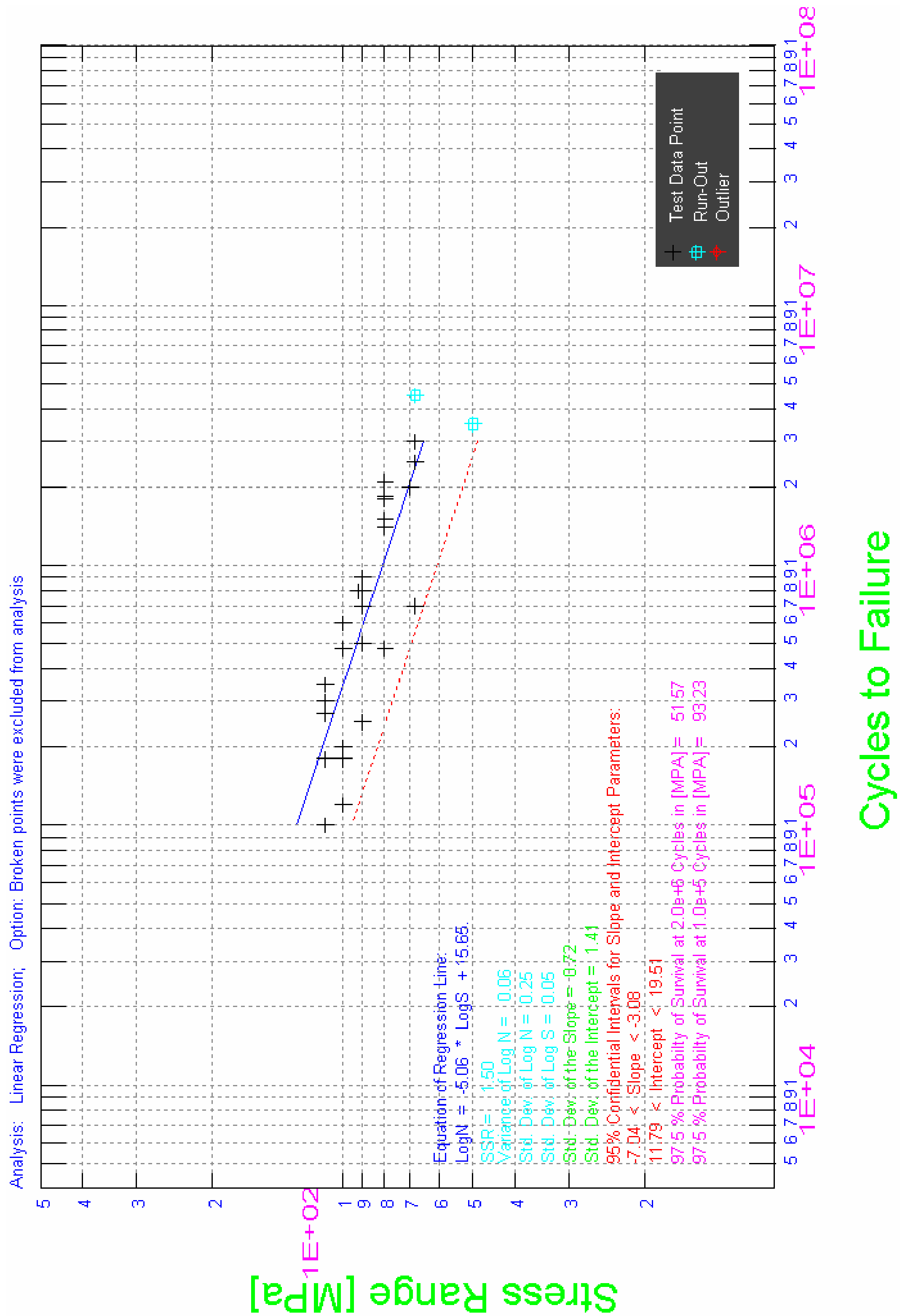

Figure 51 Wöhler Diagram for AA6082-T6 Friction Stir Welds (R=0.5)

8.2.1.3 Additional Wöhler Diagram for Aluminum 6082-T4

Another Wöhler Diagram was found in the literature for AA6082-T4. The Diagram derives from a testing program to determine the fatigue properties of transverse butt welding of extruded plates in aluminum alloy 6082-T4. The plate thickness was 5 mm. The results of mechanical strength tests on these specimens are listed in**Table 29**.

Table 29 Mechanical Properties of AA6082
8.2.1.3.1

Yield [N/mm^2]	Ultimate [N/mm^2]	Elongation [%]
153	258	26

The geometry and dimensions of the specimens used in S-N tests are shown in **Figure 52**.

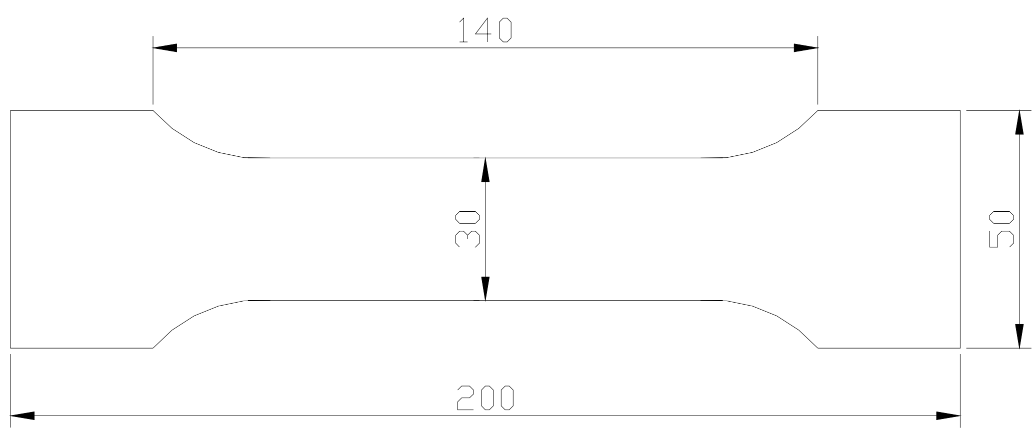

Figure 52 Specimen Geometry

In this case there is also information on process parameters: the Friction Stir Welding was performed by means of a 7.5 kW Köpings milling machine. The rotating tool consists of a 15 mm diameter cylindrical part made of high strength die steel, H13. The high strength steel pin had a diameter of 6 mm. Other information on FSW process is listed in **Table 30**. The specimens were tested under axial loading in a servo-hydraulic fatigue testing machine equipped with an actuator of 10kN load capacity. Testing was performed at a room temperature of approximately 20°C. Test frequency was 10 Hz.

The tests were run at a load ratio of R = +0.5. The applied load ranges were selected to produce fatigue lives in the range of 10^5 to 10^6 cycles. Failure was defined to have taken place when the specimen had separated into two parts. The Wöhler Diagram is presented in **Figure 53**.
The regression line is **(5):**

$$LogN = -5.33xLogS + 15.62 \qquad \textbf{(5)}$$

Other information about the regression analysis is presented in **Table 31**.

Table 30 Friction Stir Welding Process parameters

FSW Parameters	Value	Description
Travel speed	500 mm/min	Millimeter-per-minute horizontal speed
Rotating speed	1150 rev./min	Rotating speed of pin tool

Table 31 Details of mean life S-N curve obtained from regression analysis of test results

<table>
<tr><th colspan="2">S-N curve:
$N(\Delta S)^m = C$</th><th rowspan="2">Standard deviation of logN</th><th colspan="2">Fatigue strength at $2*10^6$ cycles</th></tr>
<tr><th>m</th><th>C</th><th>Stress range ΔS_{2mill}</th><th>Percent of base material fatigue strength</th></tr>
<tr><td>5.35</td><td>$4.164*10^{15}$</td><td>0.05</td><td>56</td><td>50</td></tr>
</table>

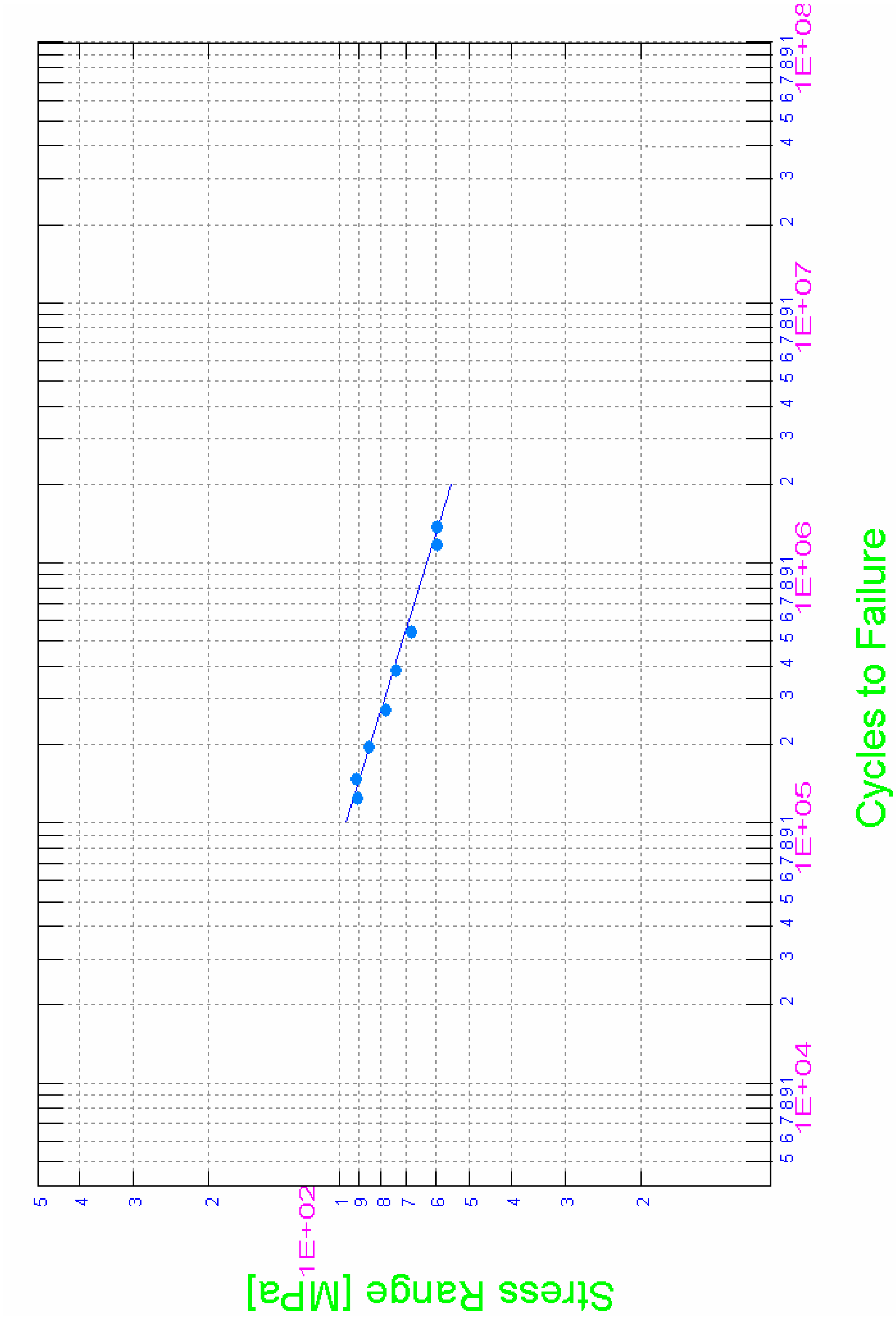

Figure 53 Wöhler Diagram for friction stir welds in aluminum alloy 6082-T4

8.2.2 Fatigue Behavior of Friction Stir Welds on Other 6XXX Aluminum Alloys

8.2.2.1 Experimental Data on Aluminum Alloy A6N01-T5

Experimental data from fatigue tests on an aluminum deck fabricated by friction stir welding [61] were carried out for the deck and "beam-type" specimens provided by cutting the deck in the transverse direction. The aluminum is A6N01S-T5. The chemical composition of the aluminum alloy is in **Table 32** together with the values specified in the Japanese Industrial Standard (JIS).

Table 32 Chemical Composition of A6N01S-T5

	Si	**Fe**	**Cu**	**Mn**	**Mg**	**Cr**	**Zn**	**Ti**
Measured values (%)	0.51-0.53	0.16	0.08-0.09	0.14-0.15	0.69	0.01	0.01	0.02-0.03
JIS-values (%)	0.40-0.90	≤ 0.35	≤ 0.35	≤ 0.50	0.40-0.80	≤ 0.30	≤ 0.25	≤ 0.10

The chemical composition of this aluminum alloy is similar to the one specified for aluminum alloy 6008, **Table 33**.

Table 33 Tab. 15 Chemical Composition of Aluminum Alloy 6008

Si	**Fe**	**Cu**	**Mn**	**Mg**	**Cr**	**Zn**	**Ti**
0.50-0.90	≤ 0.35	≤ 0.30	≤ 0.30	0.40-0.70	≤ 0.30	≤ 0.20	≤ 0.10

The beam-type specimens, provided by cutting the deck in the transverse direction, have the friction stir weld in the middle of the top and bottom flanges. The load of R = +0.1 was applied on the 10 cm width at the span centre, **Figure 54**. The fatigue crack was initiated on the lower surface of the bottom flange at the FSW. It propagated on the cross section of the specimen, and the specimen broke into two pieces due to brittle fracture.

The equation of the regression line for the beam-type specimens **(6)** shows a slope approximately equal to 3.

$$LogN = -3.23xLogS + 12.3 \qquad \textbf{(6)}$$

The standard deviation ξ_N of logN about the arbitrary logS is 0.106.

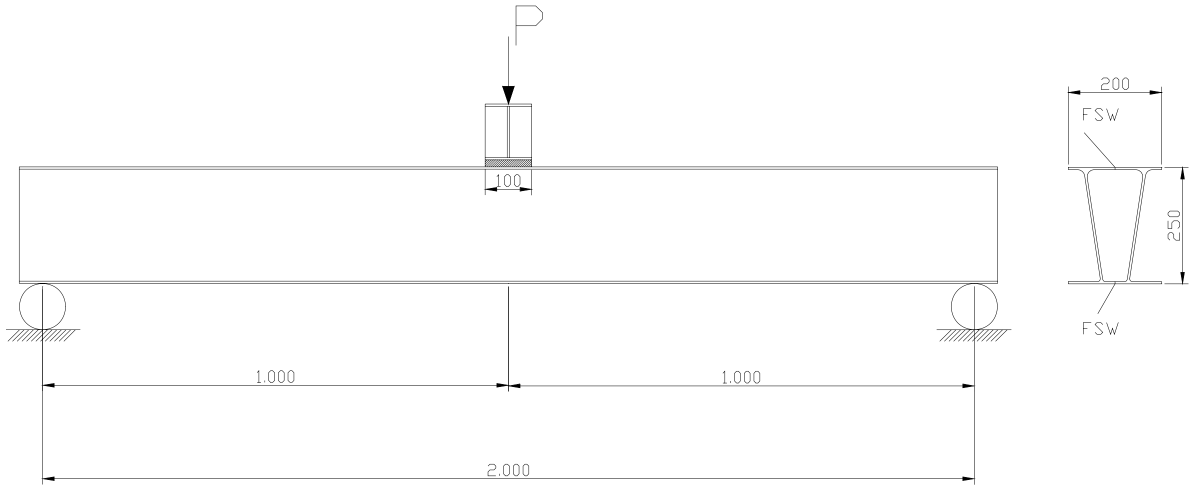

Figure 54 Beam-type Specimen

In this case, the friction stir weld is loaded longitudinally. The results of this fatigue test are much higher than the S-N curve of the longitudinal butt welds specified in “EC 9- Proposal for NAD and Corrections” (see Table Detail Category $\Delta\sigma$ – m_1:60-4.3) as shown in **Figure 55**.

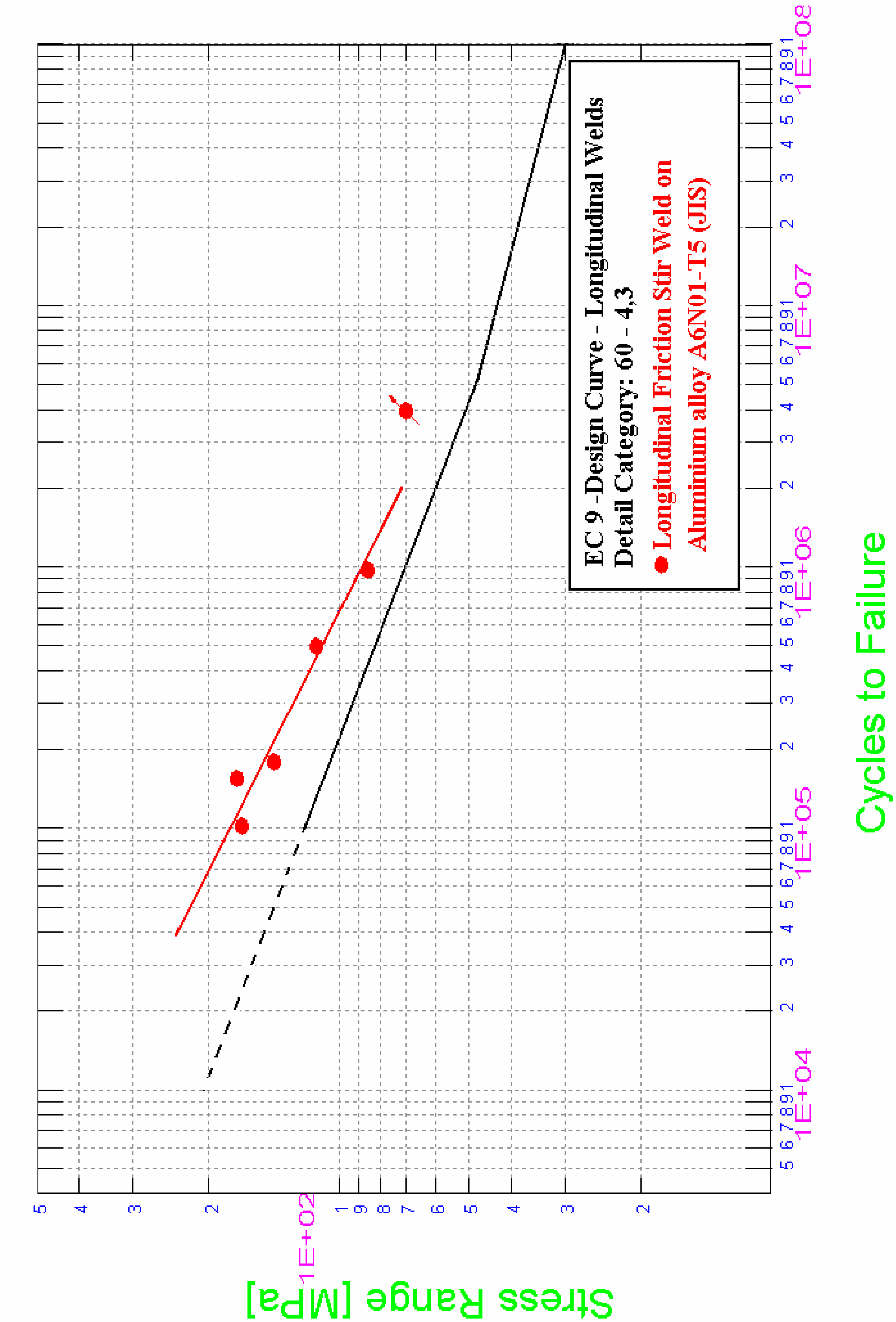

Figure 55 Comparison between Wöhler Diagram for friction stir welds in A6N01-T5 (Japanese Industrial Standard) and design curve for longitudinal butt welds

8.2.3 Experimental Data from Fatigue Tests on Transverse FSW Butt Welds on Aluminum Alloy 6013-T6

Experimental data for the fatigue strength of friction stir welds on aluminum alloy 6013-T6 are presented below [63]. The objective was to characterize the mechanical properties of butt welds produced in three different aerospace aluminum alloys using Friction Stir Welding. The FSW was performed at SAPA Finspång. The mechanical properties evaluated were tensile strength at room temperature, bend performance and fatigue strength. The properties were tested transverse to the weld. Static strength and bending properties were found superior to what is usually achieved with conventional welding methods. The fatigue strength was tested using test specimens in the as-welded condition as well as after surface milling of the top weld. Strips of thin sheet material were FSW welded at SAPA Finspång. The strips were welded in a fixture using square butt joints oriented in the longitudinal direction of the sheet. The welded blanks had the dimensions 140 x 700 mm and were used for fabrication of test specimens. The welding tool is referred to as "Standard Tool" in "Patent no. US 5813592". The pin diameter was 0.4 mm. **Table 34** outlines the welding parameters used.

Table 34 Welding Data

Alloy and condition At welding	Type of alloy	Material thickness (mm)	Rotational Speed (rpm)	Traveling Speed (mm/min)
6013 – T4	AlMgSi	1.6	2000	208

Welded blanks of each alloy were inspected using visual inspection and radiography. The visual inspection revealed that the degree of burrs formed on the advancing side of the weld was very high for the 6013 alloy. Radiographs on welds of 6013 were without remarks. The blanks of 6013 T4 were artificially aged to the T6 condition. Plain un-notched specimens were used in the fatigue testing of the FSW welds, as shown in **Figure 56**. The specimens were tested both in the as-welded condition and after flush milling of both the weld topside and the root side. By the milling operation 0.10 to 0.15 mm material was removed from the weld and the sheet adjacent to the weld. The fatigue testing was carried out with constant amplitude at the stress ratio R = +0.1. The loading frequency was 25 Hz.

Two different regression analyses have been carried out for the specimens in the as-welded condition and for the specimens after flush milling.

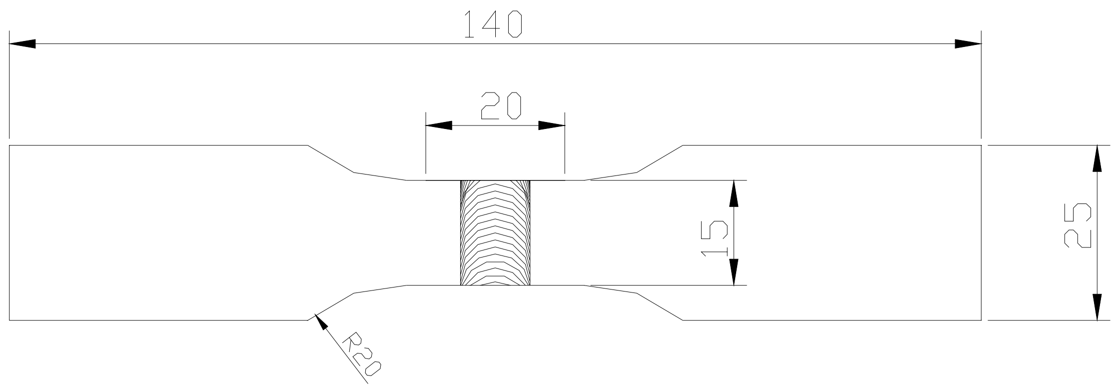

Figure 56 Specimen Geometry

The test results for the specimens in the as welded conditions are presented in **Table 35**.

Table 35 Experimental points from fatigue tests – FSW as welded

Material: Aluminum alloy 6013-T6 **R = + 0.1**			
Specimens Nr.	**Stress Range, S [N/mm^2]**	**Cycles to Failure**	**Remarks**
1	225	50000	Failure
2	225	60000	Failure
3	205	95000	Failure
4	205	100000	Failure
5	190	160000	Failure
6	190	250000	Failure
7	170	210000	Failure
8	155	600000	Failure
9	155	2000000	Failure

The equation of the regression line **(7)** and the Wöhler Diagram, **Figure 57**, are presented below.

$$LogN = -7.61xLogS + 22.60 \tag{7}$$

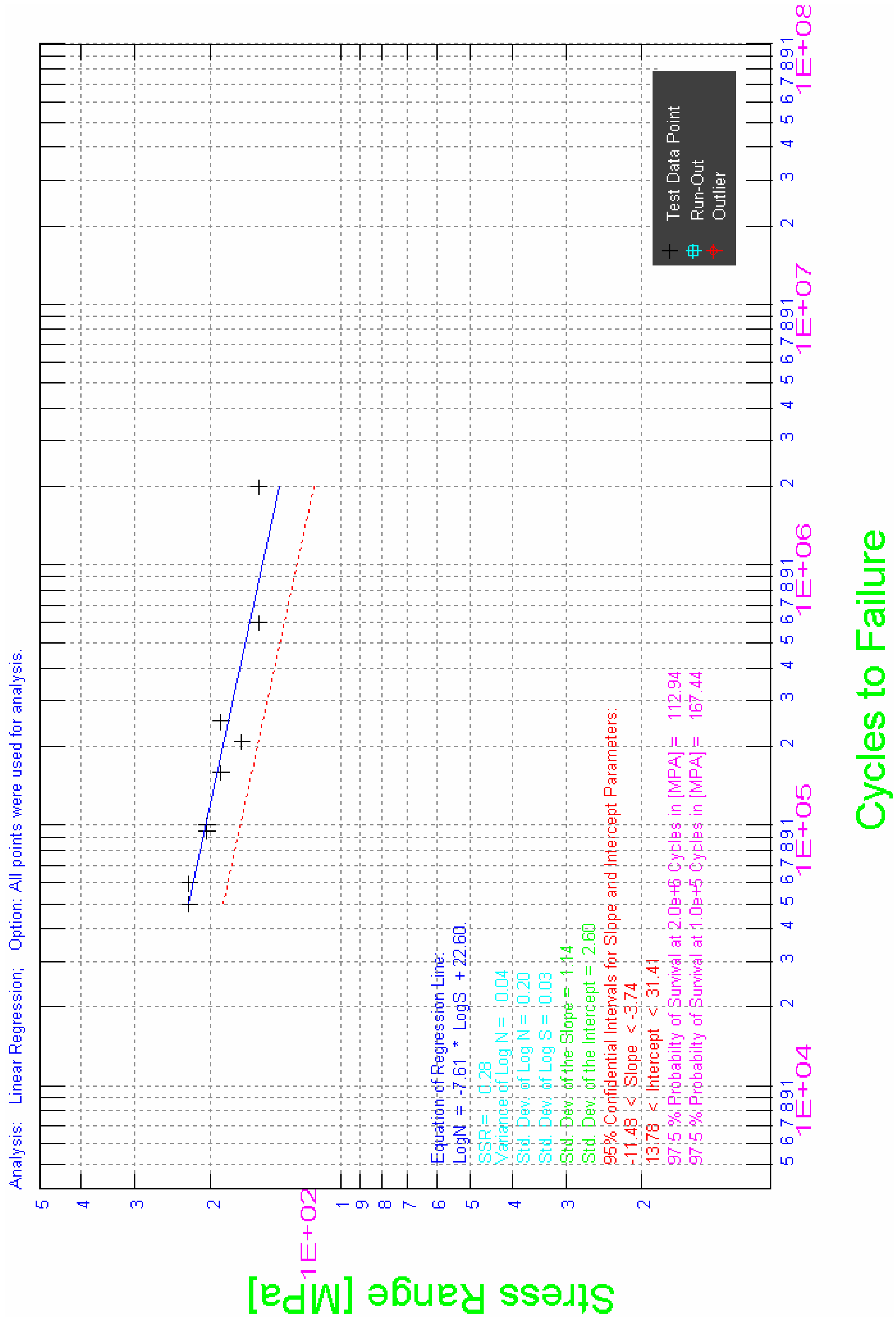

Figure 57 Wöhler Diagram for FSW butt welds in the as welded conditions on aluminum alloy 6013–T6

Other information about the regression analysis is listed in **Table 36**.

Table 36 Results of Linear Regression Analysis

Average Values:			
Mean Log[Stress]:	2.28	Mean Log[Cycles]:	5.27
Variance and Standard Deviations:			
SSR:	0.28	Std. Dev. Log S:	0.03
Variance of LogN:	0.04	Std. Dev. Slope:	1.14
Std. Dev. LogN:	0.20	Std. Dev. Intercept :	2.60
95% Confidence Intervals for Slope and Intercept Parameters:			
-11.48 < Slope <-3.74		13.78 < Intercept < 31.41	
Estimated Values:			
Estimated Mean Stress at 2E+06 Cycles to Failure [MPa]:			138.76
Estimated Mean Stress at 1E+05 Cycles to Failure [MPa]:			205.73
Estimated LogN Stress Range at 30 MPa:	LogN: 11.36	Cycles:	229652659491
Estimated LogN Stress Range at 50 MPa:	LogN: 9.67	Cycles:	4713957771
Estimated LogN Stress Range at 100 MPa:	LogN: 7.38	Cycles:	24173457
Probability of Survival:			
97.5% Probability of Survival at 2E+06 Cycles in [MPa]:			112.94
97.5% Probability of Survival at 1E+05 Cycles in [MPa]:			167.44

The test results for the specimens in the as welded conditions are presented in **Table 37**.

Table 37 Experimental points from fatigue tests – FSW as milled

Material: Aluminum alloy 6013-T6 **R = + 0.1**			
Specimens Nr.	**Stress Range, S [N/mm^2]**	**Cycles to Failure**	**Remarks**
1	240	40000	Failure
2	240	50000	Failure
3	225	110000	Failure
4	225	130000	Failure
5	205	300000	Failure
6	205	220000	Failure
7	190	350000	Failure
8	190	500000	Failure
9	190	2000000	Failure
10	190	> 6000000	Run Out

The equation of the regression line **(8)** and the Wöhler Diagram, **Figure 58**, are presented below. The unbroken specimen was excluded from analysis.

$$LogN = -11.35xLogS + 31.70 \quad \textbf{(8)}$$

Other information about the regression analysis is presented in **Table 38**.

Table 38 Results of Linear Regression Analysis

Average Values:					
Mean Log[Stress]:	2.32	Mean Log[Cycles]:			5.31
Variance and Standard Deviations:					
SSR:	0.36	Std. Dev. Log S:			0.02
Variance of LogN:	0.05	Std. Dev. Slope:			1.88
Std. Dev. LogN:	0.23	Std. Dev. Intercept :			4.38
95% Confidence Intervals for Slope and Intercept Parameters:					
-17.73 < Slope <-4.97			16.86 < Intercept < 46.53		
Estimated Values:					
Estimated Mean Stress at 2E+06 Cycles to Failure [MPa]:					172.95
Estimated Mean Stress at 1E+05 Cycles to Failure [MPa]:					225.20
Estimated LogN Stress Range at 30 MPa:		LogN:	14.93	Cycles:	59150512898188
Estimated LogN Stress Range at 50 MPa:		LogN:	12.42	Cycles:	2610009709881
Estimated LogN Stress Range at 100 MPa:		LogN:	9.00	Cycles:	1001627773
Probability of Survival:					
97.5% Probability of Survival at 2E+06 Cycles in [MPa]:					148.10
97.5% Probability of Survival at 1E+05 Cycles in [MPa]:					192.85

These results highlight that, although the fatigue strength of friction stir welds is always very high, for optimal fatigue properties milling of the FSW top surface is necessary. Actually, the fatigue tests indicated that milling of the topside of the weld increased the fatigue strength to approach that of parent material.

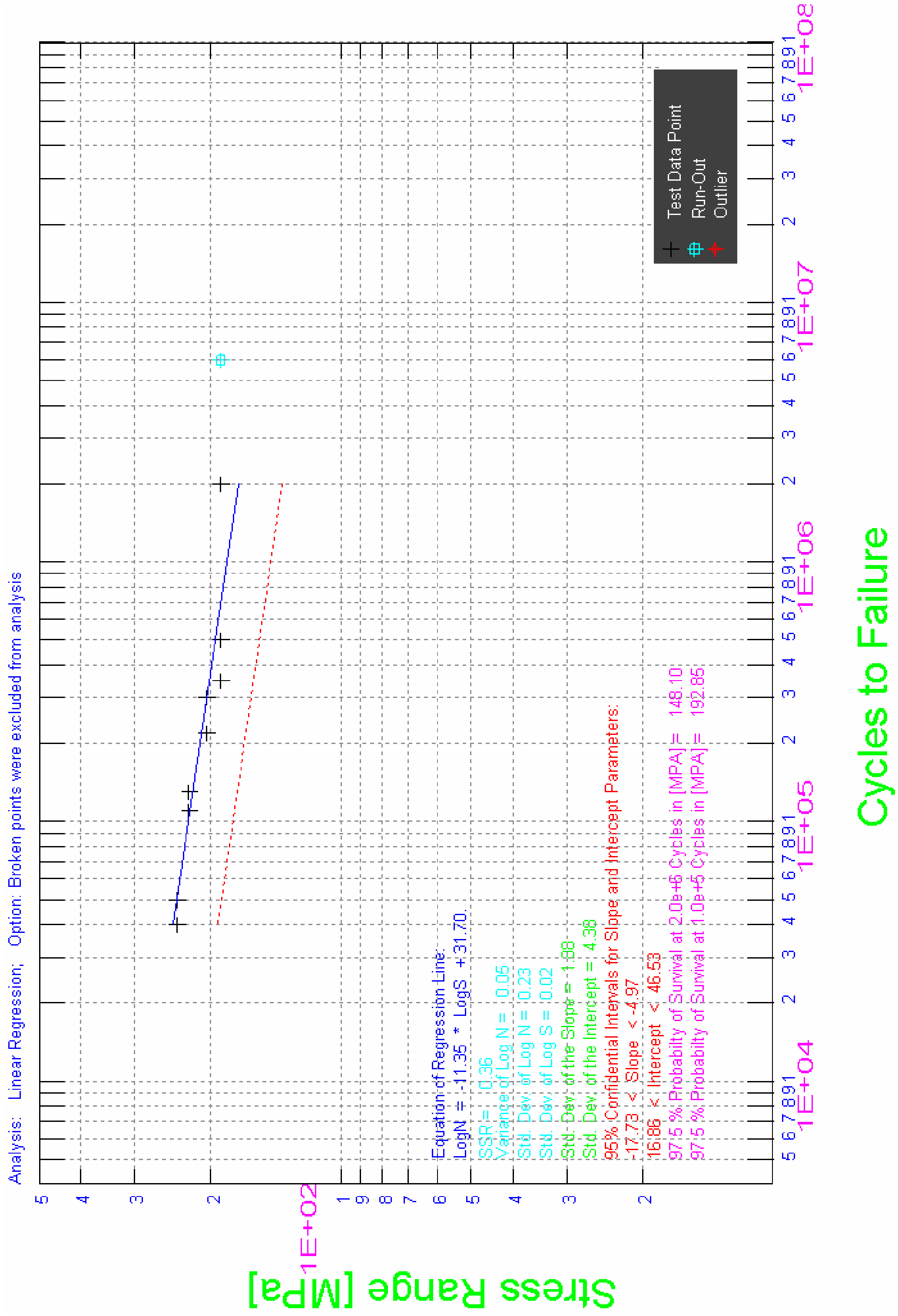

Figure 58 Wöhler Diagram for FSW butt welds in the as milled conditions on aluminum alloy 6013 – T6

8.3 Conclusions on Friction Stir Welding

All the experimental points and the regression lines (mean values) found in the literature for transverse friction stir welds without surface post-treatment on aluminum alloys 6XXX have been compared with the fatigue strength of butt welds obtained by means of other techniques, **Figure 59**. The data in the "Aluminum Data Bank" (TUM) came from fatigue tests on small specimens or on extruded beams in aluminum alloys containing transverse butt welds.

A linear regression analysis has been developed on these experimental points. The equation of the regression line **(9)** is shown below.

$$LogN = -3.77xLogS + 12.73 \quad \mathbf{(9)}$$

As expected, the experimental points found in literature for transverse butt welds obtained by means of Friction Stir Welding are in almost all cases above this regression line.

The same experimental points found in literature are shown in **Figure 60** in comparison with Design Standards in order to verify the applicability of existing design rules to this relatively new fabrication process.

The considered design standards are the ones stated in "Proposal for NAD and Corrections (November 1998)". Different detail categories were considered in order to make a comparison (see "Proposal for NAD and Corrections (November 1998)" Table 5.14 "Detail Categories for Welded Joints between Members"). The design curve for the detail category $\Delta\sigma$-m_1 55-7.0 means MIG transverse butt welds with overfill dressed flush from both sides is generally higher than the experimental points found in literature, but can not be accepted as a design curve for friction stir welds without surface post-treatment.

The best choice seems to be the detail category 40 – 4.3 the single sided butt weld unbacked with full penetration.

If a general conclusion must be reached from this literature survey on friction stir welds, it has to be stated that friction stir welding is an excellent way to join aluminum alloys. After a post-treatment of the FSW top surface, such as milling, the fatigue strength is further increased and approaches that of parent material.

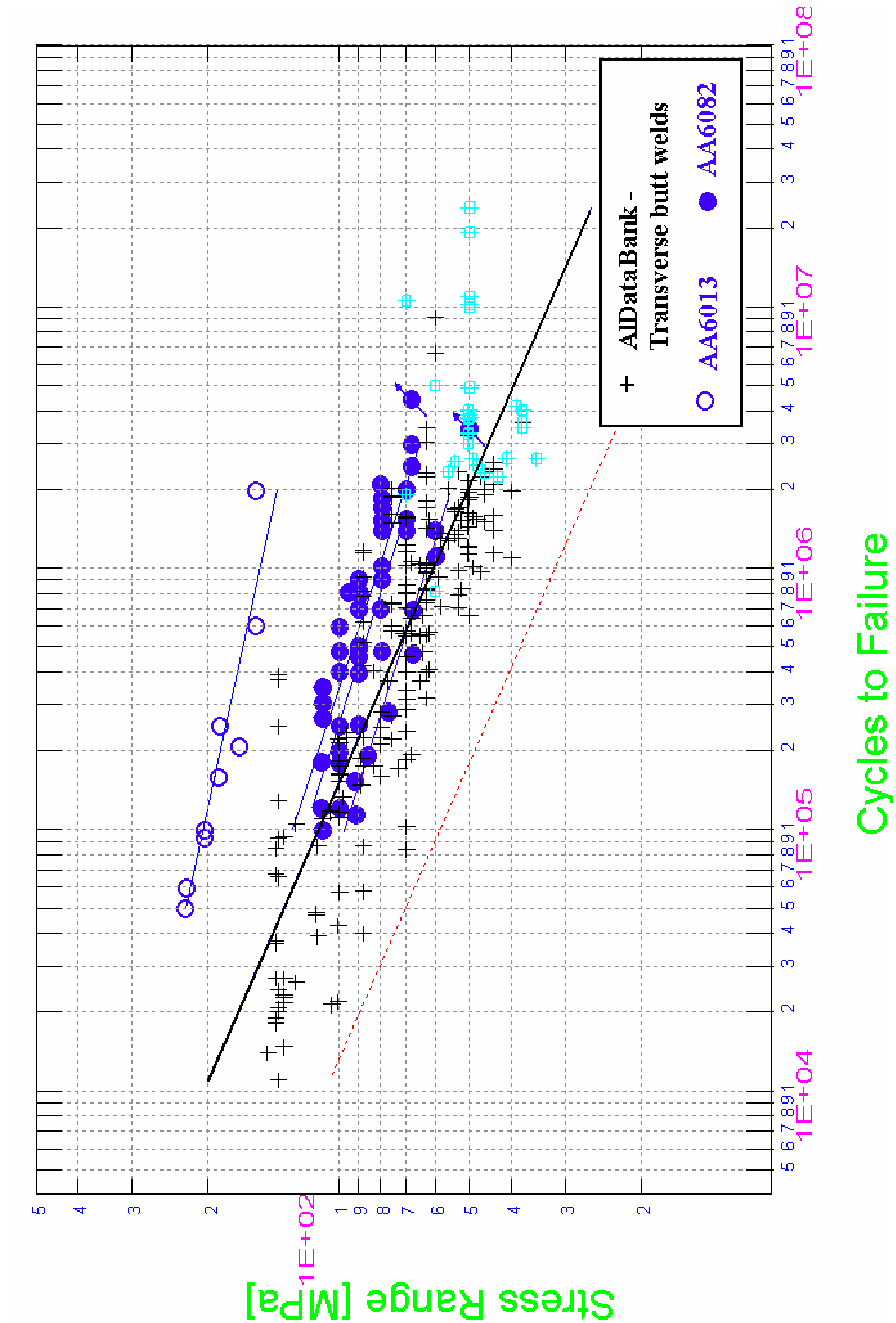

Figure 59 Transverse friction stir welds no surface post-treatment compared to fatigue strength of transverse butt welds (Aluminum Data Bank – TUM)

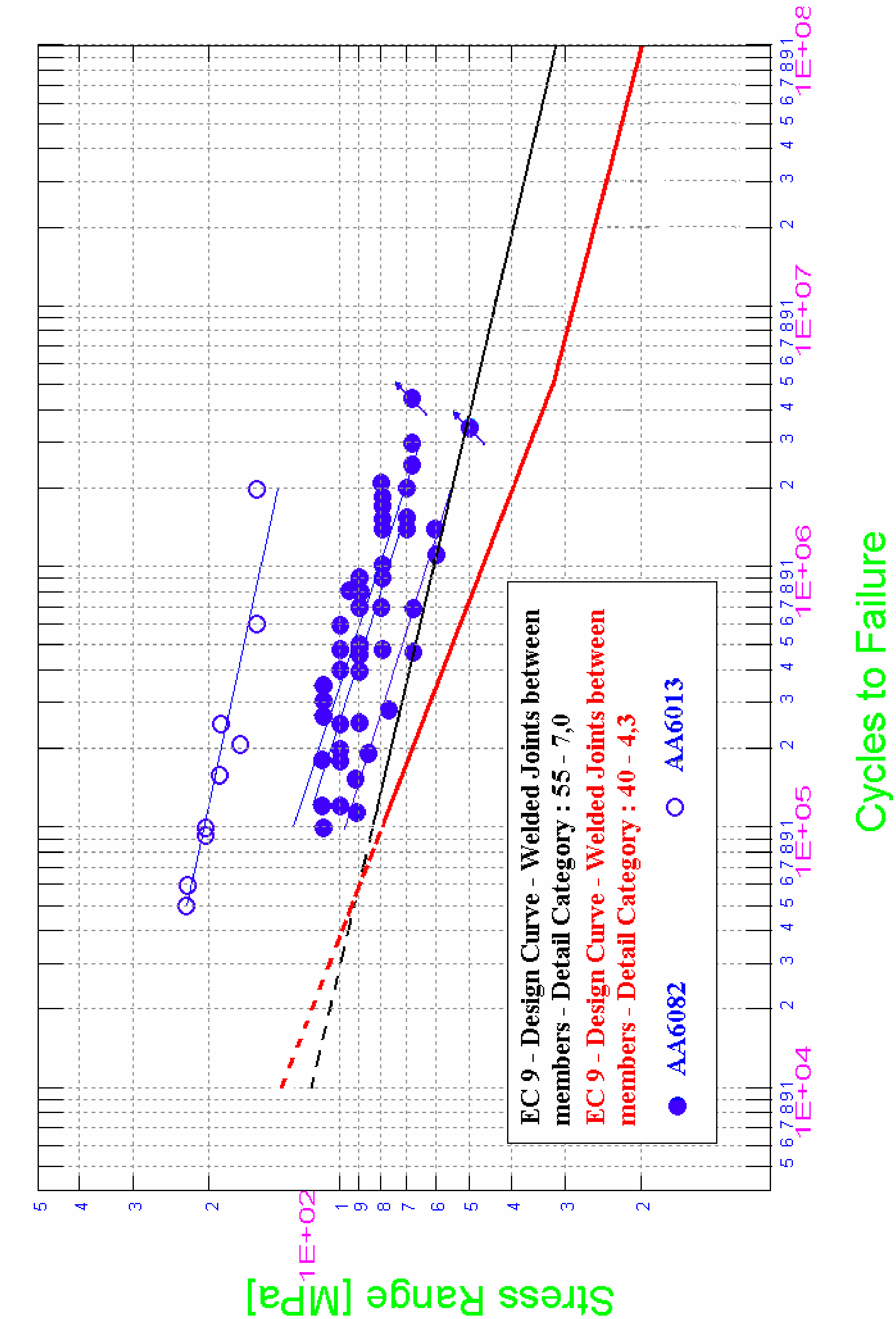

Figure 60 Transverse friction stir welds without surface post-treatment on aluminum alloys 6XXX compared with Design Standards

9. CONCLUSIONS AND RECOMMENDATIONS

Their is a significant volume of additional work that has been done and information that is available regarding fatigue of aluminum joints, friction stir welding and a comparison of fatigue performances using FSW and traditional fusion welding procedures. In addition, a lot of work has also been developed on damage tolerance and crack propagation in aluminum details. The Eurocode 9: Design of Aluminum Structures – Part 2: Structures Susceptible to Fatigue is an evolving design standard with procedures for fatigue evaluation of structural joints fabricated from aluminum. It also includes design curves and standards for damage tolerance and crack propagation providing a designer with the tools that are required to assess the likelihood of exceeding a critical crack length by a certain time in the design life of a cracked joint.

The objectives of this project associated with the survey of aluminum structural details still require work. The use of aluminum in marine structural applications continues to increase in both commercial and naval applications, with particular interest in high speed craft. This growth also brings an increased database of available information and experience although the competitive nature of the commercial industry may restrict access to and publication of detail performance. Naval programs, such as Littoral Combat Ship, also suggest the development of aluminum detail performance in combatant environments with different design procedures and requirements than typified by commercial design.

10. REFERENCES

10.1 European Standards

[1] "European Recommendations for Aluminum Alloy Structures Fatigue Design", European Convention for Constructional Steelwork, Doc. N°. 68, First Edition, Brussels 1992.

[2] Kosteas, D., Uhry, A.: „Fatigue Behaviour of Welded Aluminum Structures - European Full-Scale Tests", Part 1 (Kosteas): Analysis Results and Proposals, Part 2 (Uhry): Statistical Analysis, Part 3 (Kosteas): Data Base. Commission of the European Communities - COST 506 Program - European Aluminum Association. Munich/Voreppe, March/April 1989.

[3] Jaccard, R.: "Alusuisse Data Package onb Welded Aluminum Beams", Internal report, May 1988

[4] "AMAG Data on Welded Aluminum Beams", Laboratory Test Report, Wien, 02.05.1984

[5] Poalas, K., Kosteas, D.: „Voraussage des Ermüdungsverhaltens geschweißter Aluminumbauteile". LKI-Forschungsbericht Nr. 120 zum Forschungsvorhaben AIF 5723, Lehrstuhl für Stahlbau der Technischen Universität München, 1986.

[6] Ondra, R., Kosteas, D.: "Untersuchungen zum Schwingfestigkeitsverhalten geschweißter Verbindungen in Aluminum-Großbauteilen". LKI-Forschungsbericht Nr. 897-On zum Forschungsvorhaben AIF 7331, Lehrstuhl für Stahlbau der Technischen Univbersität München, 1991.

[7] Jaccard, R., Kosteas, D., Ondra, R.: „Data Re-Evaluation and Finalization of ERAAS Fatigue" , Part 1: Main Volume/Commentary, Part 2: Documents M-1 to M49, First Fatigue Workshop Munich February 1990, Part 3: Documents Z-1 to Z-135, Second Fatigue Workshop Zürich March 1990, Part 4:Preliminary Documents for Workshops Part 5: Data Sheets as of 12.07.1990, Part 6: Documents A-1 to A-35, Reclassification of Weldments,Part 7: Comparison of Structural Details Fatigue Strength Values, Internal Report of a joint TUM/A-L Study 1990/1991.

[8] R. Fisher, C. Menzemer: „Fatigue test results on welded aluminum beams", internal data exchange report, 1992.

[9] British Standard: „BS 8118- Structural Use of Aluminum", Part 1: Code of Practice for Design, 1992,

[10] Aluminum Association: "Specifications for Aluminum Structures", Washington, 1986

[11] "Association American Railcars", March 1988

[12] "Ontario Highway Bridge Code", Ontario, 1979

[13] Deutscher Verein für Schweißtechnik: "Richtlinien DVS 1608", Düsseldorf, 1969

[14] DIN 15018, „Krane", Ausgabe 1984

[15] Richtlinien der Deutschen Bundesbahn: "DS 804 - Vorschriften für Eisenbahnbrücken und sonstige Ingenieurbauten", Ausgabe Januar 1983

[16] Deutscher Ausschuß für Stahlbauten: "DASt-Richtlinie 011 - Feinkorn Baustähle", Februar 1979

[17] ENV 1993 -1 -1: "Eurocode 3 - Bemessung und Konstruktion von Stahlbauten", Brüssel, April 1992

[18] Voutaz B., Smith I., Hirt M.: Comportement à la fatigue de poutres en aluminum munies de goussets doudés", ICOM-Construction Métallique, Ecole Polytechnique Fédéral de Lausanne, ICOM 285, April 1993

[19] van Straalen IJ. J., Soetens F., Dijkstra O. D.: "EUREKA 269 - Fatigue tests on transverse butt welds", TNO Building and Research, 13. Oct. 1994
[20] van Straalen IJ. J., Soetens F., Dijkstra O. D.: "EUREKA 269 - Fatigue tests on longitudinal nonload carrying fillet welds", TNO Building and Research, 13. Oct. 1994
[21] van Straalen IJ. J., Soetens F., Dijkstra O. D.: "EUREKA 269 - Fatigue tests on transverse load carrying fillet welds", TNO Building and Research, 13. Oct. 1994
[22] van Straalen IJ. J., Soetens F., Dijkstra O. D.: "EUREKA 269 - Fatigue tests on transverse non-load carrying fillet welds", TNO Building and Research, 13. Oct.
[23] prENV 1999-2 (Sept. 1997) / Eurocode 9: Design of aluminum structures - Part 2: Structures susceptible to fatigue.
[24] Jaccard, R., Ogle, M. H.: Aluminum Eurocode - Design for Fatigue. In: WRC Proceedings IIW, p. 205-224.
[25] Jaccard, R., Kosteas, D., Ondra, R.: Background Document to Fatigue Design Curves for Welded Aluminum Components. IIW Doc. No. XIII-1588-95.

10.2 Friction Stir Welding

[26] Kallee S., 1999 Reibrührschweißen – Verfahren und Einsatzfälle, GKSS/TWI Workshop Mai
[27] Wayne T., Dawes C., Gittos M., Andrews D., 1998, Friction stir – where we are, and where we're going…, TWI Bulletin May/June
[28] Przydatek J., 2000, Friction Stir Welding with Lloyd's register, International Conference Lightweight Construction – Latest developments 24 and 25 February, London SW1
[29] Seetharaman V., Jata K.V., Semiatin S. L., Plastic flow and microstructure development during high temperature deformation of a friction stir welded 7050 aluminum alloy, Air Force Research Laboratory, Materials and Manufacturing Directorate, AFRL/MLLM Wright-Patterson Air Force Base, OH 45433-7817.
[30] Kallee S., 2000, Application of friction stir welding in the shipbuilding industry, International Conference Lightweight Construction – Latest Developments, 24 and 25 February London SW1
[31] Shepherd G. E., The potential for using solid phase welding to repair cracks that may occur on thin aluminum aircraft wing structure, BAE SYSTEMS Airbus UK, Filton, Bristol.
[32] Lee J.A., Carter R.W., Ding J., 1999, Friction Stir Welding for Aluminum Metal Matrix Composites (MMC'S), MSFC Center Director's Discretionary Fund Final Report, Project No. 98-09
[33] Haagensen P.J., Midling O.T., Ranes M., 1995, Fatigue performance of Friction Stir Butt Welds in a 6000 Series Aluminum Alloy, 2nd International Conference on Surface Treatment 95, Milan, Italy, 7-9 June.
[34] Johnson R., Kallee S., 1999, Stirring stuff from friction welding, Materials World, December.

[35] Hannour F., Davenport A.J., Strangwood M., 2000, Corrosion of Friction Stir Welds in High Strength Aluminum Alloys, 2nd International Symposium on Friction Stir Welding, 26-28 June, Gothenburg, Sweden.
[36] Backlund J., Norlin A., Andersson A., 15-17 April 1998, Friction stir welding – weld properties and manufacturing techniques, 7th Inalco Conference, Cambridge, ISBN 1 85573 417 6
[37] Thomas W.M., Nicholas E.D., 1997, Friction stir welding for the transportation industries, *Materials & Design*, Vol.18, Nos. 4/6, pp.269-273.
[38] Sanderson A., Punshon C.S., Russell J.D., 2000, Advanced welding processes for fusion reactor fabrication, Fusion Engineering and Design 49-50 77-87
[39] H. S. Yang, 1998, Microstructural Development in Friction Stir Welding of Aluminum Alloys Proc. of ICAA-6 (6th Int. Conf. Aluminum Alloys), Toyohashi, Japan, 1483-1488.
[40] O. Frigaad, B. Bjorneklett, O. Grong and O. T. Midling, 1998, Process Modelling Applied to Friction Stir Welding of Al-Mg-Si Alloys, Proc. of ICAA-6 (6th Int. Conf. Aluminum Alloys), Toyohashi, Japan, 1477-1482.
[41] H. Larsson, L. Karsson and L.-E. Svensson, 1998, Characteristics of Friction Stir Welds in AA5083 and AA6082 Aluminum Proc. of ICAA-6 (6th Int. Conf. Aluminum Alloys), Toyohashi, Japan, 1471-1476.
[42] J. Hagstrom and R. Sandstrom, 1998, Static and Dynamic Properties of Joints in Thin-Walled Aluminum Extrusions, Welded with Different Methods, Proc. of ICAA-6 (6th Int. Conf. Aluminum Alloys), Toyohashi, Japan, 1447-1452.
[43] M. W. Mahoney, C. G. Rhodes, J. G. Flintoff, R. A. Spurling and W. H. Bingel, 1998, Properties of Friction Stir welded 7075 -T651 Aluminum, Metall. Mater. Trans., 29A.
[44] G. Rhodes, M. W. Mahoney, W. H. Bingel, R. A. Spurling and C. C. Bampton, 1997, Effects of Friction Stir Welding on Microstructure of 7075 Aluminum, Scripta Mater., 36, 69-75.
[45] T. Hashimoto, N. Nishikawa, S. Tazaki and M. Enomoto, 1998, Mechanical properties of Joints for Aluminum Alloys with Friction Stir Welding Process, Preprints of INALCO 98 (7th Int. Conf. Joints in Aluminum), Cambridge, UK, 237-247.
[46] Dawes C. J., Thomas W. M., 1995, Friction stir joining of aluminum alloys, TWI Bulletin Nov/Dec
[47] Midling O.T., Oosterkamp L.D., Bersaas J., 15-17 April 1998, Friction stir welding aluminum – Process and applications, 7th Inalco Conference, Cambridge, ISBN 1 85573 417 6
[48] European Convention for Constructional Steelwork: European recommendations for aluminum alloy structure fatigue design, No 68
[49] W. M. Thomas E. D. Nicholas, J. C. Needham, M. G. Murch, P. Templesmith and C. J. Dawes, 1991, Friction Stir Butt Welding, International Patent Application PCT / GB92 / 02203, GB Patent Application 9125978.8, 6 Dec. and US Patent 5,460,317
[50] E. D. Nicholas, 1998, Developments in the Friction Stir Welding of Metals, Proc. of ICAA-6 (6th Int. Conf. Aluminum Alloys), Toyohashi, Japan, 139-151
[51] C. J. Dawes and W. M. Thomas 1995, Friction Stir Joining of Aluminum Alloys, TWI Bulletin, 36124-127
[52] C. J. Dawes and W. M. Thomas, 1996, Friction Stir Process Welds Aluminum Alloys, Welding J., March, 41-45

[53] P. Threadgill, 1997, Friction Stir Welds in Aluminum Alloys - Preliminary microstructural Assessment, TWI Bulletin, 38, March/April
[54] C. J. Dawes,1995, An Introduction to Friction Stir Welding and Its Development, Welding and Metal Fabrication, January, 14-16
[55] H. R. Shercliff and M. J. Russell, 1998, Analytical Modelling of Friction Stir Welding, Preprints of INALCO 98 (7th Int. Conf. Joints in Aluminum), Cambridge, UK, 185-195.
[56] O. Frigaad, O. Grong and O. T. Midling, 1998, Modelling of Heat Flow Phenomena in Friction Stir Welding of Aluminum Alloys Preprints of INALCO 98 (7th Int. Conf. Joints in Aluminum), Cambridge, UK, 197-207.
[57] L. E. Svensson, J. Karlsson, B. Karlsson, H. Larsson and L. Karlsson, 1998, Microstructure and Properties of Friction Stir Welded Aluminum Alloys Preprints of INALCO 98 (7th Int. Conf. Joints in Aluminum), Cambridge, UK,221-230.
[58] M. W. Mahoney, W. Harrigan and J. A. Wert, 1998, Friction Stir Welding SiC Discontinuously Reinforced Aluminuium, Preprints of INALCO 98 (7th Int. Conf. Joints in Aluminum), Cambridge, UK, 231-236.
[59] R. Tovo, R. De Scicolo, M. Volpone, 1999, Proprietà meccaniche e micro-strutturali di giunti “Friction Stir Welded” in lega di alluminio.
[60] M. Ericsson, R. Sandström, J. Hagström, Fatigue of friction stir welded AlMgSi-alloy 6082.
[61] I. Okura, M. Naruo, L. Gergely Vigh, N. Hagisawa, H. Toda, 2001, Fatigue of aluminum deck fabricated by friction Stir Welding, 8th INALCO 2001 International Conference on Joints in Aluminum, Munich, Germany, 28-30 March 2001
[62] T.Kawasaki, T.Makino, S. Todori, H. Takai, M. Ezumi, Y. Ina, Application of Friction Stir Welding to the Manufacturing of Next Generation “A-train” type Rolling Stock, HITACHI Ltd, Kasado administrative division, Higashi-Toyoi 794, Kudamatsu-city, Yamaguchi, JAPAN 744-8601
[63] L. Magnusson, L. Källman, Mechanical Properties of Friction Stir Welds in Thin Sheet of Aluminum 2024, 6013 and 7475

PROJECT TECHNICAL COMMITTEE MEMBERS

The following persons were members of the committee that represented the Ship Structure Committee to the Contractor as resident subject matter experts. As such they performed technical review of the initial proposals to select the contractor, advised the contractor in cognizant matters pertaining to the contract of which the agencies were aware, performed technical review of the work in progress and edited the final report.

Chairman	Mr. Chao Lin	MARAD
Members		
Contracting Officer's Technical Representative:		
	Ms. Lynell Fox	MARAD
Project Technical Committee Members:		
Executive Director:		
	LT Benjamin A. Gates	USCG
Administrative Assistant:		
	Ms. Jeannette Grant	USCG

SHIP STRUCTURE COMMITTEE LIAISON MEMBERS

LIAISON MEMBERS

American Iron and Steel Institute	
American Society for Testing & Materials	
American Society of Naval Engineers	Captain Dennis K. Kruse (USN Ret.)
American Welding Society	
Bath Iron Works	Mr. Steve Tarpy
Canada Ctr for Minerals & Energy Technology	
Colorado School of Mines	Dr. Stephen Liu
Edison Welding Institute	Mr. Rich Green
International Maritime Organization	Mr. Igor Ponomarev
Int'l Ship and Offshore Structure Congress	Dr. Jack Spencer
INTERTANKO	Mr. Dragos Rauta
Massachusetts Institute of Technology	
Memorial University of Newfoundland	Dr. M. R. Haddara
National Cargo Bureau	Captain Jim McNamara
Office of Naval Research	Dr. Yapa Rajapaksie
Oil Companies International Maritime Forum	Mr. Phillip Murphy
Tanker Structure Cooperative Forum	
Technical University of Nova Scotia	
United States Coast Guard Academy	Commander Kurt Colella
United States Merchant Marine Academy	
United States Naval Academy	Dr. Ramswar Bhattacharyya
University of British Columbia	Dr. S. Calisal
University of California Berkeley	Dr. Robert Bea
University of Houston - Composites Eng & Appl.	
University of Maryland	Dr. Bilal Ayyub
University of Michigan	Dr. Michael Bernitsas
University of Waterloo	
Virginia Polytechnic and State Institute	Dr. Alan Brown
Webb Institute	Prof. Roger Compton
Welding Research Council	
Worchester Polytechnic Institute	
Samsung Heavy Industries, Inc.	Dr. Satish Kumar

RECENT SHIP STRUCTURE COMMITTEE PUBLICATIONS

Ship Structure Committee Publications on the Web - All reports from SSC 392 and forward are available to be downloaded from the Ship Structure Committee Web Site at URL:
http://www.shipstructure.org
SSC 391 and below are available on the SSC CD-ROM Library. Visit the National Technical Information Service (NTIS) Web Site for ordering information at URL:
http://www.ntis.gov/fcpc/cpn7833.htm

SSC Report Number	Report Bibliography
SSC 445	Structural Survivability of Modern Liners, S. Schilling, 2005
SSC 444	In-Service Non-Destructive Estimation of the Remaining Fatigue Life of Welded Joints, Dexter R.J., Swanson K.M., Shield C.K. 2005
SSC 443	Design Guidelines for Doubler Plate Repairs on Ship Structures Sensharma P.K., Dinovitzer A., Traynham Y. 2005
SSC 442	Labor-Saving Passive Fire Protection Systems For Aluminum And Composite Construction E. Greene, 2005
SSC 441	Fire Degradation, Failure Prediction And Qualification Methods For Fiber Composites R. Asaro, M. Dao, 2005
SSC 440	Deterioration of Structural Integrity Due to Chemical Treatment of Ballast Water S. Tiku, 2005
SSC 439	Comparative Structural Requirements For High Speed Crafts K. Stone, 2005
SSC 438	Structural Optimization for Conversion of Aluminum Car Ferry to Support Military Vehicle Payload, R.Kramer, 2005
SSC 437	Modeling Longitudinal Damage in Ship Collisions A.J. Brown, JAW Sajdak 2005
SSC 436	Effect of Fabrication Tolerances on Fatigue Life of Welded Joints A. Kendrick, B. Ayyub, I. Assakkaf 2005
SSC 435	Predicting Stable Fatigue Crack Propagation in Stiffened Panels R.J. Dexter, H.N. Mahmoud 2004
SSC 434	Predicting Motion and Structural Loads in Stranded Ships Phase 1 A.J. Brown, M. Simbulan, J. McQuillan, M. Gutierrez 2004